Study of Some Problems on Thermoelasticity and Generalized Thermoelasticity

Sourov Roy
Department of Mathematics
Jadavpur University

A thesis submitted for the degree of
Doctor of Philosophy

2024

যাদবপুর বিশ্ববিদ্যালয়

FACULTY OF SCIENCE
DEPARTMENT OF MATHEMATICS

JADAVPUR UNIVERSITY
Kolkata - 700 032, India
Telephone : 91 (33) 2457 2269

CERTIFICATE FROM THE SUPERVISOR

This is to certify that the thesis entitled **"Study of Some Problems on Thermoelasticity and Generalized Thermoelasticity"** Submitted by **Sri Sourov Roy** who got his name registered on **17.09.2019 (Index No.: 99/19/Maths./26)** for the award of Ph. D. (Science) degree of Jadavpur University, is absolutely based upon his own work under the supervision of **Professor Abhijit Lahiri** and that neither this thesis nor any part of it has been submitted for either any degree / diploma or any other academic award anywhere before.

abhijit Lahiri 22/01/24.

(Signature of the Supervisor date with official seal)

Professor
DEPARTMENT OF MATHEMATICS
Jadavpur University
Kolkata-700 032, West Bengal

Dedicated to my beloved parents

Acknowledgements

I extend my heartfelt appreciation to my esteemed supervisor, Professor Abhijit Lahiri of Department of Mathematics at Jadavpur University, Kolkata. I am sincerely grateful to him for providing me with the invaluable opportunity to conduct my research. His guidance has been both cooperative and knowledgeable, and I am thankful for his unwavering support throughout the research process. His mentorship has allowed me to gain insights into numerous new aspects, for which I am truly grateful.

I express my gratitude to Prof. Sujit Kumar Sardar, Prof. Subhas Chandra Mondal, Prof. Dipak Kumar Kesh, Prof. Nandadulal Bairagi, Prof. Sagnik Sinha, and the other esteemed faculty members of the Department of Mathematics at Jadavpur University for their valuable insights, comments, and encouragement. Their perspectives have significantly contributed to the broadening of my research.

I acknowledge the Council of Scientific & Industrial Research(CSIR), New Delhi for providing financial assistance as Junior Research Fellow (JRF) and Senior Research Fellow (SRF) through the award letter No. 09/949(096)/2018-EMR-I.

I would like to express my heartfelt gratitude to my parents and other family members for their steadfast and continuous mental support during the progression of my research work. Their encouragement has been a cornerstone in the formation of my academic endeavors.

2024 Sourov Roy

Kolkata, W.B, India

Preface

Every natural material exhibits elastic properties, signifying their tendency to deform in response to even slight external forces. The examination of stresses and strains induced in deformable materials due to applied forces or temperature changes falls within the part of solid mechanics, specifically referred to as elasticity. Elasticity essentially provides a structured framework for predicting the way materials will respond to specific mechanical stresses or temperature changes. This yields valuable insights into the mechanical characteristics of solids across diverse scenarios. The practical significance of elasticity lies in its application to assess stresses and displacements in machine or structural components within the elastic limit. This ensures that stiffness, stability, and strength meet the required criteria.

The historical development of the theory of elasticity can be traced back to 1632 when Galileo [43] initiated an investigation into the 'tendency to break' of a heavy horizontal beam. This experimental setup involved one end of the beam being built-in while the other end remained free. Foundational experiments crucial for establishing the theory were conducted by Hooke [59], whose famous law establishing the proportionality of stress and strain laid the groundwork for the mathematical formulation of elasticity. Expanding on Hooke's foundational work, Navier [100] formulated general equations governing the equilibrium and vibration of elastic solids. Following this, Cauchy [26] provided a formulation for the linear theory of elasticity based on Navier's contributions. Remarkably, this formulation has remained virtually unchanged to the present day. The evolution of the theory witnessed significant contributions from Poisson [119], Lame [80], Kirchhoff [75], Green [46]. A detailed chronological account of these contributions can be explored in the works of Love [87], and Sokolnikoff [137] etc.

The deformation of a body is invariably linked to a modification in heat content, and correspondingly, a shift in the body's temperature. Deformation that fluctuates over time induces an alteration in the temperature field, and conversely, a temperature change gives rise to strain. The internal energy of the body, therefore, becomes a function of deformation and temperature. The branch of science dealing with these coupled processes is called 'thermoelasticity.'

The basis of classical thermoelasticity theory (CTE) was established by Duhamel [34], in which equations for the distribution of strain in an elastic medium containing temperature gradients have been derived. The present structure of the equation was given by Neumann [102], known as the Duhamel-Neumann stress-strain-temperature relation. Efforts were made by researchers like Jeffreys [62], Lessen and Duke [83], Lessen [82] to justify a coupled system of momentum and energy equations for heat conduction. However, classical thermodynamic principles couldn't satisfactorily explain the irreversible process of thermal diffusion. A breakthrough occurred when Biot [20] successfully derived the linear theory of classical coupled thermoelasticity (CCTE) based on irreversible thermodynamics, addressing the paradox that elastic changes have no impact on temperature. Chadwick [27] extended the theory to linear and non-linear versions, highlighting the inseparable nature of thermal and strain fields in dynamic problems. Contributions from Boley and Wiener [22], Nowacki [103], Johns [63], Kovalenko [76], Sneddon [136], Parkus [117], and Dhaliwal and Singh [33] further enriched the understanding and applications of classical and coupled theories. Advancements in Classical Coupled Thermoelasticity (CCTE) have aimed to extend its application to various material structures, including electromagnetic, viscoelastic, and microelastic solids. Researchers like Paria [116], Eringen [36], Parkus [117], Nowacki [104], Hetnarski [56], and Chandrasekharaiah [28] have contributed by providing closed-form solutions for these formulations, expanding the theory's versatility across a broader spectrum of material behaviors and structures.

The governing equations, initially introduced by Biot [20], consist of two coupled partial differential equations for displacement and temperature fields. However, the linear dynamical theory of thermoelasticity poses a challenge with a wave-type (hyperbolic type) equation for displacement

and a diffusion-type (parabolic type) equation for temperature. This results in unrealistic infinite-speed propagation of disturbances, contradicted by experimental evidence showing finite-speed propagation of heat pulses. Lebon [81] provided a thermodynamic basis for the theory proposed by Kaliski [65], addressing the wave-like thermal disturbance known as 'second sound' vide, Suhubi [141].

The introduction of the generalized Fourier law by Lord and Shulman [85] led to the development of generalized thermoelasticity theories. Maxwell [90] proposed a law for gases, later adapted by Cattaneo [24, 25] to derive a wave-type heat conduction equation. Subsequent researchers, including Vernotte [150], Nettleton [101], Lykov [88],and Kaliski [65] explored and analyzed this revised law, with Gurtin and Pipkin [52] proposing a more general law for rigid material with memory.

Lord and Shulman [85] present one of the two significant generalized theories of thermoelasticity, with the second being the theory of temperature-rate-dependent thermoelasticity[TRDTE]. In a thermodynamics review of thermoelastic solids (TSs), Muller [97] introduced an entropy production inequality, imposing constraints on a class of constitutive equations. Green and Laws [47] proposed a generalization of this inequality, with another version of these constitutive equations obtained by Green and Lindsay [48]. The theoretical framework under consideration is commonly known as "temperature rate-dependent thermoelasticity" or TRDTE for short. This particular theory exhibits distinct characteristics that set it apart from the Lord-Shulman (L-S) [85] theory, which incorporates a single relaxation time. Within the Green and Lindsay(G-L)[48] model, the fundamental principles of Fourier's law of heat conduction remain unaltered, while modifications are introduced to the classical energy equation and the relationships governing stress, strain, and temperature. Suhubi [141] independently and explicitly derived these equations, which include two constants acting as relaxation times, transforming all the equations of the coupled theory.

Green and Naghdi [49, 50, 51] introduced another extension of the theory, characterizing material response for thermal phenomena with three constitutive response functions labeled as Type I, Type II, and Type III. When linearized, Type I aligns with the classical heat conduction equation

(based on Fourier Law), Type II permits thermal wave propagation at finite speed without dissipation, and Type III involves a thermal damping term while also predicting finite speed of thermal wave propagation. In the area of thermoelasticity, various studies have been conducted based on the Green and Naghdi (GN) theory. Roychoudhuri and Datta [129] studied thermoelastic interactions in a solid with periodic heat sources under the GN-II model. Mukhopadhyay [94, 95, 96] tackled a thermal shock problem involving a spherical cavity in an unbounded medium using the GN-II model. Other researchers, such as Kar et al.[70, 69, 71] have explored various problems under the GN-III model, addressing different aspects of thermoelasticity.

The concept of fractional derivatives can be traced to the 17th century, with mathematicians like Leibniz and L'Hôpital playing key roles. Leibniz, in particular, engaged in correspondence with L'Hôpital, exploring the idea of non-integer order derivatives. Substantial progress in fractional calculus occurred in the 1830s, credited to Liouville[84]. Liouville formulated the theory of fractional integration and fractional differentiation, laying a robust foundation for subsequent advancements. The Riemann-Liouville fractional calculus, initially introduced by Riemann[125] and further expanded by Liouville[84], stands out as one of the most widely used definitions of fractional derivatives and integrals. This approach addresses fractional orders in a continuous manner. Caputo[23] provided an alternative definition of fractional derivatives, known as the Caputo fractional derivative. This definition has gained widespread application and offers distinct advantages in certain contexts. In the latter half of the 20th century and into the 21st century, fractional calculus experienced a surge in attention. Mathematicians and scientists across various disciplines, including engineering, physics, and biology, studied the applications and properties of fractional calculus. In recent years, the application of fractional calculus theory has become instrumental in advancing our understanding of thermoelasticity. Povstenko [121] utilized this theory to investigate thermal stresses, incorporating the Caputo time-fractional derivative into the heat conduction equation. This application facilitated the analysis of thermal stresses in an infinite body with a circular cylindrical hole. Sherief et al. [135] introduced an innovative thermoelasticity model by modifying the Fourier heat conduction law through fractional derivatives.

Their contributions included the derivation of uniqueness and reciprocity theories within the framework of fractional thermoelasticity. Sherief et al. [132] tackled a one dimensional problem for a half-space using fractional thermoelasticity theory, examining the influence of variable thermal conductivity on the half-space. Ezzat et al. [40, 41, 42] established a new model for the fractional heat conduction equation, employing the Taylor series expansion of time-fractional order developed by Jumarie [64]. Additionally, Povstenko [120] introduced fractional Cattaneo-type equations, analyzing time non-local generalizations of the Fourier law. This analysis resulted in the derivation of fractional telegraph equations and the proposal of corresponding theories in the field of thermoelasticity.

In many modern engineering materials, the constituent particles are not only subject to translational motion but also have the freedom to rotate about their own axes. This type of motion involves both deformation and microrotation. Consequently, the interaction between different parts of the material is conveyed not only through forces but also through torques, giving rise to asymmetric force stresses and couple stresses in the material. Classical elasticity theory fails to explain these phenomena. To address the analysis of material microstructures, the theory of micropolar elasticity is employed. Materials such as soils, rocks, concrete, metals, and polymers exhibit such microstructural characteristics. Classical theories of elasticity fall short in capturing the behavior of materials with intricate internal structures. Recognizing this limitation, Eringen and Suhubi [39] introduced a nonlinear theory for microelastic solids. Eringen [38, 35, 36] further expanded on this work, introducing a theory that allows material particles in solids to undergo both macro-deformations and microrotations. This extension, known as the "linear theory of micropolar elasticity," was later refined by Eringen [37] to include axial stretch, resulting in a comprehensive theory of micropolar elastic solids with stretch.

In recent years, the study of photothermal waves in semiconducting media has seen significant advancements. Semiconducting thermoelasticity is applied in microelectronics for optimizing thermal management, enabling non-destructive testing of semiconductor materials, and contributing to the development of energy harvesting devices. Additionally, its use in photothermal imaging, biomedical applications, and gas sensing technologies showcases its versatility across various fields, playing a crucial role

in material design, sensor development, and environmental monitoring. Todorovic et al. [144, 142, 143] provided valuable insights into micromechanical structures and carrier behaviors in one dimensional semiconductors. Muratikov and Glazov [98] explored photoacoustic effects in bodies with residual stresses, while Song et al. [140, 139, 138] contributed to the understanding of the photothermal effect. Othman et al. [112, 113] investigated photothermal waves using the L–S model, considering the influence of gravity. Othman et al. [114] applied the DPL model to study the temperature-dependent thermoelastic response with initial stress. Lotfy [86] explored hydrostatic initial stress effects on photo-thermal solids using DPL and L–S theories. Hobiny and Abbas [58] introduced a fractional-order G–N model for wave propagation in inhomogeneous semiconductors. Alzahrani and Abbas [15] used the G–L model to derive field variables in semiconductor media. Abbas et al. [4] employed the DPL model for a generalized theory of plasma, thermal, and elastic waves in semiconductor solids. Zenkour [157, 159] introduced refined DPL theories exploring gravity, thermal activation, and diffusion in photo-thermal semiconducting media. These studies collectively contribute to a nuanced understanding of photothermal behavior in semiconductors.

Since the advent of thermoelasticity and generalized thermoelasticity theories, Iesan's book [60], the work by Ignaczak and Ostoja-Starzewski [61], and Das's book [30] offer significant insights. Theses authored by Narasimha Murthy [99], Keshavan [72], Mitra [92], and Ghosh [44] provide comprehensive details on the foundational equations of generalized thermoelasticity theories.

This research is dedicated to the application field of continuum mechanics, focusing on exploring problems in thermoelasticity and generalized thermoelasticity. This thesis comprises four chapters, each addressing various aspects of thermoelastic models. The *introductory chapter* provides essential definitions, introduces thermoelasticity and related theories, discusses the applications of thermoelasticity.

The *second chapter* contrues two problems on generalized thermoelasticity. **Problem-1** investigates a one-dimensional problem on fractional-order generalized thermoelasticity in a half-space with an instantaneous heat source. The Laplace transform and eigenvalue approach techniques

are applied to obtain closed-form solutions for displacement, temperature, and stress, which are presented graphically. In **Problem-2**, a fractional-order thermoelasticity model with dual-phase lag is studied in a half-space isotropic elastic medium. The eigenvalue approach is employed to solve the vector-matrix differential equation obtained from normal mode analysis, and graphical representations illustrate the impact of the heat source.

The *third chapter* explores three thermoelasticity problems with microstructure. **Problem-3** focuses on a multi-phase-lag micropolar thermoelastic model in a rotating half-space medium with a moving heat source in the presence of an electromagnetic field. The eigenvalue approach is used, and graphical representations depict the impact of heat source, rotation, and magnetic field. **Problem-4** addresses fractional order three-phase-lag thermoelasticity in a micropolar thermoelastic half-space medium with voids, providing numerical computations and graphical depictions.
Problem-5 investigates the influence of electro-magnetic force in the presence of gravitational force on a prestressed micro-elongated thermoelastic layer. A three-phase-lag (TPL) heat conduction equation is employed for microelongated layer. So, TPL model is employed in conjunction with an elastic layer. The governing equations are introduced, and non-dimensionalization is applied. Normal mode analysis is employed to transform partial differential equations into ordinary ones, and the eigenvalue approach is utilized to solve these equations. The constants in the solutions are determined by the boundary conditions, and the study includes a thorough discussion and graphical representation of the obtained results.

In the *last chapter*, two thermoelastic problems in a semiconducting medium are discussed. The *fourth chapter* contains two thermoelasticity problems in semiconducting medium. **Problem-6** explores a comprehensive model that investigates the interactions of various factors on an isotropic, homogeneous semiconducting plate. The study encompasses the influences of volume fraction, photothermal phenomena, initial stress, electromagnetic fields, gravity, and rotation, all within the framework of multi-three-phase lag thermoelastic models. The investigation addresses the fundamental governing equations, accounting for voids, electromagnetic fields, photothermal effects, initial stresses, gravitational forces, rotational dynamics, and the semiconductor properties of the material, all under the

umbrella of generalized thermoelasticity. To tackle this complex problem, the normal mode analysis method is employed for solving partial differential equations with specific boundary conditions. The study incorporates a comprehensive discussion and graphical representation of the obtained results. **Problem-7** introduces fractional thermoelasticity to analyze the photothermal and memory response of a rotating semiconducting half-space medium. The semiconducting medium is subjected to an internal heat source. The propagation of photothermal waves in a prestressed semiconducting half-space with a gravity effect has been investigated. The normal mode analysis precisely resolved all coupled photo-thermoelastic equations. The eigenvalue approach is adopted to derive the analytical solution of the main variables of the medium. Temperature, horizontal and vertical displacements, stresses, and carrier density were all measured. The dependence of all field variables on the internal heat source, initial stress, rotation, electromagnetic field, fractional order parameter, and inclusion of gravity is demonstrated. The results are graphed to serve as benchmarks for future comparisons, and additional results are shown to demonstrate the physical meaning of the phenomenon.

The thesis concludes with a list of references, providing a comprehensive overview of the research conducted in the field of thermoelasticity and generalized thermoelasticity.

Contents

List of Figures

List of Tables

CHAPTER 1

General Introduction

1.1 Fundamental Concepts and Models in Thermoelasticity

1.1.1 Thermoelasticity and its Applications

Thermoelasticity involves investigating how an elastic material responds to non-uniform changes in its temperature field. This field of study expands upon elasticity theory by considering both thermal and mechanical reactions. The theories of thermoelasticity have emerged through a beneficial combination of Fourier's Law of heat conduction and established formulations in elasticity theory.

During the second half of the 20th century, the theory of thermoelasticity drew the attention of many researchers due to its extensive applications in diverse fields. Thermoelasticity, with its ability to comprehensively address the coupled processes of heat conduction and elasticity, finds various applications across structural engineering, aerospace engineering, material science, geophysics, biomedical engineering, energy systems, material testing, nuclear engineering, and more.

In structural engineering, it plays a crucial role in analyzing the behavior of structures exposed to temperature variations, ensuring integrity and safety. Aerospace engineering relies on thermoelasticity for designing components in extreme temperature conditions and optimizing material selection. Material science benefits from thermoelastic models in studying materials with specific thermal and mechanical properties, guiding the design of advanced materials. Geophysics utilizes thermoelasticity to understand the Earth's crust behavior, contributing to seismic studies and subsurface dynamics. In biomedical engineering, thermoelasticity studies thermal and mechanical responses of tissues for accurate medical imaging and therapeutic applications.

Energy systems, material testing, nuclear engineering, and other fields use thermoelasticity for design, optimization, and safety assessments. In essence, thermoelasticity provides valuable insights and tools for addressing challenges related to temperature-induced deformations across disciplines.

1.1.2 Strain-Displacement Relation

The kinematic relationship between strain and displacement is established when the displacement at a specific location within the body, denoted by Cartesian coordinates x_i (where $i = 1, 2, 3$), is represented as u_i.

$$e_{ij} = \frac{1}{2}\left(u_{i,j} + u_{j,i}\right) \tag{1.1}$$

Here, $e_{ij} = e_{ji}$. Strain-displacement relations in cylindrical co-ordinate system are given by

$$\begin{aligned} e_{rr} &= \frac{\partial u_r}{\partial r}, e_{\theta\theta} = \frac{1}{r}\frac{\partial u_\theta}{\partial \theta} + \frac{u_r}{r}, e_{zz} = \frac{\partial u_z}{\partial z} \\ e_{r\theta} &= \frac{1}{2}\left(\frac{1}{r}\frac{\partial u_r}{\partial \theta} + \frac{\partial u_\theta}{\partial r} - \frac{u_\theta}{r}\right), \\ e_{rz} &= \frac{1}{2}\left(\frac{\partial u_z}{\partial r} + \frac{\partial u_r}{\partial z}\right) \\ e_{\theta z} &= \frac{1}{2}\left(\frac{\partial u_\theta}{\partial z} + \frac{1}{r}\frac{\partial u_z}{\partial \theta}\right) \end{aligned} \tag{1.2}$$

1.1.3 Stress-Strain Relations

The most general form of Hooke's law is represented by

$$\sigma_{ij} = C_{ijkl} e_{kl} \quad (i, j, k, l = 1, 2, 3) \tag{1.3}$$

The stress component σ_{ij} corresponds to the force on unit area in the x_j direction within the plane x_i = constant. Consequently, there are nine distinct stress components. It can be demonstrated that $\sigma_{ij} = \sigma_{ji}$. In such instances, the body's stress system can be defined by just six independent stress components. where C_{ijkl} is the stiffness tensor which has 81 elements. Considering symmetry properties of both stress and strain components, these may be reduced to the form

$$\sigma_m = C_{mn} e_n, \quad (m, n = 1, \ldots, 6) \tag{1.4}$$

In equation (1.4),

$$\begin{aligned} \sigma_{11} = \sigma_1, \sigma_{22} = \sigma_2, \sigma_{33} = \sigma_3 \\ \sigma_{32} = \sigma_4, \sigma_{13} = \sigma_5, \sigma_{12} = \sigma_6 \\ e_{11} = e_1, e_{22} = e_2, e_{33} = e_3 \\ e_{32} = e_4, e_{13} = e_5, e_{12} = e_6 \end{aligned}$$

and C_{mn} is a matrix of order 6 with $C_{mn} = C_{nm}$.

In the generalized Hooke's law, the coefficients C_{mn} are symmetric due to the existence of a strain energy density function. The number of independent elastic constants in the generalized Hooke's law (Equation 1.3) includes six different constants located along the diagonal and an additional $\frac{36-6}{2} = 15$ among the remaining constants, making a total of $15 + 6 = 21$ constants. Therefore, the existence of the strain energy density function reduces the number of coefficients from 36 to 21 in the

generalized Hooke's law. an orthotropic solid has 9 independent elastic constants, a transversely isotropic material has 5, and a cubic crystalline structure has 3 independent elastic constants. On the other hand, for isotropic materials, the matrix is defined by only two independent parameters, λ and μ, known as Lamè's constants [80].

1.1.4 Thermal Stresses

Deformation occurs in a material when subjected to heat-induced changes in its dimensions. In such cases, elevated temperatures can lead to deformation and resultant stresses, even in the absence of external mechanical loads. This phenomenon is known as thermoelasticity. The temperature excess over the surroundings can result from either internal heating due to straining or external heating from a heat source denoted as T. The thermal stresses in this context are calculated using the constitutive relations given by:

$$\sigma_m = C_{mn} e_n - \gamma_m T \quad (m, n = 1, 2, 3, \ldots, 6) \tag{1.5}$$

Here, the coefficients γ_{mn} are defined as follows:

$$\gamma_{11} = \gamma_1, \quad \gamma_{22} = \gamma_2, \quad \gamma_{33} = \gamma_3, \quad \gamma_{32} = \gamma_4, \quad \gamma_{13} = \gamma_5, \quad \gamma_{12} = \gamma_6$$

These relations are commonly referred to as the Duhamel-Neumann relations. For a transversely isotropic body with principal elastic axes coinciding with the coordinate axes, the equations can be expressed as:

$$\begin{bmatrix} \sigma_{11} \\ \sigma_{22} \\ \sigma_{33} \\ \sigma_{32} \\ \sigma_{31} \\ \sigma_{12} \end{bmatrix} = \begin{bmatrix} c_{11} & c_{12} & c_{13} & 0 & 0 & 0 \\ c_{12} & c_{11} & c_{12} & 0 & 0 & 0 \\ c_{12} & c_{12} & c_{11} & 0 & 0 & 0 \\ 0 & 0 & 0 & c_{44} & 0 & 0 \\ 0 & 0 & 0 & 0 & c_{44} & 0 \\ 0 & 0 & 0 & 0 & 0 & c_{44} \end{bmatrix} \begin{bmatrix} e_{11} \\ e_{22} \\ e_{33} \\ e_{32} \\ e_{31} \\ e_{12} \end{bmatrix} - T \begin{bmatrix} \gamma_{11} \\ \gamma_{11} \\ \gamma_{33} \\ 0 \\ 0 \\ 0 \end{bmatrix} \tag{1.6}$$

In this formulation, γ_{11} and γ_{33} are expressed as functions of material constants and coefficients of linear thermal expansion (α_1 and α_3).

For isotropic bodies, where $c_{12} = \lambda$, $c_{11} = \mu$, $c_{44} = \mu$, and $\gamma_{11} = (3\lambda + 2\mu)\alpha$, the constitutive relations simplify to:

$$\sigma_{ij} = \lambda e_{kk} \delta_{ij} + 2\mu e_{ij} - \gamma T \tag{1.7}$$

Here, δ_{ij} represents the Kronecker delta.

1.1.5 Equations of Motion

The conservation of linear momentum forms the basis for the equations governing the motion of an elastic body under various types of stresses, encompassing both mechanical and thermal stressors. The inertial force within any specified volume V, bounded by the surface S, is the sum of volume and surface forces, as expressed by the conservation principle:

$$\rho \frac{\partial}{\partial t} \int_V v_i \, dv = \int_V F_i \, dv + \int_S p_i \, ds \quad (i = 1, 2, 3) \tag{1.8}$$

Here, ρ denotes the mass density, while v_i, F_i, and p_i represent the components of velocity, body force per unit volume, and surface traction on S, respectively. The relation $p_i = \sigma_{ij} n_j$ is employed, where n_i signifies the unit normal vector to S. Utilizing the Gauss divergence theorem, the equation transforms into:

$$\int_S \sigma_{ij} n_j \, ds = \int_V \sigma_{ij,j} \, dv \tag{1.9}$$

Leading to:

$$\sigma_{ij,j} + \rho F_i = \rho \frac{\partial^2 u_i}{\partial t^2} \tag{1.10}$$

Together with appropriate constitutive relations, the equations describing the motion in terms of displacement components are formulated as:

$$\mu u_{i,jj} + (\lambda + \mu) u_{j,ji} + \rho F_i = \gamma T_{,i} + \rho \ddot{u}_i \tag{1.11}$$

For a cylindrical coordinate system, the equations of motion are given by:

$$\begin{aligned}
&\frac{\partial \sigma_{rr}}{\partial r} + \frac{1}{r}\frac{\partial \sigma_{r\theta}}{\partial \theta} + \frac{\partial \sigma_{rz}}{\partial z} + \frac{\sigma_{rr} - \sigma_{\theta\theta}}{r} + F_r = \rho \frac{\partial^2 u_r}{\partial t^2} \\
&\frac{\partial \sigma_{r\theta}}{\partial r} + \frac{1}{r}\frac{\partial \sigma_{\theta\theta}}{\partial \theta} + \frac{\partial \sigma_{\theta z}}{\partial z} + \frac{2}{r}\sigma_{r\theta} + F_\theta = \rho \frac{\partial^2 u_\theta}{\partial t^2} \\
&\frac{\partial \sigma_{rz}}{\partial r} + \frac{1}{r}\frac{\partial \sigma_{\theta z}}{\partial \theta} + \frac{\partial \sigma_{zz}}{\partial z} + \frac{1}{r}\sigma_{rz} + F_z = \rho \frac{\partial^2 u_z}{\partial t^2}.
\end{aligned} \tag{1.12}$$

1.1.6 Thermo-Mechanical Coupling

An elastic body undergoes straining when subjected to mechanical loading, resulting in the performance of work. The dissipation of energy occurs as heat, creating a temperature field within the material. Consequently, it becomes crucial to appropriately

incorporate this internal heat source in the Fourier heat conduction equation to accurately compute the temperature field. The interplay between the temperature and strain fields elucidates how temperature influences the speed of elastic wave propagation, aiding in the comprehension of the temperature field induced by time-varying forces. It is important to note that the coupling component can be disregarded only in scenarios with stationary temperature fields.

1.1.7 History of Thermoelasticity Theories

The study begins with an exploration of classical linear thermoelasticity (CTE) and subsequently discusses the generalized theory of thermoelasticity. The generalized theory aims to address practical paradoxes in the classical theory by incorporating the concept of second sound.

1.1.7.1 Classical Thermoelasticity (CTE):

The foundation of classical thermoelasticity theory (CTE) was laid by Duhamel [34], who derived equations describing strain distribution in an elastic medium with temperature gradients. The Duhamel-Neumann stress-strain-temperature relation, as formulated by Neumann [102], remains fundamental in CTE. Constitutive equations in CTE describe the relationship between stress, strain, and temperature changes, incorporating material properties such as thermal expansion coefficients and elastic constants. Fourier's law of heat conduction is a central element in CTE, linking heat flux to temperature gradients.

1. **Constitutive equations:**

$$\sigma_{ij} = \lambda e_{ii}\delta_{ij} + 2\mu e_{ij} - \gamma T\delta_{ij} \quad ; \quad (i,j = 1,2,3) \tag{1.13}$$

   where $\gamma = (3\lambda + 2\mu)\alpha_t$, α_t is the coefficient of linear thermal expansion, T is the increase in temperature above the reference T_0.

2. **Strain-displacement relations:**

$$e_{ij} = \frac{1}{2}(u_{i,j} + u_{j,i}) \tag{1.14}$$

3. **Classical Fourier law:** Equations (1.11) and (1.12) are supplemented by the classical Fourier law, connecting the heat flux vector $\mathbf{q}$ with the temperature gradient ∇T through the equation:

$$q_i = -KT_{,i} \quad \text{for } i = 1,2,3 \tag{1.15}$$

where $K > 0$ is the thermal conductivity of the solid.

4. **Conservation of internal energy:**

$$-q_{i,i} + \rho Q = \rho c_e \dot{T}, \quad \text{for } i = 1, 2, 3 \tag{1.16}$$

where Q is the heat source, and c_e is the specific heat at constant strain. The dot notation ($\dot{}$) denotes the partial derivative with respect to time.

5. **Heat transport equation:** Equations (1.13) and (1.14) together yield the parabolic heat transport equation:

$$K\nabla^2 T + \rho Q = \rho c_e \dot{T} \tag{1.17}$$

6. **Equations of motion:**

   - **Stress equations of motion:**

$$\sigma_{ij,j} + \rho f_i = \rho \ddot{u}_i \tag{1.18}$$

   where σ_{ij} is given by equation (1.11).

   - **Displacement equations of motion:**

$$(\lambda + \mu) u_{j,ij} + \mu u_{i,jj} - \gamma T_{,i} + F_i = \rho \ddot{u}_i \tag{1.19}$$

The complete mathematical model of classical thermoelasticity is defined by equations (1.11), (1.15), and (1.16) (or (1.17)).

1.1.7.2 Classical Coupled Thermoelasticity (CCTE):

Biot (1956) introduced the theory of coupled dynamical thermoelasticity for isotropic materials, providing a set of linear equations expressing this theory. The fundamental equations are outlined below:

1. **Constitutive equations:**

$$\sigma_{ij} = \lambda e_{ii} \delta_{ij} + 2\mu e_{ij} - \gamma T \delta_{ij} \quad ; \quad (i, j = 1, 2, 3) \tag{1.20}$$

2. **Law of conservation of internal energy:**

$$-q_{i,i} + \rho Q = \rho c_e \dot{T} + \gamma T_0 \dot{e}_{k,k} \tag{1.21}$$

where the term $\gamma T_0 \dot{e}_{k,k}$ introduces coupling between strain and temperature [20].

3. **Classical heat transport equation:** Eliminating q_i between equations (1.16) and (1.21), the classical heat transport equation in a generalized form is derived as:

$$k\nabla^2 T + \rho Q = \rho c_e \dot{T} + \gamma T_0 \dot{e}_{k,k} \tag{1.22}$$

4. **Displacement equations of motion:**

$$(\lambda + \mu)u_{j,ij} + \mu u_{i,jj} - \gamma T_{,i} + F_i = \rho \ddot{u}_i \tag{1.23}$$

Equations (1.11), (1.15), and (1.16) (or (1.17)) together form the comprehensive mathematical framework for the classical theory of thermoelasticity.

1.1.7.3 Lord-Shulman (L-S) Model [Extended thermoelasticity (ETE)]:

Lord and Shulman (1967) introduced a thermoelastic model that adjusts Fourier's law of heat conduction by incorporating the notion of a relaxation time. This relaxation time signifies the duration necessary for accelerating heat flow.

Law of conservation of internal energy:

$$\left(1 + \tau \frac{\partial}{\partial t}\right) q_i = -KT_{,i} \tag{1.24}$$

where τ is a non-negative constant. This law is a generalization of the classical Fourier law given by (1.15). Here q_i represents the heat-flux within the material to the temperature gradient. Using (1.24) in place of (1.15), one gets the following generalization of the heat conduction equation:

$$K\nabla^2 T = \left(1 + \tau \frac{\partial}{\partial t}\right) [\rho c_e \dot{T} + T_0 \gamma \dot{u}_{k,k} - \rho Q] \tag{1.25}$$

Equation (1.25) belongs to the hyperbolic type, establishing that the heat transport equation in thermoelasticity theory avoids the paradox of infinite heat propagation speed. The predicted speed for thermal signals in (1.25) is $\left(\frac{K}{\rho c_e \tau}\right)^{\frac{1}{2}}$, indicating a wave-like thermal disturbance commonly known as 'second sound,' as discussed by Suhubi [141]. The coupled equations (1.16) and (1.24), along with constitutive equations (1.19), together form a comprehensive set of field equations known as Extended Thermoelasticity (ETE). The Extended Thermoelasticity (ETE) theory, often denoted as the L-S theory of generalized thermoelasticity, incorporates a single relaxation time parameter.

1.1.7.4 Green-Lindsay (G-L) Model [Temperature Rate Dependent Thermoelasticity (TRDTE)]:

In the G-L model, Fourier law of heat conduction is unchanged whereas the classical energy equation and the stress-strain-temperature relations are modified. Two constitutive constants α and α_0 having the dimension of time appear in the governing equations in place of one relaxation time τ in L-S model. The equations, as proposed in the G-L model, are as follows:

1. **Modified energy equation:**

$$-q_{i,i} + \rho Q = \rho c_e(\dot{T} + \alpha_0 \ddot{T}) + \gamma T_0 \dot{e_{kk}} \tag{1.26}$$

2. **Modified constitutive equation with temperature rate term:**

$$\sigma_{ij} = \lambda e_{kk}\delta_{ij} + 2\mu e_{ij} - \gamma(T + \alpha\dot{T})\delta_{ij}; \quad (i, j = 1, 2, 3) \tag{1.27}$$

3. **Fourier law:**

$$q_i = -KT_{,i} \tag{1.28}$$

4. **Coupled heat transport equation:**

$$K\nabla^2 T + \rho Q = \rho c_e(\dot{T} + \alpha_0 \ddot{T}) + \gamma T_0 \dot{e_{kk}} \tag{1.29}$$

It is known that $\alpha \geq \alpha_0 > 0$.

1.1.7.5 Green and Naghdi (G-N) Model of Type I, II and III:

For isotropic medium, the heat conduction equation in the theories proposed by Green and Naghdi can be expressed in the following way:

A. **Green and Naghdi (G-N) model I**

1. **Modified energy equation :**

$$-q_{i,i} + \rho Q = \rho c_e \dot{T} + \gamma T_0 \dot{e_{kk}} \tag{1.30}$$

2. **Heat conduction law :**

$$q_i = -K\nu_{,i}, \dot{\nu} = T \tag{1.31}$$

where ν is the thermal displacement.
Equations (1.30) and (1.31) are combined together to give the equation as

$$K\nabla^2 T + \rho\dot{Q} = \rho c_e \ddot{T} + \gamma T_0 \ddot{e_{kk}} \tag{1.32}$$

Here K(>0) is a material constant.

B. **Green and Naghdi (G-N) model II (without energy dissipation)**

1. **Modified energy equation :**

$$-q_{i,i} + \rho Q = \rho c_e \dot{T} + \gamma T_0 \dot{e_{kk}} \tag{1.33}$$

2. **Heat conduction law :**

$$q_i = -K^* \nu_{,i}, \dot{\nu} = T, \tag{1.34}$$

where ν is the thermal displacement.
Equations (1.33) and (1.34) are combined together to give the equation as

$$K^*\nabla^2 T + \rho\dot{Q} = \rho c_e \ddot{T} + \gamma T_0 \ddot{e_{kk}} \tag{1.35}$$

Here $K^*(>0)$ is a material constant. The finite thermal wave speed is equal to $\left(\frac{K^*}{\rho c_e}\right)^{\frac{1}{2}}$.

C. **Green and Naghdi (G-N) model III with energy dissipation (TEWED)**

1. **Modified energy equation :**

$$-q_{i,i} + \rho Q = \rho c_e \dot{T} + \gamma T_0 \dot{e_{kk}} \tag{1.36}$$

2. **Heat conduction law :**

$$q_i = -(KT_{,i} + K^* \nu_{,i}), \dot{\nu} = T \tag{1.37}$$

Equations (1.36) and (1.37) are combined together to give a hyperbolic equation as

$$K\nabla^2 \dot{T} + K^*\nabla^2 T + \rho\dot{Q} = \rho c_e \ddot{T} + \gamma T_0 \ddot{e_{kk}} \tag{1.38}$$

Equation (1.38) admits propagation of damped thermoelastic waves, where the damping being due to the term T in the equation.

1.1.8 Dual-Phase-Lag Model of Linear Thermoelasticity

1.1.8.1 Parabolic Thermoelasticity Theory with Dual-Phase-Lag:

Tzou's theory [146] presents a modification of ETE, replacing the Fourier law

$$\boldsymbol{q}(P,t) = -K\nabla T(P,t)$$

with an approximation of the form

$$\boldsymbol{q}(P,t+\tau_q) = -K\nabla T(P,t+\tau_T).$$

After using Taylor's expansion, the parabolic form of the above equation can be written as

$$\left(1+\tau_q\frac{\partial}{\partial t}\right)\boldsymbol{q} = -K\left(1+\tau_T\frac{\partial}{\partial t}\right)\nabla T \tag{1.39}$$

in which the temperature gradient ∇T at a precise position P of the medium at time $t+\tau_q$ corresponds to the heat flux vector $\boldsymbol{q}$ at the exact position P at time $t+\tau_T$. The constitutive relation between heat flux vector and temperature gradient has been introduced with two different phase lags, τ_T and τ_q. The phase lag of the temperature gradient can be defined as the delay time caused by the micro-structural interactions. In addition to the delay time τ_q, the phase-lag of the heat flux can be interpreted as the relaxation time of the transient thermal inertia. Here, τ_T is the phase-lag of the temperature gradient, representing the delay caused by micro-structural interactions, and τ_q is the phase-lag of the heat flux, interpreted as the relaxation time due to fast transient effects of thermal inertia. The parabolic heat conduction equation with dual-phase-lag, derived by eliminating $\boldsymbol{q}$ between equations (1.21) and (1.39), takes the form:

$$K\left(1+\tau_T\frac{\partial}{\partial t}\right)\nabla^2 T = \left(1+\tau_q\frac{\partial}{\partial t}\right)\left(\rho c_E\dot{T}+\gamma T_0\dot{e}-\rho Q\right) \tag{1.40}$$

1.1.8.2 Hyperbolic Thermoelasticity Theory with Dual-Phase-Lag:

Chandrasekharaiah [29] extends the dual-phase-lag thermoelastic model proposed by Tzou. By expanding equation (1.57) in a Taylor series up to the first-order terms in τ_T and second-order terms in τ_q, the hyperbolic thermoelasticity model is formulated as:

$$\left(\boldsymbol{q}+\tau_q\frac{\partial \boldsymbol{q}}{\partial t}+\frac{\tau_q^2}{2}\frac{\partial^2 \boldsymbol{q}}{\partial t^2}\right) = -K\left(1+\tau_T\frac{\partial}{\partial t}\right)\nabla T \tag{1.41}$$

1.1.9 Three-Phase-Lag Thermoelasticity

In the novel extension of thermoelasticity proposed by Roy Choudhuri [128], the three-phase-lag (TPL) model introduces three time parameters, namely τ_q (heat flux time lag), τ_T (temperature gradient time lag), and τ_ν (thermal displacement gradient time lag). These parameters satisfy the inequality $0 \leq \tau_\nu \leq \tau_T \leq \tau_q$. To characterize the lagging behavior using ∇v, $\boldsymbol{q}$, and ∇T as thermal displacement gradient, heat flux vector, and temperature gradient, respectively, the constitutive equation of generalized heat conduction can be expressed as:

$$\boldsymbol{q}(P, t + \tau_q) = -[K^* \nabla v(P, t + \tau_\nu) + K \nabla T(P, t + \tau_T)] \tag{1.42}$$

Here, $P(\boldsymbol{r})$ represents the point where the material volume is located at time $t + \tau_\nu$ and $t + \tau_T$, along with the heat flux flow at different instants of τ_q for a finite time $t > 0$.

Expanding the equation using Taylor's series, we obtain:

$$\boldsymbol{q} + \tau_q \frac{\partial \boldsymbol{q}}{\partial t} = -[K^* \nabla v + K \tau_T \frac{\partial}{\partial t} \nabla T + \tau_\nu^* \nabla T] \tag{1.43}$$

Here,

$$\tau_\nu^* = K + K^* \tau_\nu \text{ and } \dot{v} = T.$$

The theory's classification depends on the values of τ_q, τ_T, τ_ν, and K^*, leading to different categories:

1. **Classical Fourier's Law:** $K^* = 0$, $\tau_q = \tau_T$
2. **Lord-Shulman (L-S) Theory:** $K^* = 0$, $\tau_q = \tau$, $\tau_T = 0$ (where τ is the relaxation time)
3. **Green-Naghdi-III (G-N-III) theory:** $\tau_q = 0$, $\tau_T = 0$, $\tau_\nu = 0$
4. **Tzou's DPL model:** $K^* = 0$, $\tau_\nu = 0$.

Hyperbolic Thermoelasticity with Three-Phase-Lag

By neglecting terms above the second order of τ_q in Taylor's expansion and eliminating $-\operatorname{div} \boldsymbol{q}$, the generalized heat conduction equation reduces to:

$$K^* \nabla^2 \dot{T} + K \tau_T \nabla^2 \ddot{T} + \tau_\nu^* \nabla^2 \dot{T} = \left(1 + \tau_q \frac{\partial}{\partial t} + \frac{\partial^2}{\partial t^2} \frac{1}{2} \tau_q^2\right) F(x_1, x_2, x_3, t) \tag{1.44}$$

Where $F(x_1, x_2, x_3, t) = \left(\rho C_E \ddot{T} + \gamma T_0 \ddot{e}\right)$, and ρ, C_E, γ, T_0, and e denote density, specific heat conduction, material constant, reference temperature, and dilation, respectively.

1.1.10 Generalized Phase-Lag Theory

Zenkour [160] proposed a generalized three-phase-lag thermoelasticity model that encompasses both multi-dual-phase lag and multi-three-phase lag phenomena in a unified framework. An extension to the G-N formula is introduced by incorporating the three-phase-lag of $\boldsymbol{q}, \nabla T$, and $\nabla\vartheta$. The generalized constitutive formula for heat conduction (Fourier's law) is anticipated as

$$\boldsymbol{q}\left(P, t+\tau_q\right) = -K_{ij}\nabla T\left(P, t+\tau_T\right) - K^*_{ij}\nabla\vartheta\left(P, t+\tau_\vartheta\right) \tag{1.45}$$

where τ_ϑ represents the third relaxation time or the phase-lag of thermal displacement gradient with $0 \leq \tau_\vartheta \leq \tau_T < \tau_q$. Equation (1.45) indicates both ∇T and $\nabla\vartheta$ inclines perceived through a substantial volume located at position $P(\boldsymbol{r})$ at time $t+\tau_T$ and $t+\tau_\vartheta$ result in a heat flux $\boldsymbol{q}$ flowing at a different moment of time τ_q.

By employing Taylor's series expansion of equation (1.45) up to the multi-time-derivative and power terms in τ_q, τ_T, and τ_ϑ, one can obtain

$$\left(1+\sum_{m=1}^{M_2}\frac{\tau_q^m}{m!}\frac{\partial^m}{\partial t^m}\right)\boldsymbol{q} = -K_{ij}\left(1+\sum_{m=1}^{M_1}\frac{\tau_T^m}{m!}\frac{\partial^m}{\partial t^m}\right)\nabla T - K^*_{ij}\left(1+\sum_{m=1}^{M_1}\frac{\tau_\vartheta^m}{m!}\frac{\partial^m}{\partial t^m}\right)\nabla\vartheta \tag{1.46}$$

or

$$\left(1+\sum_{m=1}^{M_2}\frac{\tau_q^m}{m!}\frac{\partial^m}{\partial t^m}\right)\boldsymbol{q} = -\left(\sum_{m=0}^{M_1}\tau^{(m)}\frac{\partial^m}{\partial t^m}\right)\nabla T - K^*_{ij}\nabla\vartheta \tag{1.47}$$

where relations

$$\frac{\partial}{\partial t}(\nabla\vartheta) = \nabla T, \quad \tau^{(m)} = K_{ij}\frac{\tau_T^m}{m!} + K^*_{ij}\frac{\tau_\vartheta^{m+1}}{(m+1)!}, \quad m = 0, 1, 2 \tag{1.48}$$

are used. Equation (1.46) serves as an extension to the generalized heat conduction formula in the absence of any mechanical terms.

1.1.11 Fractional Order Thermoelasticity

The utilization of fractional order derivatives and integrals offers a more efficient and advantageous methodology in tackling physical problems compared to classical approaches. Classical Coupled Thermoelasticity (CTE) theory may not be well-suited for certain materials like porous materials, biological materials/polymers, or specific physical scenarios such as low temperatures or transient loading. In these cases, adopting a generalized thermoelastic or thermo-viscoelastic model based on heat conduction theory with fractional time-derivatives emerges as a more suitable and applicable alternative.

1.1.11.1 Fractional Order Thermoelasticity Model with One Relaxation Time Parameter:

Sherief [135] introduced a fractional order formula for heat conduction as

$$q_i + \tau_0 \frac{\partial^\alpha q_i}{\partial t^\alpha} = -k\nabla T, \quad 0 < \alpha \leq 1 \tag{1.49}$$

For a homogeneous and isotropic thermoelastic material, the constitutive equations are

$$\sigma_{ij} = 2\mu e_{ij} + \lambda e \delta_{ij} - \gamma(T - T_0)\delta_{ij} \tag{1.50}$$

$$k\nabla^2 T = \left(1 + \frac{\tau_0^\alpha}{\alpha!}\frac{\partial^\alpha}{\partial t^\alpha}\right)(\rho C_E \dot{T} + \gamma T_0 \dot{e} - Q), \quad 0 < \alpha \leq 1 \tag{1.51}$$

Where

$$\frac{\partial^\alpha}{\partial t^\alpha} f(x,t) = \begin{cases} f(x,t) - f(x,0), & \text{when } \alpha \to 0, \\ I^{1-\alpha}\frac{\partial f(x,t)}{\partial t}, & \text{when } 0 < \alpha < 1, \\ \frac{\partial f(x,t)}{\partial t}, & \text{when } \alpha = 1. \end{cases} \tag{1.52}$$

In the above definition, the Riemann-Liouville fractional integral operator I^α is defined as

$$I^\alpha f(t) = \frac{1}{\Gamma(\alpha)} \int_0^t (t-s)^{\alpha-1} f(s)\, ds.$$

The equation of motion is

$$\sigma_{ij,j} + F_i = \rho \ddot{u}_i, \tag{1.53}$$

1.1.11.2 Fractional Order Thermoelasticity with Two Relaxation Times:

According to Hamza et al. [55], we consider the following governing equations with two relaxation times as:
The constitutive equations are

$$\sigma_{ij} = 2\mu e_{ij} + \lambda e\delta_{ij} - \gamma(T - T_0 + \tau_1 \frac{\partial T}{\partial t})\delta_{ij} \tag{1.54}$$

The heat conduction equation with fractional derivative is

$$K\nabla^2 T = \rho C_E \left(1 + \frac{\tau_0^\alpha}{\alpha!}\frac{\partial^\alpha}{\partial t^\alpha}\right)\dot{T} + \gamma T_0 \dot{e} - Q, \quad 0 < \alpha \leq 1 \tag{1.55}$$

The equation of motion is

$$\sigma_{ij,j} + F_i = \rho \ddot{u}_i \tag{1.56}$$

1.1.12 Generalized Magneto Thermoelasticity

The study of magneto-thermoelastic interactions involves understanding the interplay among strain, temperature, and electromagnetic fields in an elastic solid. This area of research holds significant practical importance due to its diverse applications. When a solid is subjected to a load, internal motion is induced. In the presence of a strong external magnetic field (represented as $\boldsymbol{H}$), secondary electromagnetic fields arise due to this internal motion. These secondary fields, in turn, interact with the primary magnetic field. Accounting for such interactions, Maxwell's electrodynamics equations for a slowly moving thermally and electrically conducting homogeneous isotropic medium body are provided by Kaliski et al. [68, 67, 66] as follows:

$$\begin{gathered} \nabla \times \boldsymbol{h} = \boldsymbol{J} + \dot{\boldsymbol{D}}, \\ \nabla \times \boldsymbol{E} = -\dot{\boldsymbol{B}} \\ \nabla.\boldsymbol{h} = 0, \nabla.\boldsymbol{E} = 0, \\ \boldsymbol{B} = \mu_0 \left(\boldsymbol{H} + \boldsymbol{h}\right), \ \boldsymbol{D} = \varepsilon_0 \boldsymbol{E}. \end{gathered} \tag{1.57}$$

The Lorentz force is given by

$$\boldsymbol{F} = (F_1, F_2, F_3) = \mu_0 \left(\boldsymbol{J} \times \boldsymbol{H}\right). \tag{1.58}$$

where $\boldsymbol{E}$ and $\boldsymbol{h}$ denote perturbations of the electric and magnetic fields respectively, $\boldsymbol{D}$ is the electric induction, $\boldsymbol{H}$ is the total magnetic field i.e., $\boldsymbol{H} = \boldsymbol{H_0} + \boldsymbol{h}$, $\boldsymbol{E}$ is the electric current, $\boldsymbol{u}$ is the displacement vector, ε_0 and μ_0 are electric and magnetic permeability of the medium respectively.

1.2 Vector-Matrix Differential Equations with Solutions

In the course of our research, we have addressed problems related to generalized, magneto, and fractional order thermoelasticity. We employed techniques such as Laplace transform, Fourier transform and normal mode analysis to express the governing equations of various thermoelasticity models in a vector-matrix differential equation form.

Most of the thermoelasticity and generalized thermoelasticity (coupled or uncoupled) problems have been solved by using potential functions. This method is not always suitable as discussed by Dhaliwal and Sherief [33] and Sherief and Anwar [133, 134]. The boundary and initial conditions for physical problems can be effectively summarized by focusing on the directly relevant physical quantities rather than the potential function. In the context of natural variables, the solution to the physical problem is convergent, while other representations involving potential functions may not always exhibit convergence.

The alternative to the potential function approach is **State-Space approach**. This method is essentially an expansion in a series in terms of the coefficient matrix of the field variables in ascending powers and applying Caley-Hamilton theorem, which requires extensive algebra. Subsequently, we solved these equations utilizing the eigenvalue approach [78, 79]. The details of this method are discussed below.

Eigenvalue approach to solve the vector-matrix differential equation :

Type-I

Consider the vector matrix differential equation of the form:

$$\frac{d\underset{\sim}{v}}{dx} = A\underset{\sim}{v} \tag{1.59}$$

where $\underset{\sim}{v} = [v_1, v_2, \ldots..v_n]^T$ and $A = (a_{ij})\,; i, j = 1, 2, \ldots n.$
are real vector and matrix respectively.

Let

$$A = V\Lambda V^{-1} \tag{1.60}$$

where $\Lambda = \begin{bmatrix} \lambda_1 & & & 0 \\ & \lambda_2 & & \\ & & \ddots & \\ 0 & & & \lambda_n \end{bmatrix}$ is a diagonal matrix whose elements $\lambda_1, \lambda_2, \ldots\ldots \lambda_n$

are the distinct eigenvalues of A. Let $V_1, V_2, \ldots, V_n$ be the eigenvectors of A corresponding to $\lambda_1, \lambda_2, \ldots, \lambda_n$ respectively, and

$$V = \left[\ V_1,\ \ V_2, \ldots..,\ \ V_n\ \right] = (x_{ij})\,(say); i, j = 1, 2, \ldots, n$$

Substituting (1.60) in (1.59) and premultiplying by V^{-1}, we get,

$$V^{-1}\frac{dv}{dx} = \Lambda V^{-1}\underset{\sim}{v}$$

or

$$\frac{d}{dx}\left(V^{-1}\underset{\sim}{v}\right) = \Lambda\left(V^{-1}\underset{\sim}{v}\right)$$

If we define

$$y = V^{-1}\underset{\sim}{v} \tag{1.61}$$

we need to solve the equations

$$\frac{dy}{dx} = \Lambda y \tag{1.62}$$

This is a set of n decoupled differential equations. Consider the r^{th} equation, which is typical

$$\frac{dy_r}{dx} = \lambda_r y_r \tag{1.63}$$

The solution is $y_r = c_r e^{\lambda_i x}, \quad r = 1, 2, \ldots, n$

where C_r are scalars to be determined from the boundary conditions.

Since from (1.61), $v = Vy$, we write

$$\underset{\sim}{v} = \sum_{r=1}^{n} V_r y_r \tag{1.64}$$

which can be explicitly written as,

$$\begin{bmatrix} v_1 \\ v_2 \\ \vdots \\ v_n \end{bmatrix} = \begin{bmatrix} x_{11} \\ x_{21} \\ \vdots \\ x_{n1} \end{bmatrix} y_1 + \begin{bmatrix} x_{12} \\ x_{22} \\ \vdots \\ x_{n2} \end{bmatrix} y_2 + \ldots\ldots\ldots\ldots\ldots\ldots + \begin{bmatrix} x_{1n} \\ x_{2n} \\ \vdots \\ x_{nn} \end{bmatrix} y_n \tag{1.65}$$

Substituting equation (1.65) in (1.64) we get the complete solution of (1.59) in the form

$$v_r = C_1 X_{r1} e^{\lambda_1 x} + C_2 X_{r2} e^{\lambda_2 x} + \ldots\ldots\ldots.. + C_n X_{rn} e^{\lambda_n x} \quad r = 1, 2, \ldots, n \tag{1.66}$$

Type-II

Consider the vector matrix differential equation of the form :

$$\frac{d\underset{\sim}{v}}{dx} = A\underset{\sim}{v} + \underset{\sim}{f} \tag{1.67}$$

Here $f = [f_1, f_2, \ldots\ldots\ldots\ldots f_n]^T$; $f_1, f_2, \ldots, f_n$ are scalar functions of x; v and A are as defined in (1.59).

Substituting (1.60) in (1.67) and premultiplying the resulting equation by V^{-1}, we obtain

$$\begin{aligned} V^{-1}\frac{d\underset{\sim}{v}}{dx} &= \Lambda\left(V^{-1}\underset{\sim}{v}\right) + V^{-1}\underset{\sim}{f} \\ or, \quad \frac{d}{dx}\left(V^{-1}\underset{\sim}{v}\right) &= \Lambda\left(V^{-1}\underset{\sim}{v}\right) + V^{-1}\underset{\sim}{f} \end{aligned} \tag{1.68}$$

As in (1.61), substituting $y = V^{-1}\underset{\sim}{v}$, we require to solve the system of equations,

$$\frac{d\underset{\sim}{y}}{dx} = \Lambda\underset{\sim}{y} + V^{-1}\underset{\sim}{f} \tag{1.69}$$

Clearly, this equation (1.69) represents a set of n-decoupled differential equations. A typical r^{th} equation of this set may be taken as

$$\frac{dy_r}{dx} = \lambda_r y_r + Q_r, \quad Q_r = V_r^{-1} f \tag{1.70}$$

Let $V^{-1} = w_{ij}; i, j = 1, 2, \ldots, n$; then $Q_r = \sum_{i=1}^{n} \omega_{ri} f_i, r = 1, 2, \ldots, n$

The solution of this equation may be written as,

$$y_r = e^{\lambda_r x}\left[y_r e^{-\lambda_r x}\right]_{x_o} + e^{\lambda_r x}\int_{x_o}^{x} Q_r e^{-\lambda_r x} dx \tag{1.71}$$

As in (1.67), the complete solution can now be written as,

$$\underset{\sim}{v} = \sum_{r=1}^{n} V_r y_r \tag{1.72}$$

Type-III (a)

Consider the differential equation in the form :

$$L\underset{\sim}{v} = A\underset{\sim}{v}, \; L = \frac{d^2}{dx^2} + \frac{1}{x}\frac{d}{dx} - \frac{n^2}{x^2} \tag{1.73}$$

This operator L is of frequent occurrence in problems on cylinders. Substituting (1.59) in (1.73) and premultiplying by V^{-1}, we get

$$Ly = \Lambda y, \quad y = V^{-1}\underset{\sim}{v} \tag{1.74}$$

as a system of decoupled equations. A typical r^{th} equation of (1.74) is

$$\begin{aligned} & Ly_r = \lambda_r y_r \\ \text{or,} & \frac{d^2 y_r}{dx^2} + \frac{1}{x}\frac{dy_r}{dx} - \left(\lambda_r + \frac{n^2}{x^2}\right) y_r = 0 \end{aligned} \tag{1.75}$$

Case (i)

When $\lambda_r = \alpha_r^2$, the solution of equation (1.75) can be written as

$$y_r = A_r K_n(\alpha_r X) + B_r I_n(\alpha_r X), \tag{1.76}$$

n is integer and A_r, B_r are constants. K_n, I_n are modified Bessel functions of the second and first kinds of order n.

Case (ii)

When $\lambda_r = -\alpha_r^2$, the solution can be written as

$$y_r = A_r J_n(\alpha_r X) + B_r Y_n(\alpha_r X), \tag{1.77}$$

n is integer, J_n, Y_n are Bessel functions of the first and second kinds of order n.

Hence the complete solution in this case can be written as $v = \sum_{r=1}^{n} V_r y_r$, the explicit form of which is given as in equation (1.72).

Type-III (b)

We often encounter problems on a spherical body in which we have to consider a differential equation of the form :

$$L\underset{\sim}{v} = A\underset{\sim}{v}, \quad L = \frac{d^2}{dr^2} + \frac{2}{r}\frac{d}{dr} - \frac{2}{r^2} \tag{1.78}$$

Substituting (1.59) in (1.78) and premultiplying the resulting equation by V^{-1}, we get

$$Ly = \Lambda\underset{\sim}{y}, \quad \text{where} \quad \underset{\sim}{y} = V^{-1}\underset{\sim}{v} \tag{1.79}$$

as a system of uncoupled equations. A typical p^{th} equation in (1.79) can be taken as

$$Ly_p = \lambda_p y_p \tag{1.80}$$

which in explicit form can be written as

$$(\frac{d^2}{dr^2} + \frac{2}{r}\frac{d}{dr} - \frac{2}{r^2})y_p = 0 \tag{1.81}$$

If we take $\lambda_p = r_p^2$, then a solution of (1.80) can be written as

$$y_p = A_p \left(\frac{1}{r^2}e^{-r_p r} + \frac{r_p}{r}e^{-r_p r}\right) \tag{1.82}$$

Thus using (1.79) and (1.82) the complete solution can be written as

$$\underset{\sim}{v} = \sum_{p=1}^{n} V_p y_p \tag{1.83}$$

Type-IV

Consider the vector-matrix differential equation :

$$L\underset{\sim}{v} = A\underset{\sim}{v} + \underset{\sim}{f}, \quad L = \frac{d^2}{dx} + \frac{1}{x}\frac{d}{dx} - \frac{n^2}{x^2} \tag{1.84}$$

where $f = [f_1, f_2, \ldots, f_n]^T$ and f_1, f_2, f_n are real functions of x or constants.

Substituting (1.59) in (1.84) and premultiplying by V^{-1} we get,

$$Ly = \Lambda y + V^{-1}\underset{\sim}{f}, \quad y = V^{-1}\underset{\sim}{v} \tag{1.85}$$

which is reduced to a system of decoupled ordinary differential equations with Bessel operator as in (1.84). A typical r^{th} equation of (1.85) can be written as,

$$\begin{aligned} &Ly_r = \lambda_r y_r + Q_r, Q_r = V_r^{-1} f_r, r = 1, 2, \ldots, n \\ \text{or} \quad &\frac{d^2 y_r}{dx^2} + \frac{1}{x}\frac{dy_r}{dx} - \left(\lambda_r + \frac{n^2}{x^2}\right) y_r = Q_r \end{aligned} \tag{1.86}$$

We now proceed to write down a particular integral of (1.86) by the method of variation of parameters.

Let $u_1(x)$ and $u_2(x)$ be the two linearly independent solutions of the equation

$$\frac{d^2 y_r}{dx} + \frac{1}{x}\frac{dy_r}{dx} - \left(\lambda_r + \frac{n^2}{x^2}\right) y_r = 0 \tag{1.87}$$

A particular integral of (1.86) can be taken as

$$P.I. = -u_1 \int \frac{u_2 Q_r}{W} dx + u_2 \int \frac{u_1 Q_r}{W} dx \tag{1.88}$$

where $W = \begin{vmatrix} u_1 & u_2 \\ u_1' & u_2' \end{vmatrix}$ is the Wronskian of u_1, u_2.

Thus considering all the aspects as mentioned in III and IV, we write down the solution for y_r as,

$$y_r = A_r u_1(x) + B_r u_2(x) - u_1 \int \frac{u_2 Q_r}{W} dx + u_2 \int \frac{u_1 Q_r}{W} dx \tag{1.89}$$

Hence $y_1, y_2, \ldots.., \quad y_n$ are all determined from (1.89) and the complete solution can be determined by using the form of equation (1.84).

1.3 Numerical Inversion of the Laplace Transform

Let the Laplace transform $F(p)$ of $u(t)$ be given by

$$F(p) = \int_0^\infty e^{-pt} u(t) dt, p \geq 0 (p = \text{ transform parameter }) \tag{1.90}$$

For the Laplace inversion here we use the Zakian algorithm and Bellman method.

1.3.1 Zakian Algorithm to Obtain the Inversion of Laplace Transform:

The Zakian algorithm is one of a class of algorithms in which $f(t)$ is computed as a sum of weighted evaluations of $F(p)$:

$$f(t) = \sum_{i=1}^{N} K_i F(p_i) \tag{1.91}$$

where the values of K_i, p_i and N are dictated by a particular method. The development of Zakian's algorithm is given in Rice and Duong [124] as well as in Zakian's original article [155]. A significant feature of the derivation is the specification that the time function can be related to a finite series of exponential functions:

$$\sum_{i=1}^{N} K_i e^{\alpha_i t} \tag{1.92}$$

This significance of this specification is that Zakian's algorithm is very accurate for overdamped and slightly underdamped systems. But it is not accurate for systems with prolonged oscillations. Given $F(p)$ and a value of time t, the following equation implements Zakian's algorithm and allows us to calculate the numerical value of $f(t)$:

$$f(t) = \frac{2}{t} \sum_{i=1}^{5} REAL\left(K_i, F\left(\frac{\alpha_i}{t}\right)\right) \tag{1.93}$$

Zakian's algorithm is simple to implement and is quickly computed. But note that the initial value, $f(t)$ at $t = 0$, cannot be computed. Also, when there are oscillatory systems, $f(t)$ becomes inaccurate after approximately the second cycle. Table 1.1 gives the set of five complex constants for α_i and for K_i as in Zakian [155].

i	α_i	K_i
1	$12.83767675 + \boldsymbol{i}1.666063445$	$-36902.08210 + \boldsymbol{i}196990.4257$
2	$12.22613209 + \boldsymbol{i}5.012718792$	$+61277.02524 - \boldsymbol{i}95408.62551$
3	$10.93430308 + \boldsymbol{i}8.409673116$	$-28916.56288 + \boldsymbol{i}18169.18531$
4	$8.776434715 + \boldsymbol{i}11.92185389$	$+4655.361138 - \boldsymbol{i}1.901528642$
5	$5.225453361 + \boldsymbol{i}15.72952905$	$-118.7414011 - \boldsymbol{i}141.3036911$

Table 1.1: Set of Five Constants for α_i and K for the Zakian Method

1.3.2 Numerical Inversion of the Laplace Transforms using Bellman Method:

To avoid complexity of the inversion of Laplace-Fourier transform in space-time domain, an efficient computer programme has been developed for numerical computation for physical variables like stress, strain, temperature by using Method of Bellman et. al where we have taken the roots(t_i) of Legendre Polynomial of degree 7 as the seven values of time (t=t_i, i=1...7, where t_1=0.025775, t_2=0.138382, t_3=0.352509, t_4=0.693147, t_5=1.21376, $t_{6=}$2.04612 and t_7=3.67119). Also, Inverse Fourier Transforms are calculated numerically by infinite integral using seven point Gaussian quadrature formulas for different values of Space variables.

We assume that $u(t)$ is sufficiently smooth to permit the approximate method we employ. Putting

$$x = e^{-t} \tag{1.94}$$

in equation (1.90) we get,

$$F(p) = \int_0^1 x^{p-1} g(x)\, dx \tag{1.95}$$

where,

$$\mathrm{u}(-\log x) = g(x) \tag{1.96}$$

Applying the Gaussian quadrature formula in (1.95) we get

$$\sum_{i=1}^{N} w_i {x_i}^{p-1} g(x_i) = F(p) \tag{1.97}$$

Where x_i are the roots of the shifted Legendre polynomial $p_N(x) = 0$ and $w_i(x)$ are the corresponding coefficients. Thus x_i and w_i are known. The equation (1.97) can be written as

$$w_1 {x_1}^{p-1} g(x_1) + w_2 {x_2}^{p-1} g(x_2) + \ldots\ldots\ldots + w_N {x_N}^{p-1} g(x_N) = F(p) \tag{1.98}$$

We now put $p = 1, 2, \ldots\ldots N$ in equation (1.98), and as such the resulting equations become

$$\begin{aligned}
&w_1 g(x_1) + w_2 g(x_2) + \ldots\ldots + w_N g(x_N) = F(1)\\
&w_1 x_1 g(x_1) + w_2 x_2 g(x_2) + \ldots + w_N x_N g(x_N) = F(2)\\
&\ldots\ldots\ldots\ldots\ldots\ldots\ldots\ldots\ldots\ldots\ldots\ldots\ldots\ldots\ldots\ldots\\
&\ldots\ldots\ldots\ldots\ldots\ldots\ldots\ldots\ldots\ldots\ldots\ldots\ldots\ldots\ldots\ldots\\
&w_1 {x_1}^{N-1} g(x_1) + w_2 {x_2}^{N-1} g(x_2) + \ldots\ldots + w_N {x_N}^{N-1} g(x_N) = F(N)
\end{aligned} \tag{1.99}$$

The solution of unknowns $g(x_i)$ can be written as

$$\begin{bmatrix} g(x_1)\\ g(x_2)\\ .\\ .\\ .\\ g(x_N) \end{bmatrix} = \begin{bmatrix} w_1 & w_2 \ldots\ldots\ldots w_N\\ w_1 x_1 & w_2 x_2 \ldots\ldots w_N x_N\\ & . \quad . \quad .\\ & . \quad . \quad .\\ w_1 x_1 & w_2 x_2 \ldots\ldots w_N x_N \end{bmatrix}^{-1} \begin{bmatrix} F(1)\\ F(2)\\ .\\ .\\ F(N) \end{bmatrix} \tag{1.100}$$

The inverted matrix in the above equation is readily available in Bellman [19].

Hence $g(x_1), g(x_2), \ldots\ldots\ldots, g(x_N)$ are evaluated by solving the above system.

Now $\mathrm{u}(-\log x_1) = g(x_1), \mathrm{u}(-\log x_2) = g(x_2), \ldots\ldots, \mathrm{u}(-\log x_N) = g(x_N)$. For $N = 7$, we get

Roots of the shifted Legendre polynomial x_i	$\mathrm{u}(-\log x_i) = g(x_i)$
$x_1 = -0.94910791$	3.671194951
$x_2 = -0.74153119$	2.046127431
$x_3 = -0.40584515$	1.213762484
$x_4 = 0$	0.69314718
$x_5 = 0.40584515$	0.352508528
$x_6 = 0.74153119$	0.138382
$x_7 = 0.94910791$	0.025775394

Table 1.2: Roots of the Legendre polynomial

CHAPTER 2

Generalized Thermoelasticity

Problems

- Problem-1: ***A Study on Fractional Order Thermoelastic Half Space.***
- Problem-2: ***Two-Dimensional Dual-Phase-Lag Thermoelastic Problem in a Half-Space Medium Subjected to a Heat Source.***

2.1 Problem-1

A Study on Fractional Order Thermoelastic Half Space*

2.1.1 Introduction

In 1956, Biot [20] developed the dynamical coupled theory of thermoelasticity (CTE), which predicts an infinite speed of heat transportation in an elastic medium. To remove that type of pardox and predict finite speed propagation for heat propagation, the modified generalized thermoelastic theories have been developed by Lord and Shulman [85](LS model) and later Green and Naghdi [49, 50, 51](GN models I,II,III). Lord and Shulman try to remove the paradox of infinite velocity of thermal disturbances inherent in the CTE. They use a wave-type heat conduction law instead of classical Fourier law and include a single relaxation time. Dhaliwal and Sherief [33] extended the theory, introducing the anisotropic case. In 1972, Green and Lindsay [46] introduced two relaxation time parameters and modified the energy equation and constitutive equations in a theory of generalized thermoelasticity. Abel [6] first introduced fractional derivatives in the solution of integral equation that arises in the tautochrone problem. Fractional calculus was successfully used to modify many mathematical models in the field of solid mechanics.

Kimmich [74] considered anomalous diffusion and characterised it by the time-fractional diffusion wave equation using Riemann-Lioville fractional integral. Cattaneo [25] introduced a law of heat conduction by modifying the classical Fourier law in the form

$$q_i + \tau_0 \frac{\partial^\alpha q_i}{\partial t^\alpha} = -k\nabla \mathrm{T}. \tag{2.1}$$

However, Youssef and Al-lehaibi [153] introduced another formula for heat conduction as

$$q_i + \tau_0 \frac{\partial q_i}{\partial t} = -kI^{\alpha-1}\nabla \mathrm{T}, 0{<}\alpha{\leq}1 \tag{2.2}$$

In the above equation, the Riemann-Liouville fractional integral operator I^α is defined as:

$$I^\alpha \mathrm{f}\,(\mathrm{t}) = \frac{1}{\Gamma(\alpha)} \int_0^{\mathrm{t}} (\mathrm{t}-\tau)^{\alpha-1} \mathrm{f}(\tau)\mathrm{d}t, 0{<}\alpha{\leq}1 \text{ and } I^0 \mathrm{f}\,(\mathrm{t}) = \mathrm{f}\,(\mathrm{t})$$

*Published in Int. J. of Applied Mechanics and Engineering, 2020, vol. 25, no. 4, pp. 191-202

and α is the fractional order parameter. The author also proved the uniqueness theorem and, using the state-space approach, presented one- and two-dimensional applications without any heat source term in the energy equation.

We consider a one-dimensional problem for a half-space in the context of the Lord and Shulman model with a heat source in fractional ordered generalized thermoelasticity. We have applied the eigenvalue approach and Laplace transform with numerical inversion. The obtained results are also presented graphically.

2.1.2 Nomenclature

λ, μ	Lame's constants
ρ	Density
τ_0	Relaxation times
T	Temperature
T_0	Reference temperature
k	Thermal conductivity
σ_{ij}	Components of stress tensor
e_{ij}	Components of strain tensor
u_i	The displacement components
α_T	The thermal expansion coefficient
C_E	Specific heat
q_i	Heat flux components
δ	Thermal viscosity
V	Longitudinal wave speed
v	Velocity of the heat source
γ	$\alpha_T(3\lambda + 2\mu)$, Volume coefficient of thermal expansion
ϵ	$\frac{\gamma}{\rho C_E}$, Dimensionless coupling constant

2.1.3 Basic Equations and Formulation of the Problem

We consider a homogeneous,isotropic, thermoelastic conducting solid that is unstressed and unstrained initially and subjected to an instantaneous heat source. We consider the problem in half-space region $R = \{x : 0 \leq x < \infty\}$. The problem is to determine the subsequent distribution of temperature and deformation fields with regard to the conductivity of the medium.

Now the basic heat equation is

$$kI^{\alpha-1}T_{,ii} = \left(\frac{\partial}{\partial t} + \tau_0\frac{\partial^2}{\partial t^2}\right)(\rho C_E T + \gamma T_0 e) - \rho Q - \rho\tau_0\dot{Q} \tag{2.3}$$

The constitutive equation takes the form

$$\sigma_{ij} = 2\mu e_{ij} + \lambda e_{kk}\delta_{ij} - \gamma T\delta_{ij} \tag{2.4}$$

The equation of motion without body forces takes the form

$$\sigma_{ij,j} = \rho\ddot{u}_i \tag{2.5}$$

For a one-dimensional medium, we assume that

$$u_x = u(x,t), u_y = u_z = 0 \tag{2.6}$$

The strain component in the form

$$e = \frac{\partial u}{\partial x} \tag{2.7}$$

Hence, the heat equation, the equation of motion, and the constitutive equation may be written as, respectively,

$$kI^{\alpha-1}\frac{\partial^2 T}{\partial t^2} = \left(\frac{\partial}{\partial t} + \tau_0\frac{\partial^2}{\partial t^2}\right)(\rho C_E T + \gamma T_0 e) - \rho\left(1 + \tau_0\frac{\partial}{\partial t}\right)Q \tag{2.8}$$

$$(\lambda + 2\mu)\frac{\partial^2 u}{\partial x^2} - \gamma\frac{\partial T}{\partial x} = \rho\frac{\partial^2 u}{\partial x^2} \tag{2.9}$$

$$\sigma_{xx} = (\lambda + 2\mu)\frac{\partial u}{\partial x} - \gamma T \tag{2.10}$$

The following non-dimensional variables are used as follows:

$$\theta = \frac{T - T_0}{T_0}, x' = V\delta x, u' = V\delta u, t' = V^2\delta t, \tau_0' = V^2\delta\tau_0, \sigma_{xx}' = \frac{\sigma_x}{\mu},$$
$$Q' = \frac{\rho Q}{kT_0V^2\delta^2}, \text{where} \quad V^2 = \frac{\lambda + 2\mu}{\rho}, \beta^2 = \frac{\lambda + 2\mu}{\mu}, b = \frac{\gamma T_0}{\mu}, g = \frac{\gamma}{\rho C_E}, \delta = \frac{\rho C_E}{k}.$$

Therefore, the equations (2.8-2.10) becomes

$$I^{\alpha-1}\frac{\partial^2\theta}{\partial t^2} = \left(\frac{\partial\theta}{\partial t} + \tau_0\frac{\partial^2\theta}{\partial t^2}\right) + g(\frac{\partial^2\theta}{\partial x\partial t} + \tau_0\frac{\partial^3\theta}{\partial x\partial t^2}) - \rho\left(1 + \tau_0\frac{\partial}{\partial t}\right)Q \tag{2.11}$$

$$\beta^2\frac{\partial^2 u}{\partial x^2} - b\frac{\partial\theta}{\partial x} = \beta^2\frac{\partial^2 u}{\partial t^2} \tag{2.12}$$

$$\sigma = \beta^2\frac{\partial u}{\partial x} - b(1 + \theta) \tag{2.13}$$

The half-space R is subjected to an instantaneous heat source, representing its energy continuously along positive direction of x-axis with a constant velocity. So the heat source is taken as $Q = Q_0\delta(x - vt)$, where Q_0 is constant of heat sources and $\delta(.)$ is the Dirac delta function.

2.1.4 Solution

Using the Laplace transform defined for any function $f(t)$ as follows

$$\overline{f}(x,s) = \int_0^\infty f(x,t)e^{-st}dt$$

where s is the transform parameter such that Re(s)>0 and applying both sides of equations (2.11-2.13) and assuming that $u, \frac{\partial u}{\partial t}, \theta, \frac{\partial \theta}{\partial t}$ are equals to zero.
Therefore, the equations (2.11-2.13) becomes

$$\overline{\sigma} = \beta^2 \frac{\partial^2 \overline{u}}{\partial x^2} - b(1+\overline{\theta}) \tag{2.14}$$

$$\frac{d^2\overline{u}}{dx^2} = s^2\overline{u} + a\frac{d\overline{\theta}}{dx} \tag{2.15}$$

$$\frac{d^2\overline{\theta}}{dx^2} = s^\alpha\ (1+\tau_0 s)\,\overline{\theta} + \ gs^\alpha\ (1+\tau_0 s)\,\frac{d\overline{u}}{dx} - \frac{Q_0 s^{\alpha-1}\ (1+\tau_0 s)e^{-\frac{sx}{v}}}{v} \tag{2.16}$$

where $a = \frac{b}{\beta^2}$.

Equations (2.15-2.16) can be written in the form of a vector-matrix differential equation using Lahiri *et al.* [79] as follows:

$$\frac{d\overline{z}}{dx} = A\overline{z} + \overline{f} \tag{2.17}$$

where

$$\overline{z} = (\overline{\theta},\overline{u}, \frac{d\overline{\theta}}{dx}, \frac{d\overline{u}}{dx})^T, \tag{2.18}$$

$$A = \begin{bmatrix} 0 & 0 & 1 & 0 \\ 0 & 0 & 0 & 1 \\ a_{31} & 0 & 0 & a_{34} \\ 0 & a_{42} & a_{43} & 0 \end{bmatrix} \tag{2.19}$$

$$\overline{f} = (f_1, f_2, f_3, f_4)^T \tag{2.20}$$

$$f_1 = 0, \quad f_2 = 0, \quad f_3 = -\frac{Q_0 s^{\alpha-1}\ (1+\tau_0 s)\,e^{-\frac{sx}{v}}}{v}, \quad f_4 = 0 \tag{2.21}$$

$$a_{31} = s^\alpha\ (1+\tau_0 s), a_{34} = gs^\alpha\ (1+\tau_0 s) \tag{2.22}$$

$$a_{42} = s^2\ , \quad a_{43} = a \tag{2.23}$$

The eigenvalues of the matrix A can be determined from the characteristic equation of the matrix A as

$$\lambda^4 - [s^\alpha(1+\tau_0 s)\,(1+ga) + s^2]\lambda^2 + s^{\alpha+2}(1+\tau_0 s) = 0 \tag{2.24}$$

Therefore, the coefficient matrix A has four eigenvalues, which are $\lambda_1, \lambda_2, -\lambda_1, -\lambda_2$, respectively. The solution of the equation (2.24) is

$$\lambda_i^2 = \frac{\left[s^\alpha\left(1+\tau_0 s\right)\left(1+ga\right)+s^2\right] \pm \sqrt{\left[s^\alpha(1+\tau_0 s)\left(1+ga\right)+s^2\right]^2 - 4s^{\alpha+2}(1+\tau_0 s)}}{2}, \quad i = \pm 1, \pm 2. \tag{2.25}$$

Now consider the negative eigenvalues λ_1, λ_2 of A for the physical nature of the problem. The eigenvectors of the coefficient matrix A corresponding to the eigenvalues $\lambda_1, \lambda_2, -\lambda_1, -\lambda_2$ of A, respectively, are

$$X_1 = (X)_{\lambda=\lambda_1}, \quad X_2 = (X)_{\lambda=\lambda_2}, \quad X_3 = (X)_{\lambda=-\lambda_1}, \quad X_4 = (X)_{\lambda=-\lambda_2} \tag{2.26}$$

where

$$X = [\lambda^2 - s^2, a\lambda, \lambda(\lambda^2 - s^2), a\lambda^2] \tag{2.27}$$

We define the inverse of the matrix $V = (X_1, X_2, X_3, X_4)$ as $V^{-1} = (\omega_{ij})$. for $i, j = 1, 2, 3, 4$.

The solution to the differential equation (2.17) is given by

$$\overline{z} = \sum_{i=1}^{4} X_i y_i, \tag{2.28}$$

where $y_r = C_r e^{\lambda_r x} + e^{\lambda_r x}\int_{-\infty}^{\infty} Q_r e^{-\lambda_r x}$ and $Q_r = \sum_{j=1}^{4} \omega_{rj} f_j$. Here, C_r represents arbitrary constants that are determined by boundary conditions.

Now, using equations (2.14-2.16) and (2.28), the displacement component, heat component, and stress component can be written as

$$\overline{u}(x,s) = C_1\lambda_1 e^{\lambda_1 x} + C_2\lambda_2 e^{\lambda_2 x} - aQ_1 e^{-\frac{sx}{\upsilon}}\left[\frac{\lambda_1}{\lambda_1 + \frac{s}{\nu}} + \frac{\lambda_2}{\lambda_2 + \frac{s}{\nu}}\right] \tag{2.29}$$

$$\begin{aligned}\overline{\theta}(x,s) = {} & C_1(\lambda_1^2 - s^2)e^{\lambda_1 x} + C_2(\lambda_2^2 - s^2)e^{\lambda_2 x} \\ & -Q_1 e^{-\frac{sx}{\upsilon}}\left[\frac{(\lambda_1^2 - s^2)}{\lambda_1 + \frac{s}{\nu}} + \frac{(\lambda_2^2 - s^2)}{\lambda_2 + \frac{s}{\nu}}\right]\end{aligned} \tag{2.30}$$

$$\begin{aligned}\overline{\sigma}(x,s) = {} & b[C_1 s^2 e^{\lambda_1 x} + C_2 s^2 e^{\lambda_2 x} - 1 \\ & -Q_1 e^{-\frac{sx}{\upsilon}}\left[\left(\frac{\lambda_1^2 - s^2}{\lambda_1 + \frac{s}{\nu}} + \frac{\lambda_2^2 - s^2}{\lambda_2 + \frac{s}{\nu}}\right) - \frac{s}{\nu}\left(\frac{\lambda_1}{\lambda_1 + \frac{s}{\nu}} + \frac{\lambda_2}{\lambda_2 + \frac{s}{\nu}}\right)\right]]\end{aligned} \tag{2.31}$$

where $Q_1 = -\frac{Q_0 s^{\alpha-1}(1+\tau_0 s)}{2v\lambda_1(\lambda_1^2 - \lambda_2^2)}$ and C_1, C_2 are arbitrary constants.

2.1.5 Initial and Boundary Conditions

We consider two boundary conditions for the half-space problem to obtain the coefficients C_1 and C_2 of equations (2.29-2.31).

2.1.5.1 Case-1:

(a) mechanical boundary condition is $\sigma(0,t) = 0$,
(b) thermal boundary condition is $\theta(0,t) = \theta_0 H(t)$,
where θ_0 is the constant temperature and $H(t)$ is the Heaviside unit step function. The Laplace transformed boundary conditions for $t > 0$ are

$$\overline{\sigma}(0,s) = 0, \tag{2.32}$$

$$\overline{\theta}(0,s) = \frac{\theta_0}{s}. \tag{2.33}$$

Now from equations (2.29-2.31), we get

$$C_1 = \frac{\left(\lambda_2{}^2 - s^2\right) R - M}{\left(\lambda_2{}^2 - \lambda_1{}^2\right)}, \text{ and } C_2 = \frac{M - \left(\lambda_1{}^2 - s^2\right) R}{\left(\lambda_2{}^2 - \lambda_1{}^2\right)},$$

where $R = \frac{1}{s^2} - \frac{Q_0 s^{\alpha-3}\,(1+\tau_0 s)}{2v\lambda_1(\lambda_1{}^2-\lambda_2{}^2)}\left[\left\{\frac{\left(\lambda_1{}^2-s^2\right)}{\lambda_1+\frac{s}{\nu}} + \frac{\left(\lambda_2{}^2-s^2\right)}{\lambda_2+\frac{s}{\nu}}\right\} + \frac{s}{v}\left\{\frac{\lambda_1}{\lambda_1+\frac{s}{\nu}} + \frac{\lambda_2}{\lambda_2+\frac{s}{\nu}}\right\}\right]$,
and $M = \frac{\theta_0}{s} - \frac{Q_0 s^{\alpha-1}\,(1+\tau_0 s)}{2v\lambda_1(\lambda_1{}^2-\lambda_2{}^2)}\left[\frac{\left(\lambda_1{}^2-s^2\right)}{\lambda_1+\frac{s}{\nu}} + \frac{\left(\lambda_2{}^2-s^2\right)}{\lambda_2+\frac{s}{\nu}}\right]$.

2.1.5.2 Case-2:

(a) mechanical condition is $\sigma(0,t) = 0$,
(b) thermal boundary condition is $\theta(0,t) = \begin{cases} 0, & t \le 0 \\ \theta_1 \frac{t}{t_0}, & 0 < t \le t_0 \\ \theta_1, & t > t_0 \end{cases}$
where θ_1 is a constant and t_0 is ramping time parameter.
Taking Laplace transformation of the boundary condition becomes

$$\overline{\sigma}(0,s) = 0, \tag{2.34}$$

$$\overline{\theta}(0,s) = \frac{\theta_1}{t_0}\left(\frac{1 - e^{-t_0 s}}{s^2}\right). \tag{2.35}$$

Similarly, from equations (2.29-2.31), we get

$$C_1 = \frac{\left(\lambda_2{}^2 - s^2\right) R - M}{\left(\lambda_2{}^2 - \lambda_1{}^2\right)} \; and \; C_2 = \frac{M - \left(\lambda_1{}^2 - s^2\right) R}{\left(\lambda_2{}^2 - \lambda_1{}^2\right)},$$

where $R = \frac{1}{s^2} - \frac{Q_0 s^{\alpha-3}\ (1+\tau_0 s)}{2v\lambda_1(\lambda_1{}^2-\lambda_2{}^2)} \left[\left\{ \frac{\left(\lambda_1{}^2-s^2\right)}{\lambda_1+\frac{s}{\nu}} + \frac{\left(\lambda_2{}^2-s^2\right)}{\lambda_2+\frac{s}{\nu}} \right\} + \frac{s}{v} \left\{ \frac{\lambda_1}{\lambda_1+\frac{s}{\nu}} + \frac{\lambda_2}{\lambda_2+\frac{s}{\nu}} \right\} \right]$
and $M = \frac{\theta_1}{t_0} \left(\frac{1-e^{-t_0 s}}{s^2} \right) - \frac{Q_0 s^{\alpha-1}\ (1+\tau_0 s)}{2v\lambda_1(\lambda_1{}^2-\lambda_2{}^2)} \left[\frac{\left(\lambda_1^2-s^2\right)}{\lambda_1+\frac{s}{\nu}} + \frac{\left(\lambda_2{}^2-s^2\right)}{\lambda_2+\frac{s}{\nu}} \right]$.

2.1.6 Numerical Representation

The inverse of the Laplace transform of the expressions given in equations (2.29–2.31) for displacement, temperature, and stress, respectively, in the space-time domain are very complex. So, we develop an efficient computer programme for the inversion of the Laplace transforms. We follow the method of Bellman *et al.* [19] for this inversion of the Laplace transform. The numerical computations for the field variables are performed for the time instants. $t_1 = 0.025775$, $t_2 = 0.138382$, $t_3 = 0.352509$, $t_4 = 0.693147$, $t_5 = 1.21376$, $t_6 = 2.04612$, $t_7 = 3.67119$, which are the roots of the Legendre polynomial of degree seven, vide Bellman et al. [19]. Here copper is taken as the thermoelastic material, and the taken parameters (in S.I. units) are below [151]:

$$\alpha = 7.76 \times 10^{10}\text{N/m}^2, \quad \mu = 3.86 \times 10^{10}\text{N/m}^2, \quad \tau_0 = 0.001,$$
$$T_0 = 293K, \quad k = 386\ \text{N/Ks}, \quad \alpha_T = 1.7810^{-5}\text{K}^{-1}$$
$$v = 0.08, \quad \delta = 888.6m/\text{s}^2, \quad \rho = 8954Kg/\text{m}^3, \quad \beta^2 = 4, \quad \epsilon = 0.0168.$$

2.1.7 Graphical Representation

Now we consider the obtained graphs of two cases.

2.1.7.1 Case-1:

(i) **Figure 2.4:** This figure exhibits the variation of displacement against the space variable x for $\alpha = 0.1$. The displacement u attains its maximum value near $t = t_6$ for $x = 0$ and then decreases rapidly, similar to $t = t_4$ and $t = t_2$. However, for $\alpha = 0.8$, the graph is also significant.

(ii) **Figure 2.5:** This figure shows the temperature distribution against the space variable x for $\alpha = 0.1$. It attains its maximum value near $t = t_7$ for $x = 0.2$ and then decreases rapidly. Similarly, near $t = t_5$, the figure increases up to $x = 0.2$ and then decreases towards zero. However, for $t = t_2$, the graph decreases up to $x = 0.4$; thereafter, it increases and converges to zero. At $\alpha = 0.8$, the graphs are likely similar, but their attained maximum and minimum values vary.

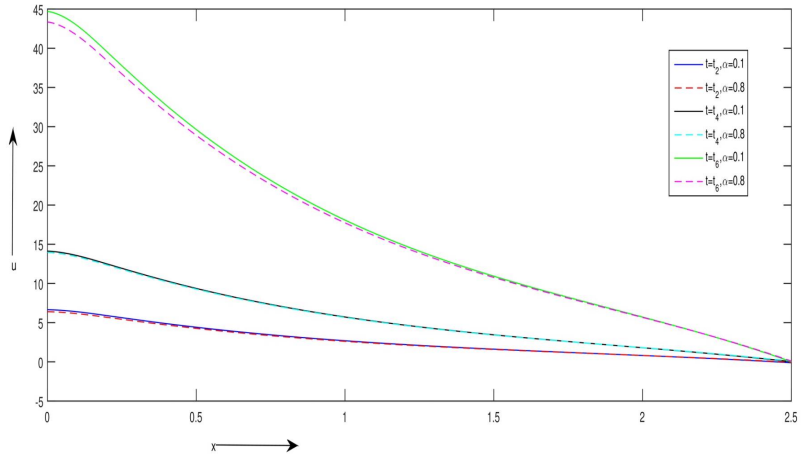

Figure 2.1: The displacement distribution u against x

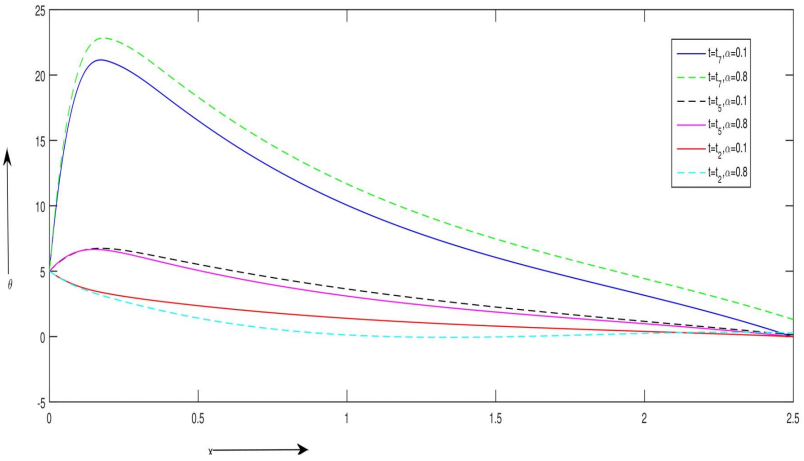

Figure 2.2: The temperature distribution against x

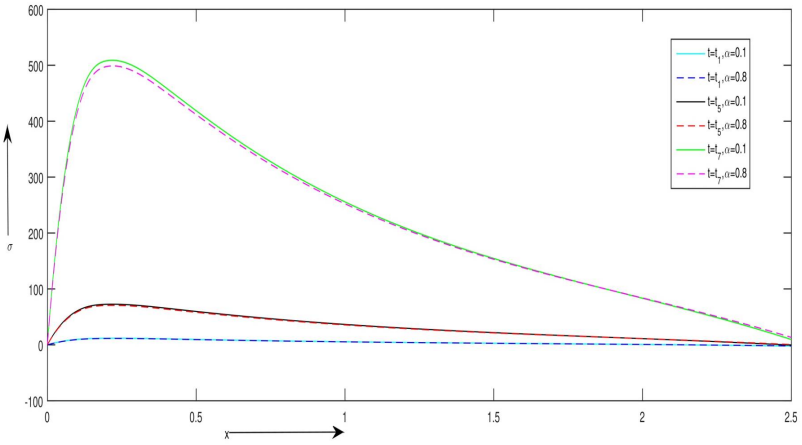

Figure 2.3: The stress distribution against x

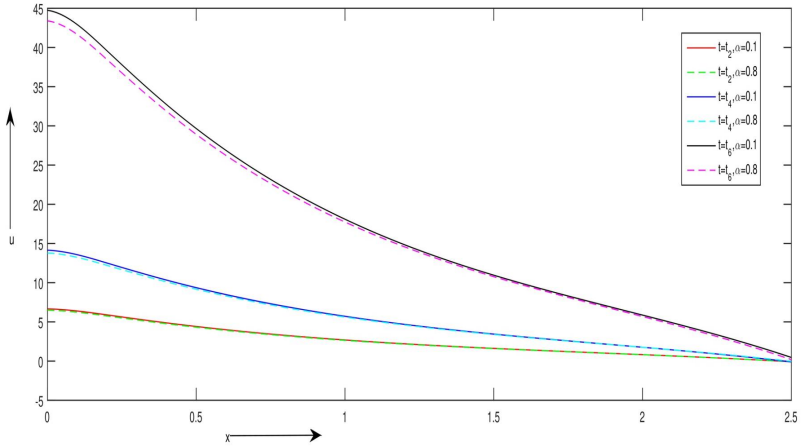

Figure 2.4: The displacement distribution against x

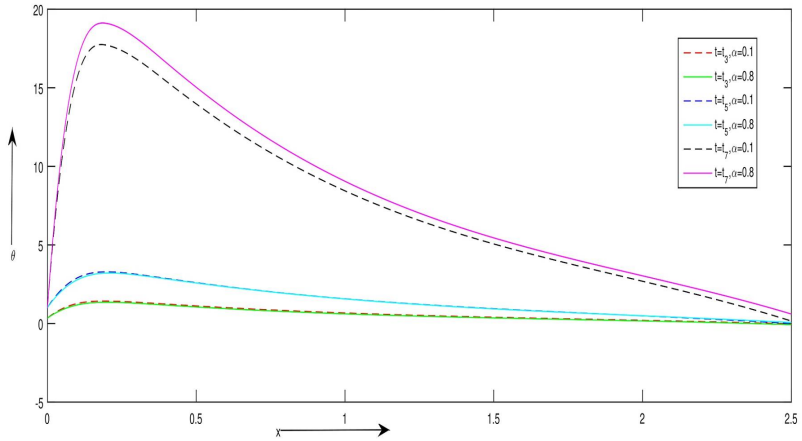

Figure 2.5: The temperature distribution against x

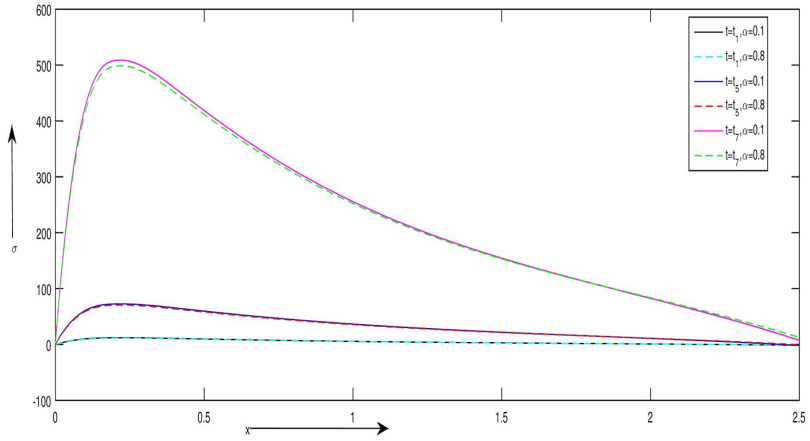

Figure 2.6: The stress distribution against x

(iii) **Figure 2.6:** This figure shows the stress distribution against the space variable x for $\alpha = 0.1$. It attains its maximum value near $t = t_7$ for $x = 0.2$ and then decreases rapidly. Similarly, for $t = t_5$ and $t = t_1$, the figure at first increases and thereafter decreases towards zero. For $\alpha = 0.8$, the graphs are likely similar, but their attained peak points and lowest points vary.

2.1.7.2 Case-2:

(iv) **Figure 2.1:** The variation of displacement against the space variable x shows differences in values for $\alpha = 0.1$ and $\alpha = 0.8$ in the range $1 \leq t \leq 7$. For $\alpha = 0.1$, the displacement u attains its maximum value near $t = t_2$, $t = t_4$, and $t = t_7$ for $x = 0$, and then decreases towards zero. For $\alpha = 0.8$, the graph also starts from the maximum values near $t = t_2$, $t = t_4$, and $t = t_7$.

(v) **Figure 2.2:** For $\alpha = 0.1$, the temperature θ increases and attains the maximum value near $t = t_7$, t_5, and t_3 for $x = 0.3$, and then decreases rapidly. However, for $\alpha = 0.8$, the graph shows different peak points.

(vi) **Figure 2.3:** This figure shows the stress distribution against the space variable x. For $\alpha = 0.1$ and $\alpha = 0.8$, the value of stress attains its maximum near $t = t_7$, t_5, and t_1 for $x = 0.2$, and thereafter decreases rapidly.

2.1.8 Conclusion

Investigating the thermoelastic solid subjected to an instantaneous heat source in the context of the fractional order theory of thermoelasticity, we can get the following information:

1. The non-dimensional temperature reaches its maximum value at the location $x = vt$ when its time is specified.

2. The magnitude of the maximum value of temperature increases as the fractional order parameter increases.

2.2 Problem-2

Two-Dimensional Dual-Phase-Lag Thermoelastic Problem in a Half-Space Medium Subjected to a Heat Source

2.2.1 Introduction

In 1956, Biot [20] introduced the coupled thermoelasticity theory (CT), which for the first time showed that heat propagation takes place in waves and predicted that heat will move at an infinitely fast rate in elastic media. Lord and Shulman (LS model) [85] developed modified generalized thermoelastic theories that remove the paradox of infinite velocity of thermal disturbances inherent in the CT model and predict finite speed propagation for heat propagation. Green and Lindsay [46] first used two relaxation time parameters and modified the energy equation and constitutive equations in a theory of generalized thermoelasticity. Later Green and Naghdi (GN-I,II,III model) [49, 50, 50] use a single relaxation time and a wave-type heat conduction law in place of classical Fourier law. Dhaliwal and Sherief [33] show the theory in the anisotropic case. Recently, Ignaczak and Ostoja-Starzewski[61] showed the finite wave speeds in thermoelasticity.

A dual-phase-lag (DPL) model of high-speed heat transportation in macroscopic formulation was proposed by Tzou [146]. Tzou's model replaces conventional Fourier's law $q = -k\nabla T$ with

$$q(P, t + \tau_q) = -k\nabla T(P, t + \tau_T) \tag{2.36}$$

in which the temperature gradient ∇T at a precise position P of the medium at time $t + \tau_q$ corresponds to the heat flux vector q at the exact position P at time $t + \tau_T$. The constitutive relation between heat flux vector and temperature gradient has been introduced with two different phase lags, τ_T and τ_q. The phase lag of the temperature gradient can be defined as the delay time caused by the micro-structural interactions. In addition to the delay time τ_q, the phase-lag of the heat flux can be interpreted as the relaxation time of the transient thermal inertia. Tzou [145] discussed the application and thermal disturbances of this theory in space. Also, Mitra et al. [91] and Tzou [147] gave experimental support for the lagging behaviour. Recently, Quintanilla [122] employed the exponential stability of dual-phase lag thermoelasticity. Using this hypothesis, Othman and Abbas [109] investigated the influence of heat loading in half-space.

Abel [6] was the first to employ fractional calculus in the tautochrone problem's solution of an integral equation. This area has grown rapidly, and applications have been found in several fields, including solid mechanics, geophysics, physics, and mathematical biology. Many mathematical models in the fields of solid mechanics, bio-rheology, nonlinear dynamical systems in ecology, and so on, have been successfully modified using fractional calculus. The fractional derivative exhibits nonlocal properties, and global dependency is among the main reasons to use it. Kimmich [74] considered anomalous diffusion and characterised it by the time-fractional diffusion wave equation using the Riemann-Liouville fractional integral. Povstenko [120] demonstrated the effect of fractional heat transportation in the presence of thermal stresses. Sherief [135] introduced a fractional order formula for heat conduction as

$$q_i + \tau_0 \frac{\partial^\alpha q_i}{\partial t^\alpha} = -k\nabla T,\ 0<\alpha\leq 1 \tag{2.37}$$

Later, Youssef [153] introduced another formula for heat conduction as

$$q_i + \tau_0 \frac{\partial q_i}{\partial t} = -kI^{\alpha-1}\nabla T,\ 0<\alpha\leq 2 \tag{2.38}$$

where the Riemann-Liouville fractional integral operator is defined as

$$I^\alpha f(t) = \frac{1}{\Gamma(\alpha)} \int_0^t (t-\tau)^{\alpha-1} f(\tau) d\tau,\ 0<\alpha\leq 2,\ \text{with } I^0 f(t) = f(t) \tag{2.39}$$

Here $\Gamma(.)$ denotes the Gamma function and α is the fractional order with $0<\alpha<1$ for the weak conductivity, $\alpha=1$ for normal conductivity, and $\alpha>1$ for strong conductivity. Also, established the uniqueness theorem and provided an example of a one-dimensional model with no heat source in the energy equation. Roy and Lahiri[126] studied the effect of fractional order thermoelasticity with a heat source in half-space. Abbas and Youssef [2] considered fractional-order thermoelastic problems in porous materials. Several studies have aimed at the fractional calculus in thermoelasticity [153, 54, 53, 121, 118]. This problem can be solved using different methods, such as the state space method [152], the Eigen value approach method [109, 126], the finite element method [3], etc. The eigenvalue approach offers the advantage of directly obtaining solutions to equations in coupled form within matrix notations. This capability facilitates the application of modern control theory methodologies in addressing problems within the field of linear thermoelasticity.

We construct a two-dimensional fractional order dual-phase-lag thermoelasticity problem in a half-space medium carrying a moving heat source and also in another case shown in a stable heat source. The eigenvalue approach method is used to solve the vector matrix differential equation, which is obtained using normal mode analysis. The obtained results are also presented graphically using MATLAB programming.

Nomenclature

C_E	Specific heat
e_{ij}	Components of strain tensor
k	Thermal conductivity
T	Temperature
T_0	Reference temperature
u_i	Displacement components
q_i	Heat flux components
c_0	Longitudinal wave speed
v_0	Velocity of the heat source
α_T	Thermal expansion coefficient
δ	Thermal viscosity
λ , μ	Lame's constants
γ	$\alpha_T(3\lambda+2\mu)$, Volume coefficient of thermal expansion
ϵ	$\frac{\gamma}{\rho C_E}$, Dimensionless coupling constant
ρ	Density
τ_0	Relaxation times
σ_{ij}	Components of stress tensor
τ_q	Phase lag of heat flux
τ_T	Phase lag of temperature gradient
β	Ratio of longitudinal to shear wave speed

2.2.2 Formulation of the Problem

Following Youssef[153], Hamza et al. [55] and Tzou[146, 145], our governing equations are taken in a homogeneous, isotropic thermoelastic medium with body forces and heat source as: The constitutive equation

$$\sigma_{ij} = 2\mu e_{ij} + \lambda e_{kk}\delta_{ij} - \gamma(1 + \frac{\tau_0^\alpha}{\alpha!}D_t^\alpha)T\delta_{ij}. \tag{2.40}$$

The equation of motion with force is written as

$$\mu u_{i,jj} + (\lambda + \mu)u_{j,ji} + F_i - \gamma\left(1 + \frac{\tau_0^\alpha}{\alpha!}D_t^\alpha\right)T_{,i} = \rho\ddot{u}_i \tag{2.41}$$

The fractional-order heat conduction equation with a heat source in DPL theory

$$\begin{aligned} k(1 + \frac{\tau_\theta^\alpha}{\alpha!}D_t^\alpha)T_{,ii} = \rho C_E &\left(1 + \frac{\tau_q^\alpha}{\alpha!}D_t^\alpha + \frac{\tau_q^{2\alpha}}{2\alpha!}D_t^{2\alpha}\right)\dot{T} \\ &+ \left(1 + n\frac{\tau_q^\alpha}{\alpha!}D_t^\alpha + \frac{\tau_q^{2\alpha}}{2\alpha!}D_t^{2\alpha}\right)(\gamma T_0\dot{u}_{j,j} - \rho Q) \end{aligned} \tag{2.42}$$

We consider a two-dimensional non-dimensionalized homogeneous isotropic thermoelastic problem in a half-space medium with the presence of a heat source, which

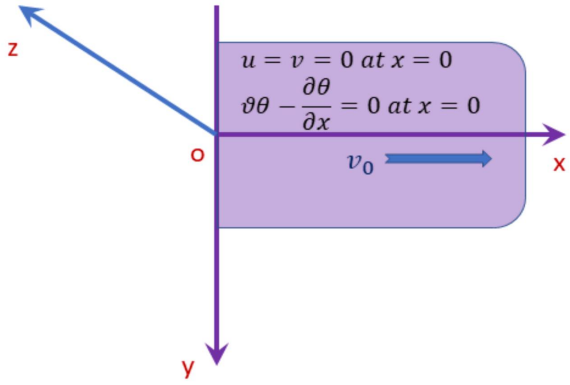

Figure 2.7: Schematic diagram

the region describes as $R = \{(x, y, z) : x \geq 0, -\infty < y < \infty, z = 0\}$ shown in Figure 2.7. In this case, t, x, and y will determine all the variables. We assume that there are no body forces, and initially, at uniform temperature T_0. Also, the displacement vectors and the temperature are all zero as x and y tend to infinity. We will use the Cartesian coordinates $(x,\ y,\ z)$ and the components of the displacement $u_i = (u, v, 0)$ to write the equations (2.40-2.42) as:

$$\begin{aligned}\left(1+\frac{\tau_\theta^\alpha}{\alpha!}D_t^\alpha\right)\left(\frac{\partial^2}{\partial x^2}+\frac{\partial^2}{\partial y^2}\right)\theta = \\ \left(1+\frac{\tau_q^\alpha}{\alpha!}D_t^\alpha+\frac{\tau_q^{2\alpha}}{2\alpha!}D_t^{2\alpha}\right)\frac{\partial\theta}{\partial t} \\ +\left(1+n\frac{\tau_q^\alpha}{\alpha!}D_t^\alpha+\frac{\tau_q^{2\alpha}}{2\alpha!}D_t^{2\alpha}\right)(\varepsilon\frac{\partial}{\partial t}(\frac{\partial u}{\partial x}+\frac{\partial v}{\partial y})-\varepsilon_4 Q)\end{aligned} \tag{2.43}$$

$$\beta^2\frac{\partial^2 u}{\partial x^2}+\frac{\partial^2 u}{\partial y^2}+(\beta^2-1)\frac{\partial^2 v}{\partial y\partial x}-\beta^2\left(1+\frac{\tau_0^\alpha}{\alpha!}D_t^\alpha\right)\frac{\partial\theta}{\partial x}=\beta^2\ddot{u} \tag{2.44}$$

$$\beta^2\frac{\partial^2 v}{\partial y^2}+\frac{\partial^2 v}{\partial x^2}+(\beta^2-1)\frac{\partial^2 u}{\partial y\partial x}-\beta^2\left(1+\frac{\tau_0^\alpha}{\alpha!}D_t^\alpha\right)\frac{\partial\theta}{\partial y}=\beta^2\ddot{v} \tag{2.45}$$

Now the stress components from Equation (2.40) take the form of

$$\sigma_{xx}=\beta^2(\frac{\partial u}{\partial x}+\frac{\partial v}{\partial y})-2\frac{\partial v}{\partial y}-\beta^2\left(1+\frac{\tau_0^\alpha}{\alpha!}D_t^\alpha\right)\theta \tag{2.46}$$

$$\sigma_{yy}=\beta^2(\frac{\partial u}{\partial x}+\frac{\partial v}{\partial y})-2\frac{\partial u}{\partial x}-\beta^2\left(1+\frac{\tau_0^\alpha}{\alpha!}D_t^\alpha\right)\theta \tag{2.47}$$

$$\sigma_{xy} = (\frac{\partial u}{\partial y} + \frac{\partial v}{\partial x}) \tag{2.48}$$

where non-dimensionalized variables are taken as

$$(x^*, y^*, u^*) = c_0\eta(x, y, u),\ (t^*, {t_0}^*, {\tau_0}^*, {\tau_q}^*, {\tau_T}^*, \upsilon^*) = {c_0}^2\eta(t, t_0, \tau_0, \tau_q, \tau_T, \upsilon),$$

$$\theta^* = \frac{\gamma}{\lambda + 2\mu}\theta, {\sigma_{ij}}^* = \frac{\sigma_{ij}}{\mu}, Q^* = \frac{\gamma Q}{(\lambda + 2\mu)K{c_0}^2\eta^2}, \beta = \sqrt{\frac{\lambda + 2\mu}{\mu}},\ \varepsilon = \frac{\gamma^2 T_0}{(\lambda + 2\mu)\rho c_E}.$$

Here $c_0 = \sqrt{\frac{\lambda+2\mu}{\rho}}$ is the longitudinal wave speed and $\eta = \frac{\rho c_E}{K}$ is the thermal viscosity. So the above equations (2.40–2.42) are written as equations (2.43-2.48) dropping the $*$ marks.

2.2.3 Solution of the Problem

The solution of the considered physical variables can be decomposed in terms of normal mode as follows:

$$(u, v, \theta, \sigma_{jk}, Q)\,(x, y, t) = \left(\overline{u}, \overline{v}, \overline{\theta}, \overline{\sigma_{jk}}, \overline{Q}\right)(x)\, e^{(\omega t + iby)};\ \mathrm{j, k = x, y}\ ; \tag{2.49}$$

where ω is a complex constant, $i = \sqrt{-1}$, and b is the wave number in the y-direction. $\overline{u}(x), \overline{v}(x), \overline{\theta}(x), \overline{\sigma_{jk}}(x), \overline{Q}(x)$ are the amplitudes of $u, v, \theta, \sigma_{ij}, Q$.

Using the above equation (2.49) in equations (2.43-2.48), we get the vector matrix differential equation as

$$\frac{d\overline{z}}{dx} = A\overline{z} + \overline{f} \tag{2.50}$$

where

$$\overline{z} = \left(\overline{u}, \overline{v}, \overline{\theta}, \frac{d\overline{u}}{dx}, \frac{d\overline{v}}{dx}, \frac{d\overline{\theta}}{dx}\right)^T \tag{2.51}$$

$$A = \begin{bmatrix} 0 & 0 & 0 & 1 & 0 & 0 \\ 0 & 0 & 0 & 0 & 1 & 0 \\ 0 & 0 & 0 & 0 & 0 & 1 \\ a_{41} & 0 & 0 & 0 & a_{45} & a_{46} \\ 0 & a_{52} & a_{53} & a_{54} & 0 & 0 \\ 0 & a_{62} & a_{63} & a_{64} & 0 & 0 \end{bmatrix} \tag{2.52}$$

and

$$\overline{f} = (0,\ 0,\ 0,\ 0,\ 0, a_{67})^T \tag{2.53}$$

Components of matrix A and $\overline{f}$ are given in Appendix-A. Let us now proceed to solve equation (2.50) by the eigenvalue approach proposed by Lahiri et al.[79]. The characteristic equation of matrix A takes the form in

$$\Lambda^6 + \overline{f_1}\Lambda^4 + \overline{f_2}\Lambda^2 + \overline{f_3} = 0 \tag{2.54}$$

Here the coefficients $\overline{f_1}$, $\overline{f_2}$, and $\overline{f_3}$ are defined in Appendix-B. Therefore, the co-efficient matrix A has six eigenvalues, which are $\pm\Lambda_j$, $j = 1, 2, 3$, respectively. The solution of the equation (2.54) is

$$\begin{gathered} {\Lambda_j}^2 = \sqrt{\omega^2\beta^2 + b^2},\ j = 1 \\ {\Lambda_j}^2 = \frac{(ad+c+\omega^2+2b^2) \pm \sqrt{(ad+c+\omega^2+2b^2)^2 - 4adb^2 + 4(\omega^2+b^2)(c^2+b^2)}}{2}, j = 2, 3 \end{gathered} \tag{2.55}$$

Now the eigenvectors of the co-efficient matrix A correspond to the eigenvalue Λ of A. be

$$\vec{X} = [\mathrm{x}_1, \mathrm{x}_2, \mathrm{x}_3, \mathrm{x}_4, \mathrm{x}_5, \mathrm{x}_6]^T \tag{2.56}$$

Here $\mathrm{x}_i, i = 1, 2, 3, 4, 5, 6$ are given in Appendix-C.
We consider the negative eigenvalues Λ_1,Λ_2,Λ_3 of A for the physical nature of the problem. The eigenvectors corresponding to the eigenvalues $\pm\Lambda_j$, $j = 1, 2, 3$ of A be are

$$\begin{gathered} X_1 = (\vec{X})_{\Lambda=\Lambda_1}, X_2 = (\vec{X})_{\Lambda=\Lambda_2}, \\ X_3 = (\vec{X})_{\Lambda=\Lambda_3}, X_4 = (\vec{X})_{\Lambda=-\Lambda_1}, \\ X_5 = (\vec{X})_{\Lambda=-\Lambda_2}, X_6 = (\vec{X})_{\Lambda=-\Lambda_3} \end{gathered} \tag{2.57}$$

We construct the inverse of the matrix.

$$V = (X_1, X_2, X_3, X_4, X_5, X_6) = (X_{ij})\ as\ V^{-1} = (\omega_{ij}),\ \ i,\ j = 1, 2, 3, 4, 5, 6 \tag{2.58}$$

Then the solution of the differential equation (2.50) is

$$\overline{z} = \sum_{j=1}^{3} X_j y_j \tag{2.59}$$

where

$$y_r = C_r e^{\Lambda_r x} + e^{\Lambda_r x} \int_{-\infty}^{\infty} Q_r e^{-\Lambda_r x}\ \ and\ Q_r = V^{-1}\overline{f} = \omega_{r6} a_{67} \tag{2.60}$$

where C_r is an arbitrary constant that is to be evaluated using initial and boundary conditions.

Hence, the solution of the equation (2.50) in the form of equation (2.59) can be written using the equation (2.49) as

$$u = e^{(\omega t + iby)} \sum_{j=1}^{3} X_{1j}(C_j e^{\Lambda_j x} - \frac{Q_j}{\Lambda_j}) \tag{2.61}$$

$$v = e^{(\omega t+iby)} \sum_{j=1}^{3} X_{2j}(C_j e^{\Lambda_j x} - \frac{Q_j}{\Lambda_j}) \tag{2.62}$$

$$\theta = e^{(\omega t+iby)} \sum_{j=1}^{3} X_{3j}(C_j e^{\Lambda_j x} - \frac{Q_j}{\Lambda_j}) \tag{2.63}$$

Using equations (2.61-2.63) and simplifying the above equations, we get the stress components as follows:

$$\sigma_{xx} = e^{(\omega t+iby)} \left(\sum_{j=1}^{3} C_j K_{1j} e^{\Lambda_j x} - E_1 \right) \tag{2.64}$$

$$\sigma_{xy} = e^{(\omega t+iby)} \left(\sum_{j=1}^{3} C_j K_{2j} e^{\Lambda_j x} - E_2 \right) \tag{2.65}$$

$$\sigma_{yy} = e^{(\omega t+iby)} \left(\sum_{j=1}^{3} C_j K_{3j} e^{\Lambda_j x} - E_3 \right) \tag{2.66}$$

where $K_{ij}, E_i, i = 1, 2, 3$ are given in Appendix-C. We will use the following boundary conditions to complete the solutions:

2.2.4 Application

2.2.5 Case-1:

We consider the problem of a half-space R with conditions
Mechanical Boundary Condition:

$$u\,(0, y, t) = v\,(0, y, t) = 0 \tag{2.67}$$

and **Thermal Boundary Condition:**

$$\upsilon\theta - \frac{\partial \theta}{\partial x} = r \ at \ x = 0. \tag{2.68}$$

Where υ is the Biot's number and r is the intensity of the heat sources.

Now using (2.49), we get

$$\overline{u}\,(0, y, t) = \overline{v}\,(0, y, t) = 0, \text{and } \upsilon\overline{\theta}(0, y, t) - \tfrac{d\overline{\theta}(0,y,t)}{dx} = r^* \tag{2.69}$$

This condition gives

$$\begin{array}{c} \sum_{j=1}^{3}(C_j - \frac{Q_j}{\Lambda_j})X_{1j} = 0, \\ \sum_{j=1}^{3}(C_j - \frac{Q_j}{\Lambda_j})X_{2j} = 0, \\ \sum_{j=1}^{3}(C_j(\upsilon - \Lambda_j) - \frac{Q_j}{\Lambda_j})X_{3j} = r^* \end{array} \tag{2.70}$$

Where X_{ij} are given in equation (2.58). Now solving the above equations (2.70) using the below process, we get the values of arbitrary constants $C_j,\ j = 1, 2, 3$ as

$$\begin{bmatrix} C_1 \\ C_2 \\ C_3 \end{bmatrix} = \begin{bmatrix} X_{11} & X_{12} & X_{13} \\ X_{21} & X_{22} & X_{23} \\ (\upsilon - \Lambda_1)X_{31} & (\upsilon - \Lambda_2)X_{32} & (\upsilon - \Lambda_3)X_{33} \end{bmatrix}^{-1} \begin{bmatrix} H_1 \\ H_2 \\ r^* + H_3 \end{bmatrix} \tag{2.71}$$

Where

$$H_i = \sum_{j=1}^{3} \frac{Q_j}{\Lambda_j} X_{ij}, i = 1, 2, 3. \tag{2.72}$$

2.2.6 Case-2:

Another boundary condition is given below to find out the arbitrary constants of the equations (2.61–2.66).

Mechanical Boundary Condition:

$$\sigma_{xx}(0, y, t) = 0, \sigma_{xy}(0, y, t) = 0 \tag{2.73}$$

and **Thermal Boundary Condition:**

$$\theta(0, y, t) = r, \text{where r is the intensity of heat source.} \tag{2.74}$$

Now using (2.49), we get

$$\begin{array}{c} \overline{\sigma_{xx}}(0, y, t) = \overline{\sigma_{xy}}(0, y, t) = 0 \\ and \ \ \overline{\theta}(0, y, t) = r^* \end{array} \tag{2.75}$$

Which gives

$$\begin{array}{c} \sum_{j=1}^{3} C_j K_{1j} = E_1 \\ \sum_{j=1}^{3} C_j K_{2j} = E_2 \\ \sum_{j=1}^{3} X_{3j}(C_j - \frac{Q_j}{\Lambda_j}) = r^* \end{array} \tag{2.76}$$

Again, solving the equation (2.76), we get the values of the arbitrary constants as

$$\begin{bmatrix} C_1 \\ C_2 \\ C_3 \end{bmatrix} = \begin{bmatrix} K_{11} & K_{12} & K_{13} \\ K_{21} & K_{22} & K_{23} \\ X_{31} & X_{32} & X_{33} \end{bmatrix}^{-1} \begin{bmatrix} E_1 \\ E_2 \\ r^* + L_3 \end{bmatrix} \tag{2.77}$$

Where $K_{1j}, K_{2j}, E_j, L_3, j = 1, 2, 3$ are given in Appendix-C. and We solve the problem numerically as below:

2.2.7 Numerical and Graphical Representation

We performed an analysis of the problem earlier. To validate the problem in physical phenomena,copper is taken as the thermoelastic material, and the parameters (in S.I. units) are given below (following Youssef[151],Mittal and Kulkarni[93]).

$$\begin{gathered}\lambda = 7.76 \times 10^{10} N/m^2, \mu = 3.86 \times 10^{10} N/m^2, \vartheta = 0.08, \delta = 888.6 ms^2, \\ \rho = 8954 Kg/m^3,\ T_0 = 293K,\ k = 386 N/Ks, \tau_T = 0.1, \tau_q = 0.15 \\ \alpha_T = 1.7 \times 10^3 Kgm^3,\ \beta^2 = 4,\ \epsilon = 0.0168,\ \ r^* = 20,\ \ b = 1.3,\ \omega = 1.2, \upsilon = 2.\end{gathered} \tag{2.78}$$

Using the above data, the temperature distribution, displacement u distribution, displacement v distribution, the stress σ_{xx} distribution, the stress σ_{xy} distribution, and the stress σ_{yy} distribution are calculated numerically and presented as graphical representations. Here we discuss the graphs with the effects of different heat sources, fractional parameters, phase lag parameters, and time.

2.2.8 Case-1:

Figure 2.8-2.13 represent the various distributions at constant time $t = 0.3$ and fixed $y = 1.0$ with different values of the fractional parameter and different values of heat source.

In the context of the dual-phase-lag model ($\tau_T = 0.1, \tau_q = 0.15$), we discuss the first four figures. In figure 1, the temperature distribution starts with a maximum value at the origin without a heat source ($Q = 0$) and a heat source ($Q = 2, 4$). As x increases, the temperature decreases towards zero. But an increase in the value of the heat source shows a decrease in temperature. For the remaining figures in case-1, Q=0 is taken to compute.

In figures 2.9 and 2.10, the displacement distributions u, v start with a minimum value of zero at the origin, where the fractional order parameter α is 0.2, 0.6, and 1.0. In all cases, up to $x = 0.6$, they increase and reach their maximum value at $x = 0.6$. After $x = 0.6$, everything gradually decreases towards zero. As the fractional order parameter α increases, the absolute values of u and v also increase.

In figure 2.11, the fractional order parameter α has significant effects on the stress distribution σ_{xx}, where an increase of α causes a decrease in the absolute values of the stress, and the rate of change of them with respect to x also increases when α increases, which is also compatible with the definition of thermal conductivity.

In figures 2.12-2.13, we take fixed α=0.6 and other constants remain the same, excluding the phase-lag parameter. The stress σ_{xy} distribution starts with negative

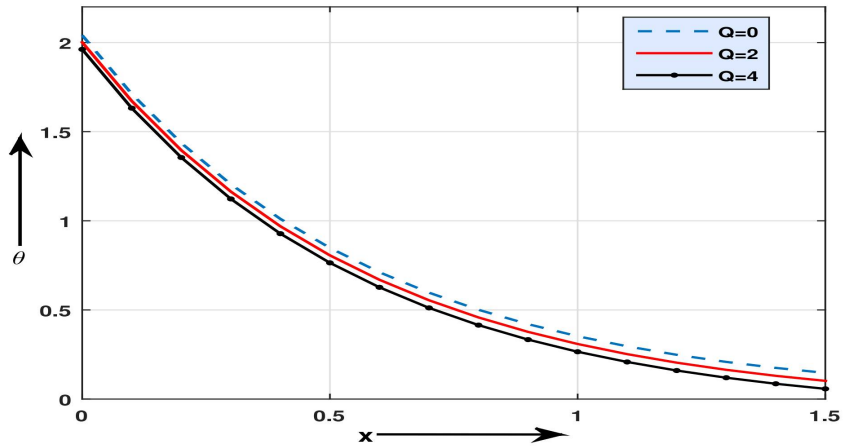

Figure 2.8: The temperature distribution with different values of the heat source.

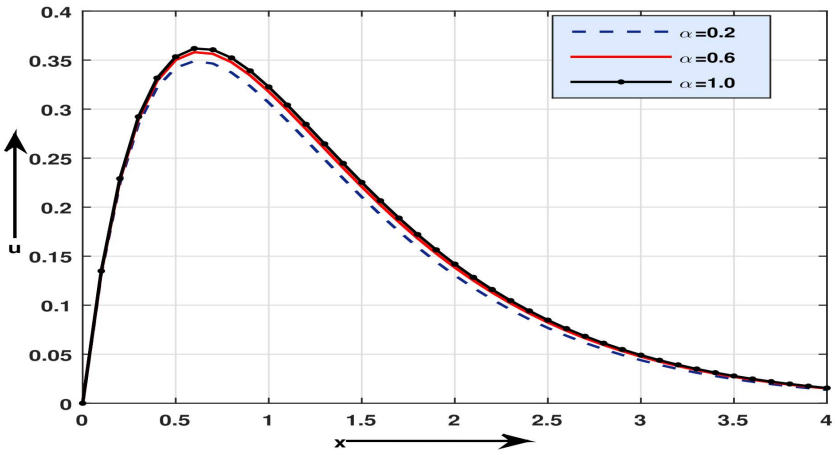

Figure 2.9: The displacement u distribution with different values of the fractional parameter.

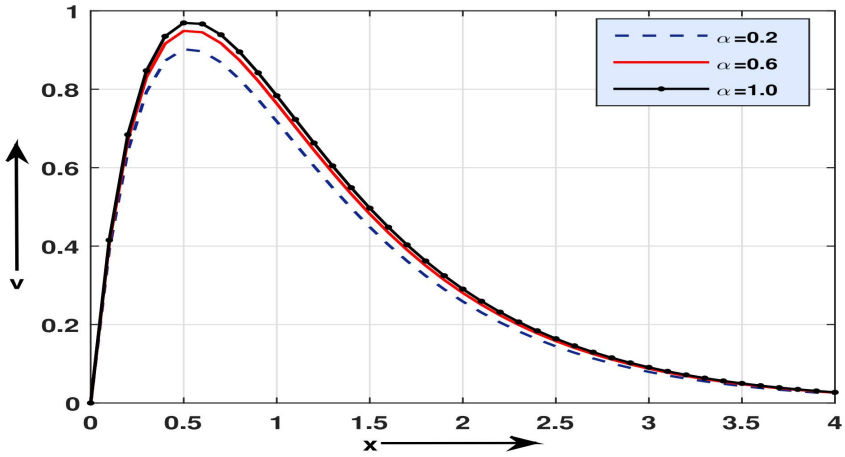

Figure 2.10: The displacement v distribution with different values of the fractional parameter.

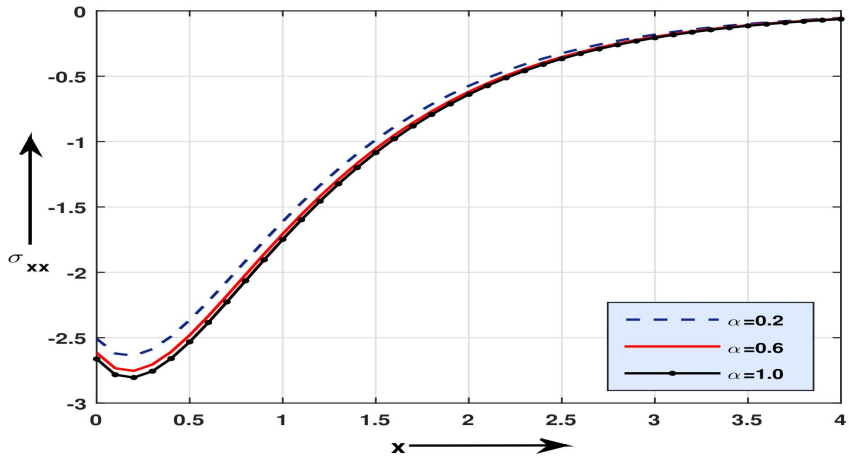

Figure 2.11: The stress σ_{xx} distribution with different values of the fractional parameter.

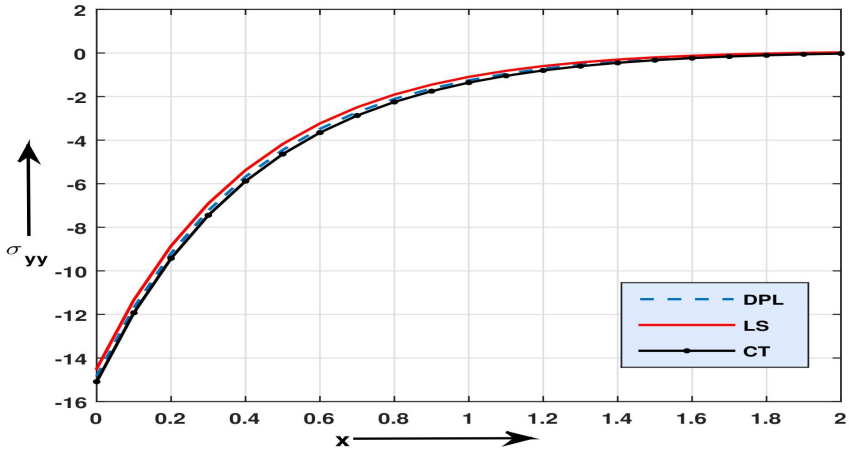

Figure 2.12: The stress σ_{yy} distribution with different values of the phase lag parameter.

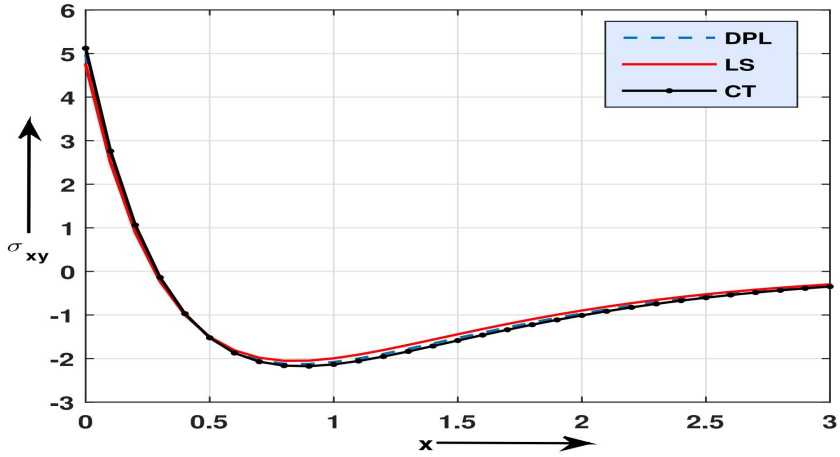

Figure 2.13: The stress σ_{xy} distribution with different values of the phase lag parameter.

value for Dual-Phase-Lag($\tau_T = 0.1$,$\tau_q = 0.15$) model, LS($\tau_T = 0$,$\tau_q = 0.15$ with ${\tau^2}_q$=0) model and CT($\tau_T = 0$,$\tau_q = 0$) theory at origin, but as x increases, the value goes towards zero. The stress σ_{yy} distribution starts with a maximum value at the initial position, but as x increases, it decreases, and after x = 0.2, it goes towards a negative value and attains a minimum value at x = 0.8. Then it increases towards zero. In both figures, the curve of the DPL model lies between the curves of the LS and CT models. Both stress distributions have a significant effect on DPL, LS, and CT theory, and for CT theory, both stress distributions take the lowest values.

2.2.9 Case-2:

We consider $\overline{Q} = Q_0 v_0$ as a moving heat source, where Q_0 is the magnitude of the heat source and v_0 is the velocity of the line heat source along the x-axis.

Figures 2.14-2.17 represent the temperature distribution, the displacement u distribution, the displacement v distribution, and the stress σ_{yy} distribution, the stress σ_{xx} distribution, and the stress σ_{xy} distribution, respectively, at constant $y = 1.0$ with different values of the fractional parameter α, phase-lag-parameter, and time. In this case, $Q_0 = 9$ and $v_0 = 3$ are taken for the representation.

We discuss DPL thermoelasticity in figures 2.14, 2.15, and 2.17 with different values of α. In figure 2.14, the fractional order parameter α has a significant effect on the temperature distribution, where increasing on α causes increasing on and the rate of change of with respect to x also increases when α increases at fixed t = 0.1.

In figure 2.15, when fractional order $\alpha = 0.6$ and time t=0.1 are fixed and other constants are the same as equation (2.78), the displacement distribution starts with negative values for DPL, LS, and CT theory. u-distribution up to x = 1.2 for LS model is greater than that of the DPL model and CT model. After x = 1.2, the result is reversed.

In figures 2.16-2.17, the fractional order parameter has significant effects on the stress σ_{xx}, σ_{xy} distribution. Both start at zero initially, which shows that they satisfy the boundary condition. Increasing the fractional parameter α causes decreasing the absolute values of the stresses, and the rate of change of them with respect to x also increases when α increases. For the fixed value of x, the stress σ_{xy}-distribution has the lowest value for the fractional parameter $\alpha = 0.2$ in the range $0 \leq x \leq 1.0$. For $x \geq 1.0$ the distribution gradually increases towards zero.

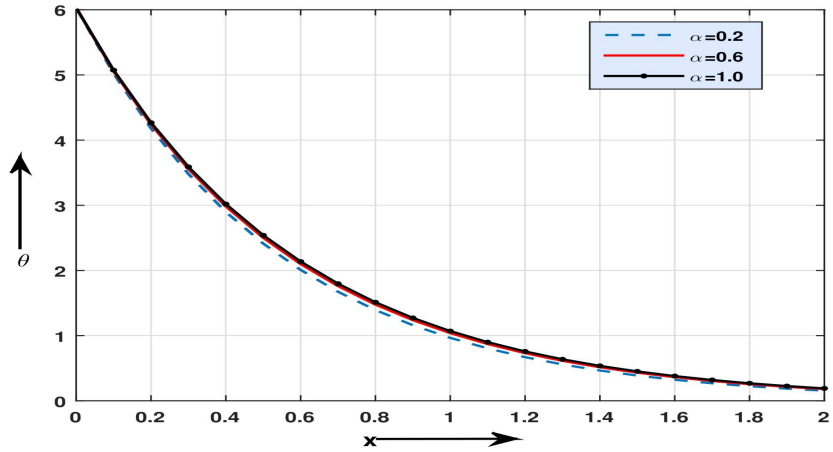

Figure 2.14: The temperature distribution with different values of the fractional parameter.

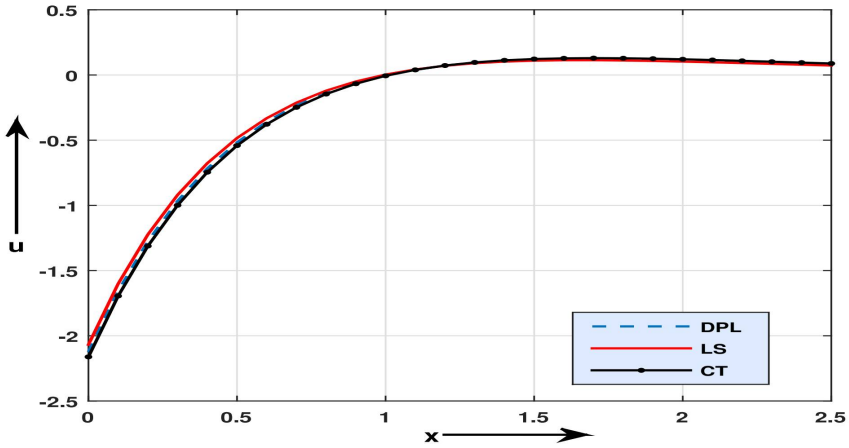

Figure 2.15: The displacement u distribution with different values of the phase-lag parameter.

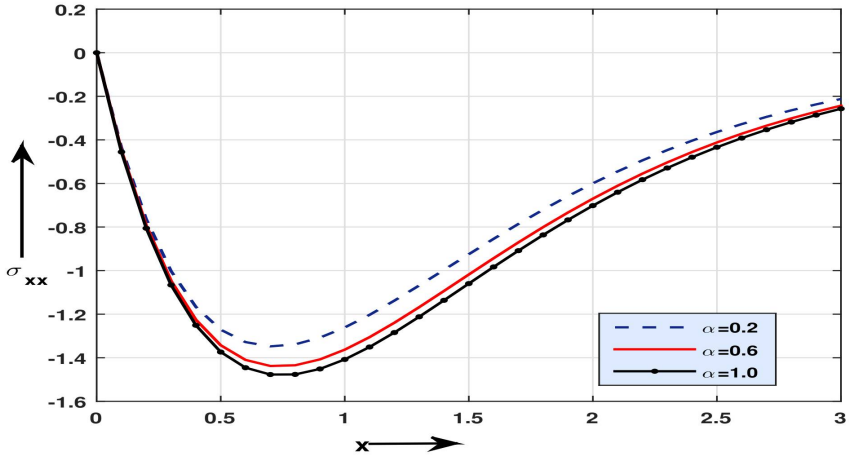

Figure 2.16: The stress σ_{xx} distribution with different values of the fractional parameter.

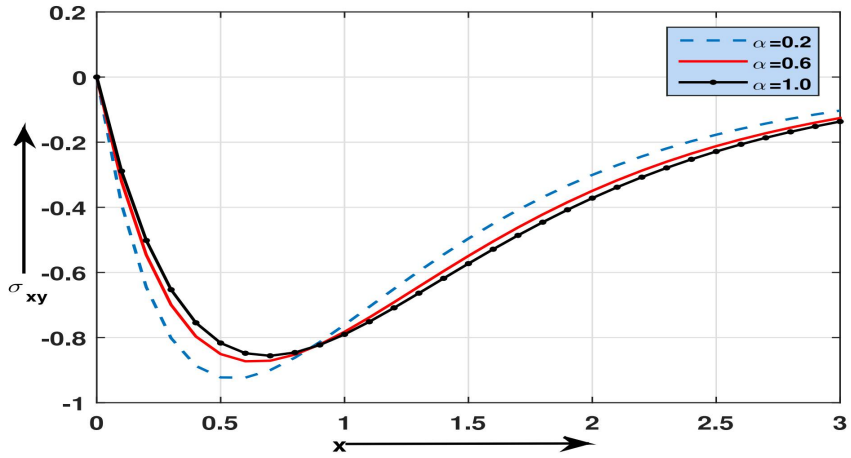

Figure 2.17: The stress σ_{xy} distribution with different values of the fractional parameter.

2.2.10 Conclusion

In this work, the effect of the heat source, fractional order, phase lag parameters, and time on the temperature distribution, displacement components, and stress components that have been studied for a two-dimensional problem in a half-space thermoelastic material is considered in the context of the fractional order generalized thermoelasticity theory carrying a heat source. The field distributions are shown graphically with the comparison of three different thermoelastic models. We found that the fractional order parameter has significant effects on all the studied fields, and the results support the definition of the classification of the thermal conductivity of the materials. We also observed significant effects of phase lag parameters when comparing the LS model, CT model, and DPL model.

2.2.11 Appendix

The components of matrix A in equation (2.49) are obtained as

$$\begin{gathered} a_{41} = \tfrac{\omega^2+b^2\beta^2}{\beta^2}, a_{45} = \tfrac{ib(1-\beta^2)}{\beta^2}, a_{46} = a; \\ a_{52} = (\omega^2+b^2)\beta^2, a_{53} = iab\beta^2, a_{54} = ib(1-\beta^2); \\ a_{62} = ibc\epsilon\omega, a_{63} = (c\omega+b^2), a_{64} = c\epsilon\omega, a_{67} = -\varepsilon_1\overline{Q}. \\ Where\ a = (1+\tfrac{\tau_0^\alpha}{\alpha!}\omega^\alpha)\ \ d = \epsilon\frac{\left(1+\frac{\tau^\alpha q}{\alpha!}\omega^\alpha+\frac{\tau^{2\alpha}q}{2\alpha!}\omega^{2\alpha}\right)}{\left(1+\frac{\tau^\alpha\theta}{\alpha!}\omega^\alpha\right)}\ ,\ c = \frac{\left(1+\frac{\tau^\alpha q}{\alpha!}\omega^\alpha+\frac{\tau^{2\alpha}q}{2\alpha!}\omega^{2\alpha}\right)}{\left(1+\frac{\tau^\alpha\theta}{\alpha!}\omega^\alpha\right)} \\ and\ \varepsilon_1 = -c\frac{\gamma}{\rho C_E(\lambda+2\mu)} \end{gathered} \tag{2.79}$$

The coefficients of various powers of Λ in Eq. (2.50) are obtained as

$$\begin{gathered}\overline{f}_1 = -a_{41} - a_{52} - a_{63} - a_{45}a_{54} - a_{46}a_{64} \\ \overline{f}_2 = a_{41}a_{52} - a_{53}a_{62} - a_{46}a_{54}a_{62} + a_{41}a_{63} + a_{52}a_{63} + a_{45}a_{54}a_{63} + a_{46}a_{52}a_{64} - a_{45}a_{53}a_{64} \\ \overline{f}_2 = a_{41}(a_{53}a_{62} - a_{52}a_{63})\end{gathered} \tag{2.80}$$

Here $\mathrm{x}_i, i = 1, 2, 3, 4, 5, 6$ are given below

$$\begin{gathered}x_1 = a_{45}a_{53}\Lambda + a_{46}\Lambda\left(\Lambda^2 - a_{52}\right), \\ \mathrm{x}_2 = a_{46}a_{54}\Lambda^2 + a_{53}\left(\Lambda^2 - a_{41}\right), \\ \mathrm{x}_3 = \left(a_{52} - \Lambda^2\right)\left(a_{41} - \Lambda^2\right) - a_{54}a_{64}\Lambda^2, \\ \mathrm{x}_4 = \Lambda\mathrm{x}_1, \quad \mathrm{x}_5 = \Lambda\mathrm{x}_2, \mathrm{x}_6 = \Lambda\mathrm{x}_3.\end{gathered} \tag{2.81}$$

$$\begin{gathered}K_{11} = \beta^2\Lambda_1 X_{11} + ib(\beta^2 - 2)X_{21} - \beta^2 a X_{31} \\ K_{12} = \beta^2\Lambda_2 X_{12} + ib(\beta^2 - 2)X_{22} - \beta^2 a X_{32} \\ K_{13} = \beta^2\Lambda_3 X_{13} + ib(\beta^2 - 2)X_{23} - \beta^2 a X_{33}\end{gathered} \tag{2.82}$$

$$\begin{gathered}K_{21} = \Lambda_1 X_{21} + ibX_{11} \\ K_{22} = \Lambda_2 X_{22} + ibX_{12} \\ K_{23} = \Lambda_3 X_{23} + ibX_{13}\end{gathered} \tag{2.83}$$

$$\begin{gathered}K_{31} = (\beta^2 - 2)\Lambda_1 X_{11} + ib\beta^2 X_{21} - \beta^2 a X_{31} \\ K_{32} = (\beta^2 - 2)\Lambda_2 X_{12} + ib\beta^2 X_{22} - \beta^2 a X_{32} \\ K_{33} = (\beta^2 - 2)\Lambda_3 X_{13} + ib\beta^2 X_{23} - \beta^2 a X_{33}\end{gathered} \tag{2.84}$$

$$\begin{gathered}E_1 = \sum_{j=1}^{3} \frac{Q_j}{\Lambda_j}(ib\left(\beta^2 - 2\right)X_{2j} - \beta^2 a X_{3j}) \\ E_2 = \sum_{j=1}^{3} ib\frac{Q_j X_{1j}}{\Lambda_j} \\ E_3 = \sum_{j=1}^{3} \frac{Q_j}{\Lambda_j}\left(ib\beta^2 X_{2j} - \beta^2 a X_{3j}\right) \\ L_3 = \sum_{j=1}^{3} \frac{Q_j X_{3j}}{\Lambda_j}\end{gathered} \tag{2.85}$$

CHAPTER 3

Generalized Thermoelasticity with Microstructure

Problems

- Problem-3: ***Multi-Phase-Lag Heat Conduction Model in a Rotating Micropolar Thermoelastic Medium with a Moving Heat Source.***
- Problem-4: ***Fractional Order Thermoelastic Model with Voids in Three-Phase-Lag Thermoelasticity.***
- Problem-5: ***Dynamic Response of Initially Stressed Microelongated Layer to Gravitational and Electromagnetic Forces.***

3.1 Problem-3

Multi-Phase-Lag Heat Conduction Model in a Rotating Micropolar Thermoelastic Medium with a Moving Heat Source.

3.1.1 Introduction

Biot [20] presented the coupled thermoelasticity theory, which combines elasticity theory with the classical Fourier law of heat transportation. In the physical domain, the transmission of heat in an elastic medium always occurs at a finite rate. However, this hypothesis falls short of guaranteeing an acceptable speed of heat transfer. To overcome the unlimited rate of heat transmission, Lord and Shulman [85] designed a novel model that uses a single relaxation time and a hyperbolic form of the energy equation instead of the standard Fourier law of heat equation. This theory automatically implies that heat and elastic waves propagate at specific speeds since the heat equation is expressed in wave form. Green and Lindsay [46] incorporated temperature rate-dependent thermoelasticity with two relaxation time parameters into the constitutive equations without violating Fourier's law of heat transportation. Both the equation of motion and the energy equation are adjusted and take on a hyperbolic form, predicting a finite rate of thermal signal. The finite speed of waves in thermoelasticity was recently shown in detail by Ignaczak and Ostoja-Starzewski [61].

The behavior of many contemporary artificial solids, such as those of the viscoelastic and polymer types, cannot be characterized by a linear thermoelasticity model because these materials have microstructures. The impact of the body's microstructure becomes considerable in the case of elastic vibrations with high frequencies and short wavelengths. This effect of microstructure results in the formation of new types of waves that are not observed in conventional elasticity theory. Thus, classical thermoelasticity theory is presently insufficient to present a complete analysis and description of the experimental results for the granular structure. Eringen [35, 36, 37] first used the term micropolar elasticity to describe such materials. Micro-rotation and macro-deformations can occur in solids under this theory, allowing both force stress and couple stress to exist in a micropolar solid. Later, Aouadi [16], Deswal and Kalkal [32] developed this theory, including the effects of temperature.

By including two-phase delays related to the heat flux vector for temperature gradients, Tzou [146, 148] constructed the two-phase delay heat equation theory. This

hypothesis is referred to as the dual-phase-lag (DPL) model. Two-phase lag parameters are related to the fastest impacts of thermal inertia. In the lagging behavior, Tzou [145] provided experimental support. Later, Roy Choudhuri [128] developed the new three-phase-lag (TPL) thermoelasticity theory. Recently, Quintanilla [122] employed the exponential stability of dual-phase-lag thermoelasticity. Tzou and Guo [149] developed a lagging technique for heat transmission theory with non-local properties. Zenkour [161] introduced the multi-phase-lag thermoelastic problem with a diffusion-type equation. Abouelregal et al. [11, 12] studied higher-order time derivatives in generalized thermoelasticity as well as micropolar thermoelasticity. Sardar et al. [130] also construed a thermoelastic problem in an anisotropic medium with multi-phase-lag thermoelasticity. Zenkour et al. [156, 157, 158, 159] illustrated the multi-phase-lag thermoelastic problem with various variables like gravity, electromagnetic, and photothermal effects. There has been a rise in interest in the issue of thermoelasticity in the context of a magnetic field for wider use in numerous sectors. Electro-magneto-thermoelasticity is used to characterize domains such as nuclear reactors, high-energy gradient fields, and physics. Das and Lahiri [31], Ghosh and Lahiri [45] solved the thermoelastic problems in the context of magneto-thermoelasticity. Biswas [21] has explored the interactions between the electromagnetic environment and the thermoelastic properties of the orthotropic medium. Because most large objects, such as the Moon, the Earth, and other planets, possess angular velocity, the Earth itself acts as a potent magnet. Studying how thermo-elastic waves spread when they encounter a magnetic field while moving through a rotating material is crucial. Kumar, Sharma, and Lata [77] investigated the effects of two temperatures and magneto-thermoelasticity due to Hall current in a transversely isotropic medium. Abouelregal [12] and Bayones et al. [18] analyzed the impact of rotation on an electromagnetic porous semiconducting medium with different thermoelastic models. Othman and Singh [106] investigated five theories and the rotational impact on micropolar thermoelasticity. Othman et al. [113] studied the effect of initial stress and gravity on a magneto-thermo-microstretch elastic medium. Othman and Abbas [4] depicted a three-phase-lag model in a micropolar thermoelastic rotating medium. Zakaria [154] discussed magneto-micropolar thermoelasticity with rotation and hall current. Abo-Dahab et al. [7] examined the outcomes for rotation, three-phase-lag, and magnetic field in a micropolar thermo-viscoelastic medium.

Most thermoelastic problems can be solved by many processes, such as (i) Potential function method: In terms of the potential function, solutions to physical issues

can be found. Initial and boundary conditions are concerned with the physical problems, not the potential function representation, which is not always stable when the physical problems have a unique and convergent solution. (ii) State-space method: The physical problem can be transformed into a matrix representation, and the coefficient matrix is expanded in series using the Cayley-Hamilton theorem. Youssef [153] used this method to solve a thermoelastic model with a moving heat source in the context of fractional thermoelasticity. (iii) Finite difference, volume, and element methods: The governing equations of the physical problem are directly expanded into the system of consistent algebraic equations. Abbas and Othman [1] depicted a comparison between the finite element method and the analytical method to solve a generalized magneto-thermoelastic problem. (iv) Eigenvalue approach method: The basic equations of the physical problem are converted into the matrix representation process, and the eigenvalue and corresponding eigenvector are extracted from the matrix of the thermoelastic problem. Othman and Abbas [109] studied the eigenvalue approach in the DPL thermoelasticity model under thermal loading due to a laser pulse. Many researchers have used the eigenvalue approach method in thermoelasticity [16, 126, 79].

In this article, the multi-phase-lag heat conduction theory is applied to two-dimensional thermoelasticity in the presence of an electromagnetic field. The normal modes transform the governing equations. Finally, using the eigenvalue approach technique in the transformed domain, the displacement component and the distribution of temperatures are determined analytically from the vector matrix differential equation.

3.1.2 Nomenclature

C_E	Specific heat
e_{ij}	Components of strain tensor
K	Thermal conductivity
T	Temperature
T_0	Reference temperature such that $\|(T - T_0)/T_0\| << 1$
$u_i, \mathbf{u}$	Displacement components
q_i	Heat flux components
c_0	Longitudinal wave speed
v_0	The velocity of the heat source
α_T	Thermal expansion coefficient
δ	Thermal viscosity
j	Micro-inertia moment
γ_T	$\alpha_T(3\lambda+2\mu+k)$, The volume coefficient of thermal expansion
λ, μ	Lame's constants
ρ	Density
τ_0, τ_1	Relaxation times
σ_{ij}	Components of stress tensor
τ_q	Phase lag of heat flux
τ_θ	Phase lag of temperature gradient
m_{ij}	The couple stress tensor
δ_{ij}	The Kronecker delta
ε_{ijk}	Permutation function
k, α, β, γ	Micropolar constants
Ω	Angular velocity
$\mathbf{E}$	Components of electric field
$\mathbf{J}$	The current density vector
μ_0	Permeability of magnetic field
ε_0	Permeability of electric field
Q	Heat source

3.1.3 Basic Equations

Following Aoudi[16] and Zenkour and El-Mekawy[161], The set of governing equations for an isotropic rotating micropolar thermoelastic medium in the appearance of an electromagnetic (Lorentz) force is provided by:

$$\sigma_{ij,j} + F_i = \rho\ddot{u}_i + (\Omega \times (\mathbf{\Omega} \times \mathbf{u}))_i + (2\mathbf{\Omega} \times \dot{\mathbf{u}})_i \tag{3.1}$$

$$m_{ij,i} + \varepsilon_{ijr}\sigma_{ir} = j\rho[\ddot{\phi} + (\Omega \times \phi)_i] \tag{3.2}$$

where $\mathbf{\Omega} = \Omega\mathbf{n}$ is the angular velocity, $\mathbf{n}$ is the unit vector along the direction of the axis of rotation, and the Lorentz force components of the form $F_i = \mu_0(\mathbf{J} \times \mathbf{H})_i$ are considered in the equation-3.1. In the presence of electromagnetic force, the medium should obey Maxwell's equation. Maxwell's equation describes the linearized electromagnetism equations for a gradually moving medium as

$$\begin{gathered} \mathbf{J} + \epsilon_0\dot{\mathbf{E}} = \vec{\nabla} \times \mathbf{h},\ \vec{\nabla} \times \mathbf{E} = -\mu_0\mathbf{h} \\ \vec{\nabla}.\mathbf{h} = 0,\ \vec{\nabla}.\mathbf{E} = 0,\ \mathbf{E} = -\mu_0(\dot{\mathbf{u}} \times \mathbf{H}). \end{gathered} \tag{3.3}$$

From the above equation (3.3), it is simple to determine the density vector of current $\mathbf{J}$ that represents displacent by removing the electric field ($\mathbf{E}$) and the magnetic field ($\mathbf{H} = \mathbf{H}_0 + \mathbf{h}$). Two extra terms have been added to the equation of motion in the rotating medium [113]: (i) the centripetal acceleration $\Omega \times (\Omega \times \mathbf{u})$ due to the time-varying motion alone, and (ii) the Coriolis acceleration $2\Omega \times \dot{\mathbf{u}}$.

The tensors of force stress and couple stress have the following components:

$$\sigma_{ij} = \mu(u_{i,j} + u_{j,i}) + \lambda u_{r,r}\delta_{ij} - k(\epsilon_{ijr}\phi_r - u_{j,i}) - \gamma_T(T - T_0 + \upsilon\frac{\partial T}{\partial t})\delta_{ij} \tag{3.4}$$

$$m_{ij} = \gamma\phi_{j,i} + \beta\phi_{i,j} + \alpha\phi_{r,r}\delta_{ij} \tag{3.5}$$

Multi-phase-lag Heat conduction in generalized thermoelasticity with heat source as:

$$\begin{aligned} K(1 + \sum_{l=1}^{L} \frac{\tau_\theta^l}{l!}\frac{\partial^l}{\partial t^l})T_{ii} = (\delta + \tau_0\frac{\partial}{\partial t} + \sum_{l=1}^{L} \frac{\tau_q^{l+1}}{(l+1)!}\frac{\partial^{l+1}}{\partial t^{l+1}})(\rho C_E\frac{\partial T}{\partial t} - \rho Q) \\ +(\delta + \tau_1\frac{\partial}{\partial t} + \sum_{l=1}^{L} \frac{\tau_q^{l+1}}{(l+1)!}\frac{\partial^{l+1}}{\partial t^{l+1}})\gamma_T T_0\frac{\partial}{\partial t}(e_{kk}) \end{aligned} \tag{3.6}$$

The relationship between strain and displacement is given below

$$e_{ij} = \frac{1}{2}(u_{i,j} + u_{ji})\, and\ e_{kk} = (\frac{\partial u}{\partial x} + \frac{\partial w}{\partial z}) \tag{3.7}$$

From the above equations, we can easily define the different definitions of thermoelasticity by changing the parameters.

i. We get Coupled thermoelasticity theory (CTE)[20] model by setting $\tau_\theta = \tau_q = \tau_0 = \upsilon = \tau_1 = 0$ and $\delta = 1$.

ii. Green-Lindsay[46] model(GL) will get if $\tau_\theta = \tau_q = \tau_1 = 0, \upsilon = \tau_0 > 0$ and $\delta = 1$.

$\tau_\theta = \tau_q = \upsilon = 0, \tau_0 = \tau_1 > 0$, and $\delta = 1$ represents the Lord-shulman[85] model(LS).

iii. By letting $N = 1, \delta = 1$and $\upsilon = 0$, $\tau_0 = \tau_1 = \tau_q \geq \tau_\theta$, this represents the simple phase lag (SPL) theory as defined by Tzou[146].

iv. By setting $L > 1, \tau_0 = \tau_1 = \tau_q$, and $\tau_\theta = \upsilon$, the definition becomes the refined multiphase thermoelasticity (RPL) theory as defined by Zenkour [156].

v. This model is confirmed as Aouadi [16] if the angular velocity term and Lorentz force term are excluded from the equations (3.1-3.2) and $\tau_q = \tau_\theta = Q = 0, \delta = 1$.

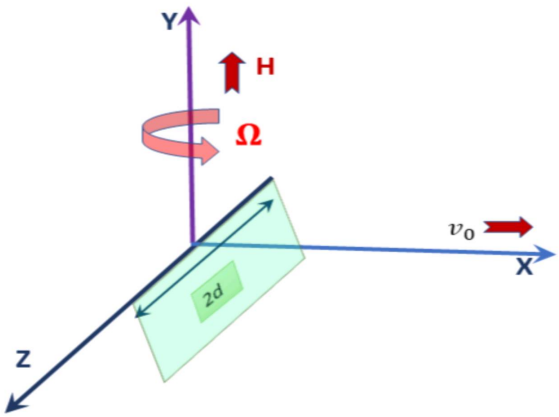

Figure 3.1: Schematic diagram

3.1.4 Formulation of the Problem

We construct a two-dimensional problem (see Figure 3.1) with initial magnetic field $\mathbf{H}_0 = (0, H_0, 0)$ in a rotating micropolar thermo-elastic semi-infinte($x \geq 0$) medium with angular velocity $\Omega = (0, \Omega, 0)$. We assume that there are body (Lorentz) forces, initially at a uniform temperature of T_0. Assume the Cartesian coordinates (x, y, z) so that the component of displacement is $\mathbf{u} = (u_1, 0, u_3), u_1 = u, u_3 = w$, and microrotation is $\phi = (0, \phi_2, 0)$. An induced magnetic field $\mathbf{h}$ and induced electrical field $\mathbf{E} = (E_1, 0, E_2)$ are produced as a result of the initial magnetic field $\mathbf{H}_0$ being applied along y-axis. So,using the equation (3.3), the components of the Lorentz force are written in the form

$$(F_1, F_2, F_3) = \mu_0 H_0^2 \left((\frac{\partial^2 u}{\partial x^2} + \frac{\partial^2 w}{\partial x \partial z}) - \varepsilon_0 \mu_0 \frac{\partial^2 u}{\partial t^2}, 0, (\frac{\partial^2 w}{\partial z^2} + \frac{\partial^2 u}{\partial x \partial z}) - \varepsilon_0 \mu_0 \frac{\partial^2 w}{\partial t^2} \right) \tag{3.8}$$

The non-dimensional variables are manipulated to simplify the equations (3.1-3.8), as below

$$\begin{gathered}
(x^*, z^*) = \frac{\eta_0}{c_0}(x, z), (t^*, \upsilon^*, \tau_0^*, \tau_1^*, \tau_\theta^*, \tau_q^*) = \eta_0(t, \upsilon, \tau_0, \tau_1, \tau_\theta, \tau_q), \\
(w^*, u^*) = \frac{\rho c_0 \eta_0}{\gamma_T T_0}(w, u), \theta^* = \frac{\theta}{T_0}, \sigma_{ij}^* = \frac{\sigma_{ij}}{\gamma_T T_0}, m_{ij}^* = \frac{\eta_0 m_{ij}}{c_0 \gamma_T T_0}, \phi_2^* = \frac{\rho c_0^2 \phi_2}{\gamma_T T_0}, \\
\Omega^* = \frac{\Omega}{\eta_0}, Q^* = \frac{Q}{\eta_0} \text{ and } c_0^2 = \frac{\mu}{\rho}, \beta = \sqrt{\frac{\lambda + 2\mu}{\mu}}, \eta_0 = \frac{\rho c_E c_0^2}{K}.
\end{gathered} \tag{3.9}$$

By using the above non-dimensional variables, we get the non-dimensional form

of equations (3.1-3.8) as follows:

$$(1+\epsilon_5)\frac{\partial^2 u}{\partial x^2}+(1-a^2+\epsilon_5)\frac{\partial^2 w}{\partial x\partial z}+a^2\frac{\partial^2 u}{\partial z^2}-\epsilon_3\frac{\partial \phi_2}{\partial z}-\frac{1}{(\epsilon_1+\epsilon_2)}(1+\upsilon\frac{\partial}{\partial t})\frac{\partial \theta}{\partial x} = (\frac{1}{\epsilon_1+\epsilon_2}+\epsilon_4)\frac{\partial^2 u}{\partial t^2}-\frac{\Omega^2}{(\epsilon_1+\epsilon_2)}u+\frac{2\Omega}{(\epsilon_1+\epsilon_2)}\frac{\partial w}{\partial t} \tag{3.10}$$

$$(1+\epsilon_5)\frac{\partial^2 w}{\partial z^2}+(1-a^2+\epsilon_5)\frac{\partial^2 u}{\partial x\partial z}+a^2\frac{\partial^2 w}{\partial x^2}-\epsilon_3\frac{\partial \phi_2}{\partial x}-\frac{1}{(\epsilon_1+\epsilon_2)}(1+\upsilon\frac{\partial}{\partial t})\frac{\partial \theta}{\partial z} = (\frac{1}{\epsilon_1+\epsilon_2}+\epsilon_4)\frac{\partial^2 w}{\partial t^2}-\frac{\Omega^2}{(\epsilon_1+\epsilon_2)}w+\frac{2\Omega}{(\epsilon_1+\epsilon_2)}\frac{\partial u}{\partial t} \tag{3.11}$$

$$\frac{\partial^2 \phi_2}{\partial x^2}+\frac{\partial^2 \phi_2}{\partial z^2}-2\epsilon_7\phi_2+\epsilon_7(\frac{\partial u}{\partial z}-\frac{\partial w}{\partial x})=\epsilon_8\frac{\partial^2 \phi_2}{\partial t^2} \tag{3.12}$$

$$(1+\sum_{n=1}^{L}\frac{\tau_\theta^n}{n!}\frac{\partial^n}{\partial t^n})(\frac{\partial^2 \theta}{\partial x^2}+\frac{\partial^2 \theta}{\partial z^2})=p_{l1}\frac{\partial \theta}{\partial t}+p_{l2}\epsilon_9\frac{\partial}{\partial t}(\frac{\partial u}{\partial x}+\frac{\partial w}{\partial z})-p_{l1}Q \tag{3.13}$$

The following form is used to represent the stress tensor and force tensor components:

$$\sigma_{xx}=(\epsilon_1+\epsilon_2)\frac{\partial u}{\partial x}+(\epsilon_1-1)\frac{\partial w}{\partial z}-(1+\upsilon\frac{\partial}{\partial t})\theta \tag{3.14}$$

$$\sigma_{xz}=\frac{\partial u}{\partial z}+\epsilon_2\frac{\partial w}{\partial x}-(\epsilon_2-1)\phi_2 \tag{3.15}$$

$$\sigma_{zx}=\frac{\partial w}{\partial x}+\epsilon_2\frac{\partial u}{\partial z}-(\epsilon_2-1)\phi_2 \tag{3.16}$$

$$\sigma_{zz}=(\epsilon_1+\epsilon_2)\frac{\partial w}{\partial z}+(\epsilon_1-1)\frac{\partial u}{\partial x}-(1+\upsilon\frac{\partial}{\partial t})\theta \tag{3.17}$$

$$m_{zy}=\frac{(\epsilon_2-1)}{\epsilon_6}\frac{\partial \phi_2}{\partial z} \tag{3.18}$$

$$m_{xy}=\frac{(\epsilon_2-1)}{\epsilon_7}\frac{\partial \phi_2}{\partial x} \tag{3.19}$$

where $\epsilon_i, i=1(1)9$ are given in Appendices, and

$$p_{l1}=(\delta+\tau_0\frac{\partial}{\partial t}+\sum_{n=1}^{L}\frac{\tau_q^{n+1}}{(n+1)!}\frac{\partial^{n+1}}{\partial t^{n+1}}), p_{l2}=(\delta+\tau_1\frac{\partial}{\partial t}+\sum_{n=1}^{L}\frac{\tau_q^{n+1}}{(n+1)!}\frac{\partial^{n+1}}{\partial t^{n+1}}).$$

For convenience,equations (3.10)-(3.19) use the above non-dimensional expression without the asteric(*) mark.

3.1.5 Normal mode analysis

Utilizing the normal mode [18], the solution of the physical quantities under investigation may be transformed as follows:

$$(\theta, w, u, m_{ij}, \sigma_{ij}, \phi_2, Q)(x, z, t) = (\bar{\theta}, \bar{w}, \bar{u}, \bar{m_{ij}}, \bar{\sigma_{jk}}, \bar{\phi_2}, \bar{Q})(x)e^{(st+iqz)}; \tag{3.20}$$

where $i = \sqrt{-1}$, s is frequency (complex constant), q is the wave number in the z-direction,and $\bar{\theta}(x), \bar{w}(x), \bar{u}(x), \bar{m_{ij}}(x), \bar{\phi_2}(x), \bar{\sigma_{ij}}(x), \bar{Q}(x)$ are the amplitude of the functions $\theta, w, u, m_{ij}, \phi_2, \sigma_{ij}, Q$ respectively.

Applying the above equation (3.20) in equations (3.10-3.13), we have a vector matrix differential equation:

$$\frac{d\overline{Y}}{dx} = A\overline{Y} + R \tag{3.21}$$

where

$$\overline{Y} = (\bar{u}, \bar{w}, \bar{\phi_2}, \bar{\theta}, \frac{d\bar{u}}{dx}, \frac{d\bar{w}}{dx}, \frac{d\bar{\phi_2}}{dx}, \frac{d\bar{\theta}}{dx})^T \tag{3.22}$$

$$A = \begin{bmatrix} 0 & 0 & 0 & 0 & 1 & 0 & 0 & 0 \\ 0 & 0 & 0 & 0 & 0 & 1 & 0 & 0 \\ 0 & 0 & 0 & 0 & 0 & 0 & 1 & 0 \\ 0 & 0 & 0 & 0 & 0 & 0 & 0 & 1 \\ a_{51} & a_{52} & a_{53} & 0 & 0 & a_{56} & 0 & a_{58} \\ a_{61} & a_{62} & 0 & a_{64} & a_{65} & 0 & a_{67} & 0 \\ a_{71} & 0 & a_{73} & 0 & 0 & a_{76} & a_{77} & 0 \\ 0 & a_{82} & 0 & a_{84} & a_{85} & 0 & 0 & 0 \end{bmatrix} \tag{3.23}$$

And

$$R = (0, 0, 0, 0, 0, 0, 0, R_8)^T \tag{3.24}$$

The appendix (3.1.10) includes a list of each element of matrix A and matrix R .

3.1.6 Solution:

To find out the solution of the equation (3.21), we use eigen value approach as [79] and [126]. Now the below equation

$$|A - \Lambda I| = 0 \tag{3.25}$$

is the characteristic equation of the matrix A, while I is the identity matrix. There are eight eigenvalues in the form $\Lambda = \pm\Lambda_i$ and $(i = 1(1)4)$. of the characteristic equation (3.25). The corresponding eigen vector $\underline{X}$ for the eigenvalue Λ obtained as

$$\underline{X} = \begin{bmatrix} \Pi_1 & \Pi_2 & \Pi_3 & \Pi_4 & \Lambda\Pi_1 & \Lambda\Pi_2 & \Lambda\Pi_3 & \Lambda\Pi_4 \end{bmatrix}^T \tag{3.26}$$

where Π_i $(i = 1(1)4)$ is given in the appendix. Now the eigenvectors related to the eigenvalues $\pm\Lambda_j$, $j = 1(1)4$ of A are written as

$$\begin{array}{ll} \Gamma_1 = (\underline{X})_{\Lambda=\Lambda_1}, & \Gamma_5 = (\underline{X})_{\Lambda=-\Lambda_1}, \\ \Gamma_2 = (\underline{X})_{\Lambda=\Lambda_2}, & \Gamma_6 = (\underline{X})_{\Lambda=-\Lambda_2}, \\ \Gamma_3 = (\underline{X})_{\Lambda=\Lambda_3}, & \Gamma_7 = (\underline{X})_{\Lambda=-\Lambda_3}, \\ \Gamma_4 = (\underline{X})_{\Lambda=\Lambda_4}, & \Gamma_8 = (\underline{X})_{\Lambda=-\Lambda_4}. \end{array} \tag{3.27}$$

We compute the inverse matrix $V^{-1} = (\omega_{ij})$, $i, j = 1(1)8$ of the matrix $V = (\Gamma_1, \Gamma_2, \Gamma_3, \Gamma_4, \Gamma_5, \Gamma_6, \Gamma_7, \Gamma_8)$. As a result, the solution to the differential equation (3.21) is

$$\overline{Y} = \sum_{j=1}^{8} \Gamma_j y_j \tag{3.28}$$

$$y_p = C_p e^{\Lambda_p x} + e^{\Lambda_p x} \int_{-\infty}^{\infty} Q_p e^{-\Lambda_p x} \; and \; Q_p = \sum_{j=1}^{8} \omega_{pj} R_j = \omega_{p8} R_8 \tag{3.29}$$

where C_p is an arbitrary constant. All the values of C_p can be assessed by using boundary and initial conditions. According to our consideration, the medium is taken as half-space medium $(x \geq 0)$. So,the field variables can be written in the following final form:

$$u = e^{(st+iqy)} \sum_{j=1}^{4} X_{1j} (C_j e^{\Lambda_j x} - \frac{Q_j}{\Lambda_j}) \tag{3.30}$$

$$w = e^{(st+iqy)} \sum_{j=1}^{4} X_{2j} (C_j e^{\Lambda_j x} - \frac{Q_j}{\Lambda_j}) \tag{3.31}$$

$$\phi = e^{(\omega t+iby)} \sum_{j=1}^{4} X_{3j} (C_j e^{\Lambda_j x} - \frac{Q_j}{\Lambda_j}) \tag{3.32}$$

$$\theta = e^{(\omega t+iby)} \sum_{j=1}^{4} X_{4j} (C_j e^{\Lambda_j x} - \frac{Q_j}{\Lambda_j}) \tag{3.33}$$

where the real part of $\Lambda_j < 0, j = 1(1)4$. Using the above equations 3.30-3.33, the simplified stress components are written as:

$$\begin{aligned} \sigma_{zx} &= e^{(\omega t+ibz)} \left(\sum_{j=1}^{4} C_j S_{1j} e^{\Lambda_j x} - M_1 \right), \\ \sigma_{zz} &= e^{(\omega t+ibz)} \left(\sum_{j=1}^{4} C_j S_{2j} e^{\Lambda_j x} - M_2 \right) \end{aligned} \tag{3.34}$$

$$\begin{aligned}
\sigma_{xz} &= e^{(\omega t+ibz)}\left(\sum_{j=1}^{4} C_j S_{3j} e^{\Lambda_j x} - M_3\right), \\
\sigma_{xx} &= e^{(\omega t+ibz)}\left(\sum_{j=1}^{4} C_j S_{4j} e^{\Lambda_j x} - M_4\right)
\end{aligned} \tag{3.35}$$

$$\begin{aligned}
m_{zy} &= e^{(\omega t+ibz)}\left(\sum_{j=1}^{4} C_j S_{5j} e^{\Lambda_j x} - M_5\right), \\
m_{xy} &= e^{(\omega t+ibz)}\left(\sum_{j=1}^{4} C_j S_{6j} e^{\Lambda_j x} - M_6\right)
\end{aligned} \tag{3.36}$$

where $X_{1j}, X_{2j}, X_{3j}, X_{4j}$,$S_{ij}$(x),$C_j$,and M_k (i=1(1)6; j=1(1)4; k=1(1)6) are given in the Appendix.

3.1.7 Initial and Boundary Condition

We consider the half-space problem with the value of initial condition as
$u = v = \phi_2 = \theta = \dot{u} = \dot{v} = \dot{\phi_2} = \dot{\theta} = 0 \;\; at \;\; t = 0$,which are used to solve the previous equations.
To evaluate the values of C_j, $j = 1, 2, 3, 4$, we consider the boundary conditions as follows:

1. **Mechanical boundary condition** as

$$\begin{aligned}
\sigma_{zz}(x, z, t) &= -F(z)H(t) \;\; at \;\; x = 0, \\
m_{xy}(x, z, t) &= \sigma_{zx}(x, z, t) = 0 \;\; at \;\; x = 0.
\end{aligned} \tag{3.37}$$

   At the origin of the coordinate system, a load called $F(z)$ is applied to the half-space medium in the direction of the normal. This is a unit strip load with width $2d$ and amplitude F_0 applied at origin. Mathematically defined as $F(z) = F_0 H(d - |z|)$ where $H(.)$ is a Heaviside function with unit step.

2. **Thermal boundary condition** as

$$\theta(x, z, t) = 0 \;\; at \;\; x = 0. \tag{3.38}$$

Now using equations (3.20) in 3.37 and 3.38, we get

$$\begin{aligned}
\bar{\sigma}_{zz}(0, z, t) &= -F_0 H(d - |z|)H(t)exp(-st - iqz) \\
\bar{m}_{xy}(0, z, t) &= \bar{\sigma}_{zx}(0, z, t) = \bar{\theta}(0, z, t) = 0
\end{aligned} \tag{3.39}$$

Now we achieve the following equations by using 3.33-3.34,3.36 in 3.37-3.38:

$$\begin{aligned}
\sum_{j=1}^{4} C_j \Lambda_j X_{3j} &= P_1 \\
\sum_{j=1}^{4} C_j S_{1j} &= P_2 \\
\sum_{j=1}^{4} C_j S_{2j} &= P_3 \\
\sum_{j=1}^{4} C_j X_{4j} &= P_4.
\end{aligned} \tag{3.40}$$

We can easily find the arbitrary constants $C_j, j = 1(1)4$ from the above equation using the inverse method of matrix as

$$\begin{bmatrix} C1 \\ C2 \\ C3 \\ C3 \end{bmatrix} = \begin{bmatrix} \Lambda_1 X31 & \Lambda_2 X32 & \Lambda_3 X33 & \Lambda_4 X34 \\ S_{11} & S_{12} & S_{13} & S_{14} \\ S_{31} & S_{32} & S_{33} & S_{34} \\ X_{41} & X_{42} & X_{43} & X_{44} \end{bmatrix}^{-1} \begin{bmatrix} P1 \\ P2 \\ P3 \\ P4 \end{bmatrix} \tag{3.41}$$

where $P_j, j = 1, 2, 3, 4$ are included in appendices.

3.1.8 Numerical and Graphical Representation

We demonstrated the analytical process earlier. We will now look at a numerical approach to validating the results. Magnesium thermoelastic material is chosen to compute the field distributions; the parameters are as follows(Abo-Dahab et al. [7]; Abouelregal [9]; Zenkour and El-Mekawy[161](in SI units)):

$$\begin{gathered}
j = 0.2 \times 10^{-19}\ \mathrm{m}^2, \mu = 4.0 \times 10^{10} \mathrm{kg\ m^{-1} s^{-2}}, \lambda = 9.4 \times 10^{10} N/m^2, \varepsilon_0 = 0.3, \\
\rho = 1.74 \times 10^3 \mathrm{kg\ m^{-3}}, T_0 = 293K,\ k = 1.0 \times 10^{10} \mathrm{kgm^{-1}\ s^{-2}}, \Omega = 0.2 \\
\alpha_t = 2.36 \times 10^{-5} \mathrm{K^{-1}}, C_E = 9.623 \times 10^2 \mathrm{Jkg^{-1} K^{-1}}, K = 2.510 \mathrm{Wm^{-1} K^{-1}}, \mu_0 = 0.1, \\
H_0 = 100, \gamma = 0.779 \times 10^{-9} \mathrm{kg\ ms^{-2}}, F_0 = 1, d = 1, \\
q = 3.5,\ s = \omega_0 + i\omega_1, \omega_0 = 2.0, \omega_1 = 0.5.
\end{gathered} \tag{3.42}$$

All the calculations were carried out in refined multi-phase-lag theory ($\tau_\theta = 0.1$, $\tau_q = \tau_0 = 0.3$, $\tau_1 = 0.5$, $\delta = 1$, and L=3) with moving heat source $Q = Q_0 v_0$ along the x-axis at time $t = 0.1$ and $z = 1$. We also consider $Q_0 = 10$ is the intensity of the heat source, and along the x-axis, $v_0 = 1$ is the velocity of the moving heat source.

In Figures 3.2-3.3, we describe the non-dimensional temperature (θ) distribution and u-displacement with the presence of an electro-magnetic field ($H_0 = 100$) and

rotation ($\Omega = 0.2$) for different speeds of the heat source and without the heat source ($Q_0 = 0$). Figure 3.2 represents temperature distribution with respect to x-axis, and it initially takes a value of zero. The curves for $Q_0 = 10, v_0 = 1.5, 3$ are different from $Q_0 = 0$. As velocity increases, the magnitude of the temperature also increases. At $x = 0.26$ all the curves touch their maximum value, and after that, they decrease towards convergence. Figure 3.3 shows the u-displacement distribution with respect to x-axis. For $Q_0 = 10$ and $v_0 = 1.5, 3$, the curves begin with a positive value. The curve takes a maximum value for $Q_0 = 0$, which is higher than the remaining curves. But as x increases, the curve gradually decreases.

Figures 3.4-3.5 describe the field distributions with different values of magnetic field(H_0). The blue dashed line describes the distributions without the existence of a magnetic field($H_1 = 0$).The red dotted line represents $H_2 = 200$, while the violate line represents $H_3 = 400$. Figure-3.4: temperature distribution (θ) begins at zero, which holds the boundary condition. An increase in the magnetic field parameter shows a lower magnitude of temperature. Figure-3.5: σ_{zx} distribution also begins at zero at $x = 0$, which also satisfies the boundary condition. When the value of the magnetic field parameter increases, the magnitude of σ_{zx} increases up to $x = 0.06$. But after that, the distribution decreases and takes its lowest value around $x = 0.5$.

Figures 3.6-3.7 depicts field distributions with different values of angular velocity ($\Omega = 0.2$, $\Omega = 0.5$, and $\Omega = 0.8$) along x-axis. Figure 3.6 clarifies that the m_{xy}-distribution begins at zero in boundary. As Ω increases, the magnitude of u decreases. Up to $x = 0.21$ the curves are decreasing and take the lowest value as negative. Figure 3.7 clarifies that the σ_{zx} distribution begins with a negative value, which also satisfies the boundary condition. When the value of the angular velocity parameter increases, the magnitude of σ_{zx} also increases.

Figures 3.8-3.11 demonstrates the five different popular theories of thermoelasticity. For this graphical presentation, we take the below numerical values with equation (3.42).

1. $\tau_\theta = \tau_q = 0$,$\tau_1 = 0.5$,$\tau_0 = 0.3$ and $\delta = 0$ for GL theory.

2. $\tau_\theta = \tau_q = \tau_1 = 0$,$\tau_0 = 0.3$ and $\delta = 1$ for LS theory.

3. $\tau_\theta = \tau_q = \tau_1 = 0$ and $\delta = 1$ for CT theory.

4. $\tau_\theta = 0.1$,$\tau_q = 0$,$\tau_1 = 0$,$\tau_0 = 0.3$ and $\delta = 1$ for SPL theory, designed by Tzou.

5. $\tau_\theta = 0.1$,$\tau_q = \tau_0 = 0.3$,$\tau_1 = 0.5$ and $\delta = 1$ and $L = 3$ for RPL theory.

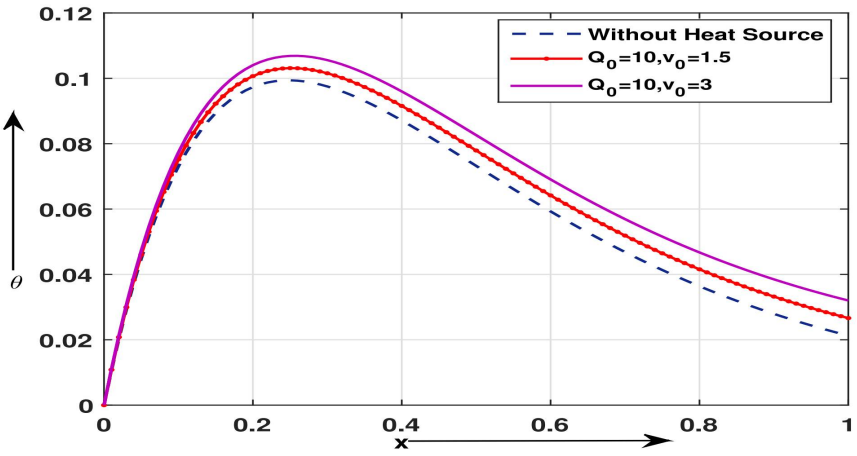

Figure 3.2: Temperature(θ) distribution verses x-axis with different velocity of heat source.

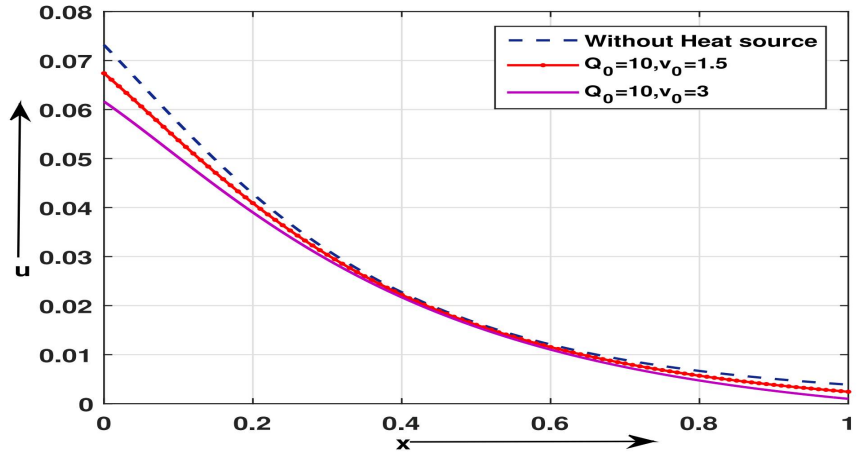

Figure 3.3: u displacement verses x-axis with different velocity of heat source.

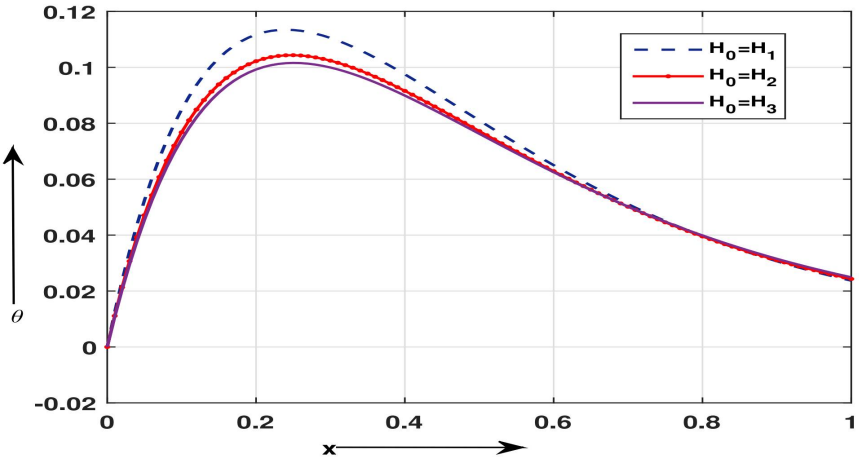

Figure 3.4: Temperature(θ) distribution verses x-axis with different value of magnetic field.

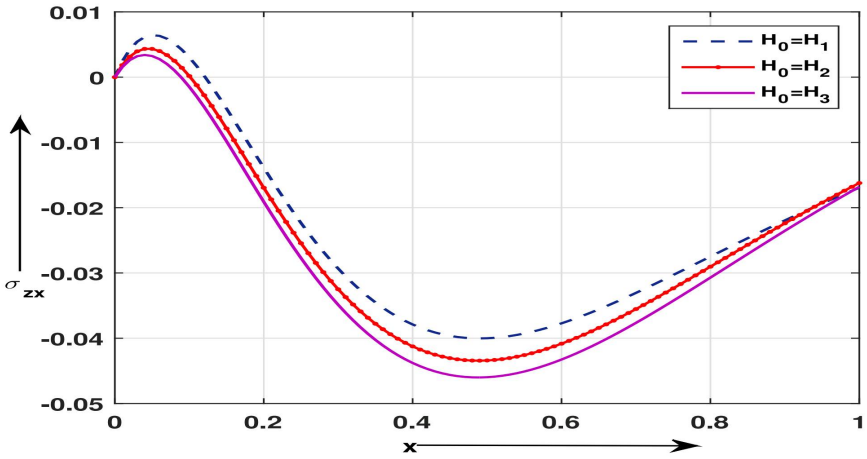

Figure 3.5: Force stress(σ_{zx}) distribution verses x-axis with different value of magnetic field.

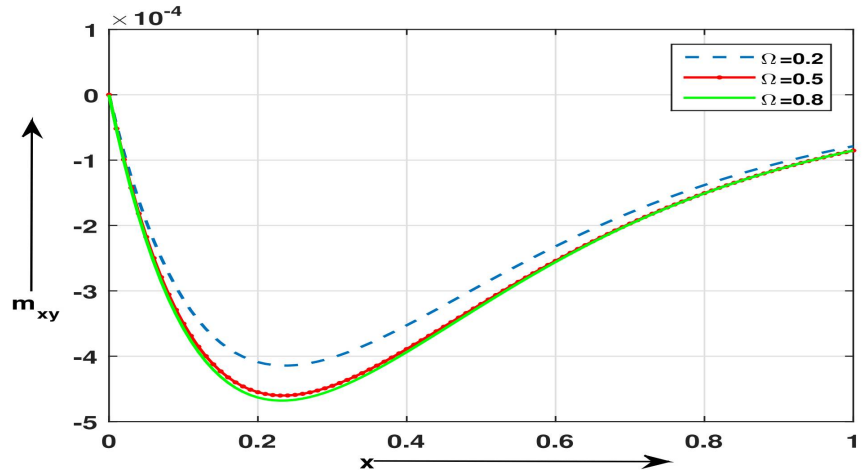

Figure 3.6: Couple stress(m_{xy}) distribution verses x-axis.

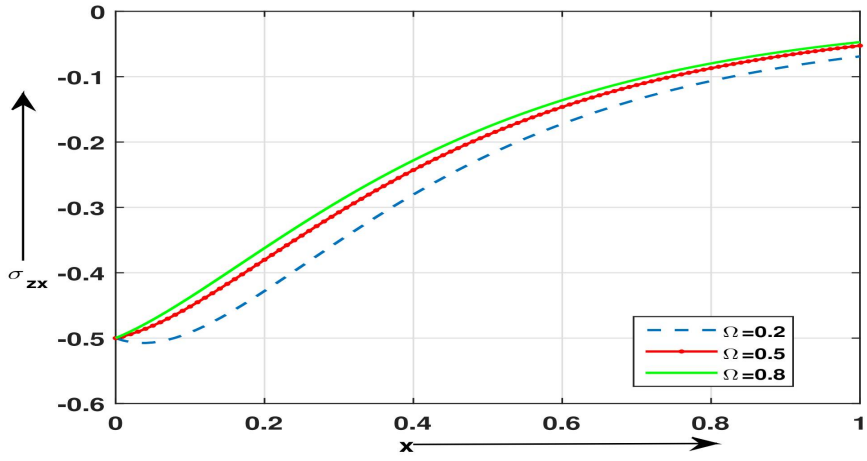

Figure 3.7: Force stress(σ_{zx}) distribution verses x-axis.

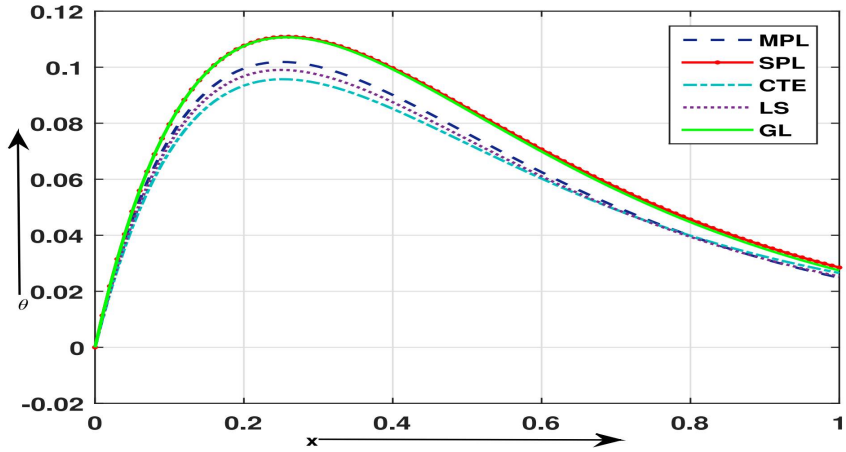

Figure 3.8: Temperature(θ) distribution verses x-axis.

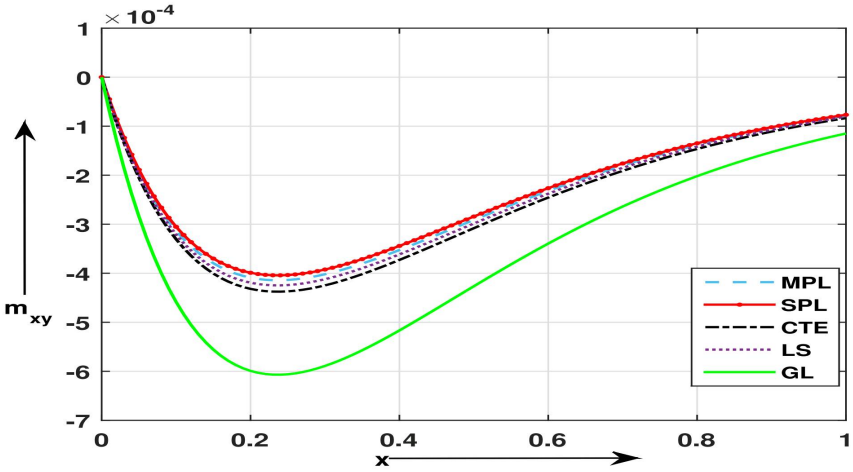

Figure 3.9: Couple stress(m_{xy}) distribution verses x-axis.

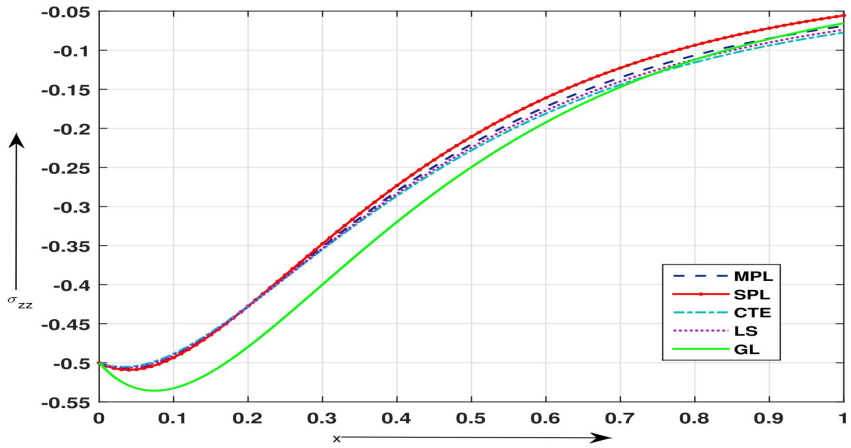

Figure 3.10: Normal force stress(σ_{zz}) distribution verses x-axis.

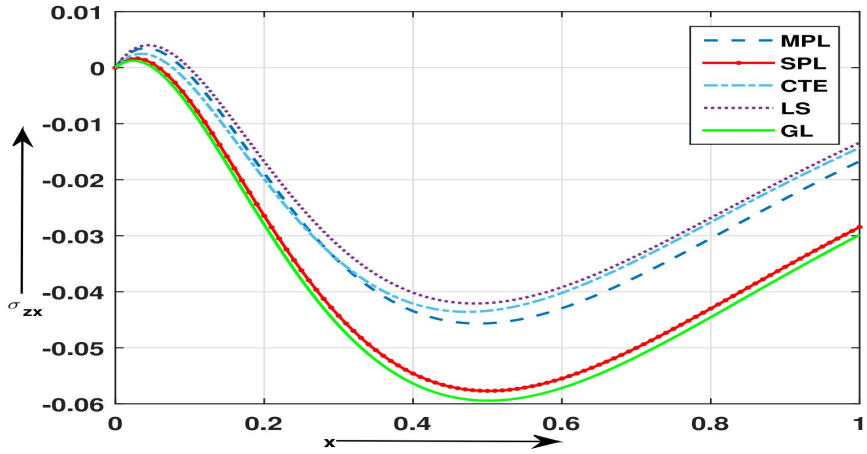

Figure 3.11: Force stress(σ_{zx}) distribution verses x-axis.

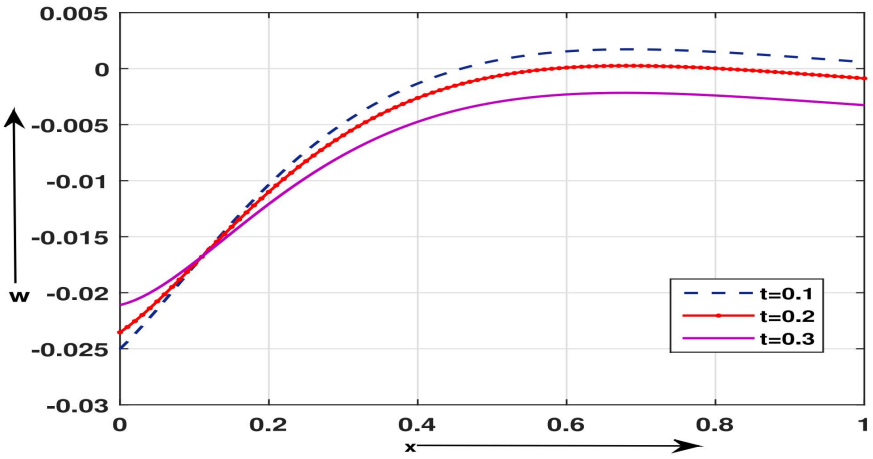

Figure 3.12: Normal Displacement (w) verses x-axis.

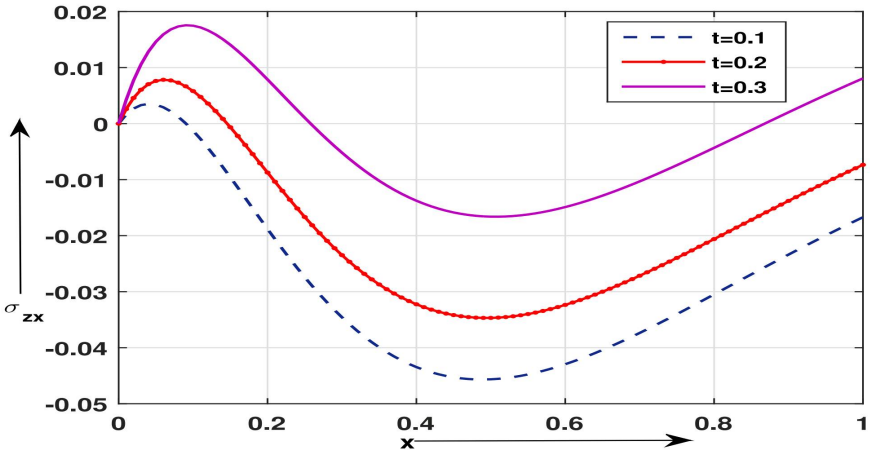

Figure 3.13: Force stress (σ_{zx}) distribution verses x-axis.

Components	CTE	LS	GL	SPL	MPL					
					N=1	N=2	N=3	N=4	N=5	N=6
θ	0.082369513	0.0805971771	0.0816307041	0.0817243938	0.0815292218	0.0815903142	0.0815931447	0.0815932383	0.0815932405	0.0815932405
σ_{zz}	-0.494364858	-0.493744768	-0.514332093	-0.494140489	-0.494072334	-0.494093683	-0.494094671	-0.494094704	-0.494094705	-0.494094705
σ_{xx}	-0.00839885612	-0.0067900074	-0.00778772531	-0.00781465649	-0.00763760544	-0.00769304157	-0.00769560969	-0.00769569458	-0.00769569659	-0.00769569662
m_{xy}	-0.000302831518	-0.000304373885	-0.000376929266	-0.00030337654	-0.000303544639	-0.000303491841	-0.000303489399	-0.000303489319	-0.000303489317	-0.000303489317
u	0.0535548415	0.0537686735	0.0530748466	0.0536349346	0.0536585574	0.0536511896	0.0536508477	0.0536508364	0.0536508361	0.0536508361
w	-0.0200768066	-0.0194978407	-0.0199276124	-0.0198645536	-0.0198006894	-0.019820663	-0.0198215888	-0.0198216194	-0.0198216201	-0.0198216201

Table 3.1: Effect of different thermoelasticity theories on temperature, displacements, and stresses

In these figures, for RPL theory, the legend of the curve is denoted as MPL. The changes in the definition of thermoelasticity show significant effects on the curves. Figure-3.8: θ distribution begins at zero for all definitions. Up to $x = 0.22$ the curves increase, attaining the maximum value. Thereafter, it decreases slowly towards its initial position. The SPL,GL model gives different results from other models. Figure-3.9: Couple stress(m_{xy}) distribution holds boundary conditions for $x = 0$. For the GL model,the curve gets its lowest value at x = 0.22, which shows a big difference from others. Figure-3.10: σ_{zz} distribution shows results for the GL model that are slower than others to achieve a stable position. The SPL model is faster than others. Figure-3.11: Up to $x = 0.06$, σ_{zx} distribution increases and reaches its maximum value near $x = 0.06$ for all definitions. The curve decreases and takes the lowest value after $0.1 \leq x \leq 0.5$. Thereafter, the results gradually go towards their initial value. The result corresponding to the LS model is the fastest to show convergence.

In these figure 3.12-3.13, changes in time show significant effects on the curves. For time $t = 0.1, 0.3, 0.5$ all the graphs are obtained. Figure 3.12 predicts a negative value as the initial value of w-distribution, but as x increases, the displacement increases towards covergence. At the initial point, w-distribution gets the lowest value for time t = 0.1, and with an increase in the time parameter, w-distribution gets higher values. Figure-3.13: For time $t = 0.3$, σ_{zx}-distribution achieves its maximum value, and for time $t = 0.1$, it achieves its lowest value. .

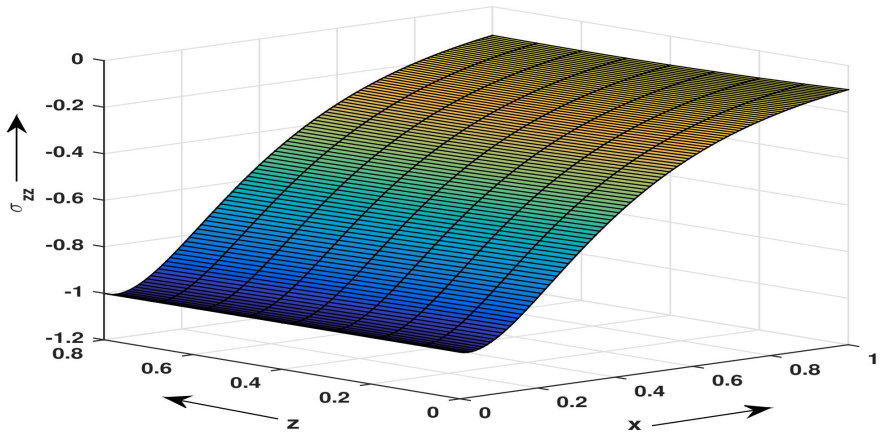

Figure 3.14: Force stress (σ_{zx}) distribution.

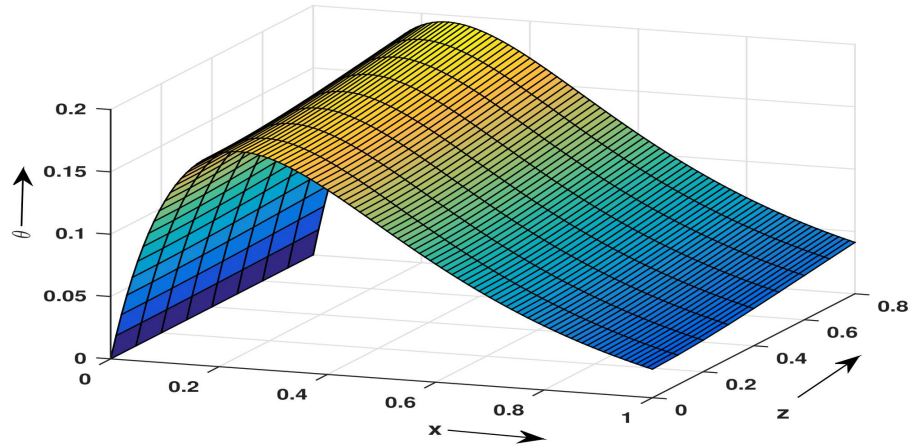

Figure 3.15: Temperature(θ) distribution.

Figure 3.14-3.15 shows the three-dimensional variation of σ_{zx} and θ variables with space variables x and z. Figure 3.14 shows that at $z = 0$, σ_{zx} distribution gets the minimum value. Between $0 \leq x \leq 1$ the curve increases and reaches its highest value at $x = 0.1$. Figure 3.15 shows θ distribution begins at zero value. Up to $x = 0.2$ the curves increase, and attaining maximum value decreases slowly towards a stable position.

The tabular data [3.1] gives all the numerical values of temperature,stress components, and displacement components. All the defined definitions of thermoelasticity in this paper using the phase lag parameter are compared with the refined multi-phase lag model. The data table allows us to identify the influence of several phase lag models and multi-phase-lags on various physical variables.

3.1.9 Conclusion

In this problem, it was investigated how the heat source, electro-magnetic field, angular velocity, and phase lag parameters of a two-dimensional problem in a half-space micropolar thermoelastic material are affected by the heat source, electro-magnetic field, angular velocity, and phase lag parameters of the media. Exact solutions to the various fields are solved analytically using normal mode analysis. Five definitions of thermoelasticity are investigated numerically and graphically. We discovered that each field under study is significantly impacted by the phase lag parameters. The moving heat source along the x-axis plays a vital role in this paper. Numerically, we show that couple stress is an effective subject in the microploar thermoelastic medium. It is found that the thermal effect is more noticeable for temperature than for normal displacement, coupling, and force stress due to mechanical loading and thermal boundary conditions. We also found significant effects of the time variable in the medium of micropolar thermoelasticity. Indeed, the findings reported in this paper should be valuable to low-temperature physicists, designers of new materials, material scientists, and those working on the development of computational techniques for thermoelastic problems.

3.1.10 Appendix

$a_{51} = \frac{A}{1+\epsilon_5}, a_{52} = \frac{2\Omega s}{(1+\epsilon_5)(\epsilon_1+\epsilon_2)}, a_{53} = \frac{iq\epsilon_3}{1+\epsilon_5} a_{56} = \frac{-iq(1-a^2+\epsilon_5)}{1+\epsilon_5}, a_{57} = 0, a_{58} = \frac{1+\upsilon s}{(1+\epsilon_5)(\epsilon_1+\epsilon_2)}$
$a_{61} = -\frac{2\Omega s}{a^2(\epsilon_1+\epsilon_2)}, a_{62} = -\frac{B}{a^2}, a_{64} = \frac{iq(1+\upsilon s)}{a^2(\epsilon_1+\epsilon_2)}, a_{65} = \frac{iq(a^2-1)}{a^2}, a_{67} = -\frac{\epsilon_3}{a^2}$
$a_{71} = -iq\epsilon_7; a_{73} = (q^2 + 2\epsilon_6 + \epsilon_8 s^2); a_{76} = \epsilon_7$
$a_{82} = iqp_{s2}\epsilon_9, a_{84} = (sp_{s1} + q^2), a_{85} = sp_{s2}\epsilon_9,$
$R_8 = -p_{s1}\frac{\bar{Q}}{c_0 T_0}, p_{s1} = \frac{(\delta+\tau_0 s+\sum_{n=1}^{N} \frac{\tau_q^{n+1}}{(n+1)!} s^{n+1})}{(1+\sum_{n=1}^{N} \frac{\tau_\theta^n}{n!} s^n)}$

$A = a^2q^2 + \epsilon_4 s^2 + \frac{s^2}{\epsilon_1+\epsilon_2} - \frac{\Omega^2}{\epsilon_1+\epsilon_2}, B = q^2 + \epsilon_4 s^2 + \epsilon_5 q^2 + \frac{s^2}{\epsilon_1+\epsilon_2} - \frac{\Omega^2}{\eta_0^2(\epsilon_1+\epsilon_2)},$
$\epsilon_1 = \frac{\lambda+\mu}{\rho c_0^2}, \epsilon_2 = \frac{\mu+k}{\rho c_0^2}, \epsilon_3 = \frac{k/\rho c_0^2}{(\epsilon_1+\epsilon_2)}, \epsilon_4 = \frac{\epsilon_0\mu_0^2 H_0^2}{\rho(\epsilon_1+\epsilon_2)}, \epsilon_5 = \frac{\mu_0^2 H_0^2}{\rho c_0^2(\epsilon_1+\epsilon_2)}, \epsilon_6 = \frac{kc_0^2}{\gamma\eta_0^2},$
$\epsilon_7 = \frac{kc_0^2}{\gamma\eta_0^2}, \epsilon_8 = \frac{\rho J\eta_0^2}{\gamma}, \epsilon_9 = \frac{\beta T_0\gamma_T}{\rho K\eta_0}, p_{s2} = \frac{(\delta+\tau_1 s+\sum_{n=1}^{N} \frac{\tau_q^{n+1}}{(n+1)!} s^{n+1})}{(1+\sum_{n=1}^{N} \frac{\tau_\theta^n}{n!} s^n)}$
$g_{11} = a_{61} + \Lambda a_{65}, \quad g_{12} = a_{62} - \Lambda^2, \quad g_{13} = a_{64},$
$g_{21} = a_{71}, \quad g_{22} = \Lambda a_{36}, \quad g_{22} = 0,$
$g_{31} = \Lambda a_{85}, \quad g_{32} = a_{82}, \quad g_{33} = a_{84} - \Lambda^2,$
$h_1 = \Lambda a_{67}, \quad h_2 = a_{73} - \Lambda^2, \quad h_3 = 0.$
$\Pi_1 = \frac{(g_{22}g_{33}h_1 - (h_2(g_{12}g_{33} - g_{13}g_{32})))}{(g_{11}g_{22}g_{33} - g_{12}g_{21}g_{33} + g_{13}g_{21}g_{32} - g_{13}g_{22}g_{31})}, \quad \Pi_2 = \frac{(h_2(g_{11}g_{33} - g_{13}g_{31}) - (g_{21}g_{33}h_1))}{(g_{11}g_{22}g_{33} - g_{12}g_{21}g_{33} + g_{13}g_{21}g_{32} - g_{13}g_{22}g_{31})}$
$\Pi_3 = -1, \quad \Pi_4 = \frac{(h_1(g_{21}g_{32} - g_{22}g_{31}) - h_2(g_{11}g_{32} - g_{12}g_{31}))}{(g_{11}g_{22}g_{33} - g_{12}g_{21}g_{33} + g_{13}g_{21}g_{32} - g_{13}g_{22}g_{31})}$
$\Pi_5 = \Lambda\Pi_1, \quad \Pi_6 = \Lambda\Pi_2$
$\Pi_7 = \Lambda\Pi_3, \quad \Pi_8 = \Lambda\Pi_4,$
$X_{ij} = j\text{-th element of } \Pi_i, j = 1, 2, 3, 4$
$S_{1j} = \Lambda_j X_{2j} + iq\epsilon_2 X_{1j} - (\epsilon_2 - 1)X_{3j} \quad S_{2j} = iq(\epsilon_1 + \epsilon_2)X_{2j} + (\epsilon_1 - 1)\Lambda_1 X_{1j} - (1 + s\upsilon)X_{4j}$
$S_{3j} = \epsilon_2\Lambda_1 X_{2j} + iqX_{1j} - (\epsilon_2 - 1)X_{3j} \quad S_{4j} = (\epsilon_1 + \epsilon_2)\Lambda_1 X_{1j} + iq(\epsilon_1 - 1)X_{2j} - (1 + s\upsilon)X_{4j}$
$S_{5j} = \frac{(\epsilon_2-1)}{\epsilon_7} iqX_{3j}, \quad S_{6j} = \frac{(\epsilon_2-1)}{\epsilon_7}\Lambda_j X_{3j}$

$M_1 = \sum_{j=1}^{4} \frac{Q_j}{\Lambda_j} (iq\epsilon_2 X_{1j} - (\epsilon_2 - 1)X_{3j}), \quad M_2 = \sum_{j=1}^{4} \frac{Q_j}{\Lambda_j}(iq(\epsilon_1 + \epsilon_2)X_{2j} - (1 + s\upsilon)X_{4j})$
$M_3 = \sum_{j=1}^{3} \frac{Q_j}{\Lambda_j}(iqX_{1j} - (\epsilon_2 - 1)X_{3j}), \quad M_4 = \sum_{j=1}^{4} \frac{Q_j}{\Lambda_j}(iq(\epsilon_1 - 1)X_{2j} - (1 + s\upsilon)X_{4j})$
$M_5 = \sum_{j=1}^{4} \frac{Q_j}{\Lambda_j}(iq\frac{(\epsilon_2-1)}{\epsilon_7}X_{3j}), \quad M_6 = 0$

$P_1 = 0 \quad P_2 = M_1$
$P_3 = M_2 - F_0 H(d - |z|)H(t)e^{(-st-iqz)} \quad P_4 = \sum_{j=1}^{3} \frac{Q_j X_{3j}}{\Lambda_j}$

3.2 Problem-4

Fractional Order Thermoelastic Model with Voids in Three-Phase-Lag Thermoelasticity*

3.2.1 Introduction

Lord and Shulman [85] derived a new model to overcome the infinite speed of heat transportation, which was established by Biot [20]. The heat equation of this theory is of the wave type; it automatically ensures finite speeds of propagation for heat and elastic waves. A linear model of thermoelasticity is incapable of characterising the behaviour of many new synthetic solids of the elastomer and polymer types. Eringen [35, 36] used the micropolar elasticity term to describe such materials.

Fractional calculus was first used by Abel [6] in the solution of an integral equation that arises in the tautochrone problem. This area has grown rapidly, and applications have been found in several fields, including solid mechanics, geophysics, physics, and mathematical biology. Many mathematical models in the fields of solid mechanics, bio-rheology, non-linear dynamical systems in ecology, and so on, have been successfully modified using fractional calculus. The fractional derivative exhibits non-local properties, and global dependency is among the main reasons for its use. Kimmich considered anomalous diffusion and characterised it with the time-fractional diffusion wave equation using the Riemann-Liouville fractional integral. Povstenko [121, 120] demonstrated the effect of fractional heat transportation in the presence of thermal stresses. Many authors[11, 135, 126, 153, 2, 118] have also discussed fractional calculus in thermoelasticity.

Recently, Tzou [146, 145] developed dual-phase-lag heat equation theory by incorporating two-phase lags associated with temperature gradient heat flux vector. Two phase lag parameters are related to the fastest effects of thermal inertia. This theory is known as the dual-phase-lag (DPL) model. The later three-phase-lag (TPL) model was developed by Roy choudhuri [128].

In this article, we explore a two-dimensional micropolar thermoelastic problem within the context of fractional-order three-phase-lag (TPL) heat conduction theory in the presence of an electromagnetic field. The governing equations are transformed using normal modes. Subsequently, the displacement components and temperature

*Published in Comput. Sci. Math. Forum 2023, 7, 57. DOI: https://doi.org/10.3390/IOCMA2023-14430

distribution are analytically determined by solving the vector matrix differential equation through the eigenvalue method in the transformed domain. A comparative analysis is conducted in this study, comparing the coupled thermoelasticity theory (CT), Lord-Shulman (LS) model, and three-phase-lag (TPL) model. Graphical presentations are utilized to illustrate and highlight the distinctions between these theoretical frameworks.

3.2.2 Nomenclature

C_E	Specific heat	ρ	Density
e_{ij}	Components of strain tensor	λ, μ	Lame's constants
K	Thermal conductivity	τ_0, τ_1	Relaxation times
T	Temperature	σ_{ij}	Components of Stress Tensor
T_0	Reference temperature	τ_q	Phase lag of heat flux
	such that $\lvert(T-T_0)/T_0\rvert << 1$	τ_θ	Phase lag of temperature gradient
$u_i, \mathbf{u}$	Displacement components	m_{ij}	The couple stress tensor
q_i	Heat flux components	δ_{ij}	The Kronecker delta
c_0	Longitudinal wave speed	ε_{ijk}	Permutation function
v_0	The velocity of the heat source	k, α, β, γ	Micropolar constants
α_T	Thermal expansion coefficient	Ω	Angular velocity
δ	Thermal viscosity	$\mathbf{E}$	Components of electric field
j	Micro-inertia moment	$\mathbf{J}$	The current density vector
γ_T	$\alpha_T(3\lambda+2\mu+k)$, The volume	μ_0	Permeability of magnetic field
	coefficient of thermal expansion	ε_0	Permeability of electric field

3.2.3 Basic Equations

The system of governing equations of an electromagnetic micropolar thermoelastic solid with voids is given by [16, 110, 128]

$$\sigma_{ji,j} + F_i = \rho \ddot{u}_i \tag{3.43}$$

$$m_{ji,j} + \epsilon_{ijr}\sigma_{jr} = J\rho\ddot{\phi}_i \tag{3.44}$$

$$\alpha\psi_{,ii} - \varepsilon\psi - \omega\dot{\psi} - \beta^* u_{i,i} + m\theta = \rho\varepsilon_1\ddot{\psi} \tag{3.45}$$

F_i corresponds to the Lorentz force, given as $F_i = \mu_0 \left(\boldsymbol{J} \times \boldsymbol{H}_0\right)_i$. The values of F_i can be determined through Maxwell's equations, as presented below:

$$\begin{gathered} \operatorname{curl} \boldsymbol{h} = \boldsymbol{J} + \varepsilon_0 \frac{\partial \boldsymbol{E}}{\partial t}, -\mu_0 \frac{\partial \boldsymbol{h}}{\partial t} = \operatorname{curl} \boldsymbol{E}, \operatorname{div} \boldsymbol{h} = 0, \\ \operatorname{div} \boldsymbol{E} = 0, \boldsymbol{h} = \operatorname{curl}(\boldsymbol{u} \times \boldsymbol{H}_0,) \text{ and } \boldsymbol{E} = -\mu_0 \left(\frac{\partial \boldsymbol{u}}{\partial t} \times \boldsymbol{H}_0\right). \end{gathered} \tag{3.46}$$

The components of the force stress and couple stress tensors are

$$\sigma_{ij} = \lambda u_{r,r}\delta_{ij} + \mu(u_{i,j} + u_{j,i}) + k(u_{j,i} - \epsilon_{ijr}\phi_r) - \beta^*\psi\delta_{ij} - \gamma_T(\theta + \nu\frac{\partial\theta}{\partial t})\delta_{ij} \tag{3.47}$$

$$m_{ij} = \alpha\phi_{r,r}\delta_{ij} + \beta\phi_{i,j} + \gamma\phi_{j,i} \tag{3.48}$$

Fractional order three-phase-lag heat conduction equation without heat source is

$$\left[K^*\left(1 + \frac{{\tau_\nu}^\alpha}{\alpha!}\frac{\partial^\alpha}{\partial t^\alpha}\right) + K\frac{\partial}{\partial t}\left(1 + \frac{{\tau_\theta}^\alpha}{\alpha!}\frac{\partial^\alpha}{\partial t^\alpha}\right)\right]\theta_{ii} = \left(1 + \frac{{\tau^\alpha}_q}{\alpha!}\frac{\partial^\alpha}{\partial t^\alpha} + \frac{{\tau^{2\alpha}}_q}{2\alpha!}\frac{\partial^{2\alpha}}{\partial t^{2\alpha}}\right) \times \left(\rho C_E\frac{\partial^2\theta}{\partial t^2} + \beta T_0\frac{\partial^2}{\partial t^2}(e_{kk}) + mT_0\frac{\partial^2\psi}{\partial t^2}\right) \tag{3.49}$$

The strain-displacement equations are

$$e_{ij} = \frac{1}{2}(u_{i,j} + u_{ji}) \text{ and } e_{kk} = u_{i,i} \tag{3.50}$$

3.2.4 Formulation of the Problem

We consider a two-dimensional scenario (refer to Figure 3.16) involving a homogeneous porous micropolar thermoelastic semi-infinite medium ($x \geq 0$) with an initial magnetic field $\mathbf{H}_0 = (0, H_0, 0)$. The medium is subject to body forces in the form of Lorentz forces, beginning at a uniform temperature of T_0. Assuming Cartesian coor-

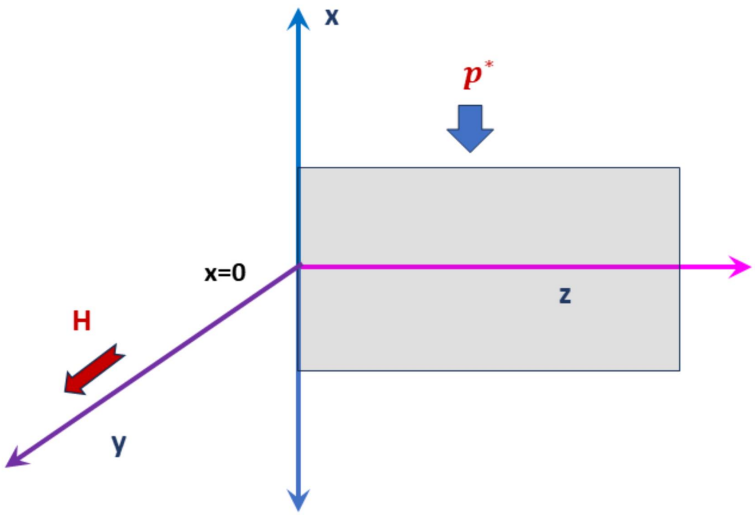

Figure 3.16: Schematic representation

dinates (x, y, z), the displacement components are $\mathbf{u} = (u_1, 0, u_3)$, where u_1 represents

u, u_3 represents w, and the microrotation is $\phi_i = (0, \phi_2, 0)$. The initial magnetic field $\mathbf{H}_0$ along the y-axis induces a magnetic field $\mathbf{h}$ and an electric field $\mathbf{E} = (E_1, 0, E_3)$.

Utilizing equation (3.46), the Lorentz force components are expressed as:

$$F_x = \mu_0 H_0^2 \left[\frac{\partial e}{\partial x} - \epsilon_0 \mu_0 \frac{\partial^2 u}{\partial t^2}\right], F_y = 0, F_z = \mu_0 H_0^2 \left[\frac{\partial e}{\partial z} - \epsilon_0 \mu_0 \frac{\partial^2 w}{\partial t^2}\right], \tag{3.51}$$

where

$$\boldsymbol{H} = \boldsymbol{H_0} + \boldsymbol{h}.$$

To simplify the equations (3.43-3.50), we use the non-dimensional variables as

$$\begin{aligned}(x^*, z^*) = \frac{\eta_0}{c_0}(x, z), (t^*, t_0^*, \tau_0^*, \tau_q^*, \tau_T^*, \upsilon^*) = \eta_0(t, t_0, \tau_0, \tau_q, \tau_T, \upsilon), (u^*, w^*) = \frac{\rho c_0 \eta_0}{\gamma_T T_0}(u, w),\\ \theta^* = \frac{\theta}{T_0}, (\sigma_{ij}^*, p_1^*, p_2^*) = \frac{1}{\gamma_T T_0}(\sigma_{ij}, p_1, p_2), m_{ij}^* = \frac{\eta_0 m_{ij}}{c_0 \gamma_T T_0}, (\psi^*, \phi_2^*) = \frac{\rho c_0^2}{\gamma_T T_0}(\psi, \phi_2).\end{aligned} \tag{3.52}$$

Now we obtain the below non-dimensionalized system of equations as

$$\begin{aligned}(1+\epsilon_5)\frac{\partial^2 u}{\partial x^2} + a_w \frac{\partial^2 w}{\partial x \partial z} + a^2 \frac{\partial^2 u}{\partial z^2} - \epsilon_3 \frac{\partial \phi_2}{\partial z} - \frac{1}{(\epsilon_1+\epsilon_2)}(1 + v\frac{\partial}{\partial t})\frac{\partial \theta}{\partial x} + \beta_1 \frac{\partial \psi}{\partial x}\\ = (\epsilon_4 + \frac{1}{(\epsilon_1+\epsilon_2)})\frac{\partial^2 u}{\partial t^2}\end{aligned} \tag{3.53}$$

$$\begin{aligned}(1+\epsilon_5)\frac{\partial^2 w}{\partial z^2} + a_w \frac{\partial^2 u}{\partial x \partial z} + a^2 \frac{\partial^2 w}{\partial x^2} - \epsilon_3 \frac{\partial \phi_2}{\partial x} - \frac{1}{(\epsilon_1+\epsilon_2)}(1 + v\frac{\partial}{\partial t})\frac{\partial \theta}{\partial z} + \beta_1 \frac{\partial \psi}{\partial z}\\ = (\epsilon_4 + \frac{1}{(\epsilon_1+\epsilon_2)})\frac{\partial^2 w}{\partial t^2}\end{aligned} \tag{3.54}$$

$$\frac{\partial^2 \phi_2}{\partial x^2} + \frac{\partial^2 \phi_2}{\partial z^2} - 2\epsilon_7 \phi_2 + \epsilon_7(\frac{\partial u}{\partial z} - \frac{\partial w}{\partial x}) = \epsilon_8 \frac{\partial^2 \phi_2}{\partial t^2} \tag{3.55}$$

$$\begin{aligned}\left[\lambda_1(1 + \frac{{\tau_v}^\alpha}{\alpha!}\frac{\partial^\alpha}{\partial t^\alpha}) + \frac{\partial}{\partial t}(1 + \frac{{\tau_\theta}^\alpha}{\alpha!}\frac{\partial^\alpha}{\partial t^\alpha})\right](\frac{\partial^2 \theta}{\partial x^2} + \frac{\partial^2 \theta}{\partial z^2})\\ = p_l\left(\frac{\partial^2 \theta}{\partial t^2} + \epsilon_9 \frac{\partial^2}{\partial t^2}(\frac{\partial u}{\partial x} + \frac{\partial w}{\partial z}) + \beta_1 \frac{\partial^2 \psi}{\partial t^2}\right)\end{aligned} \tag{3.56}$$

The components of stress tensor and force tensor are written in the below form:

$$\sigma_{xx} = (\epsilon_1 + \epsilon_2)\frac{\partial u}{\partial x} + (\epsilon_1 - 1)\frac{\partial w}{\partial x} - (1 + \nu\frac{\partial}{\partial t})\theta \tag{3.57}$$

$$\sigma_{zz} = (\epsilon_1 + \epsilon_2)\frac{\partial w}{\partial z} + (\epsilon_1 - 1)\frac{\partial u}{\partial x} - (1 + \nu\frac{\partial}{\partial t})\theta \tag{3.58}$$

$$\sigma_{xz} = \frac{\partial u}{\partial z} + \epsilon_2 \frac{\partial w}{\partial x} - (\epsilon_2 - 1)\phi_2 \tag{3.59}$$

$$\sigma_{zx} = \frac{\partial w}{\partial x} + \epsilon_2 \frac{\partial u}{\partial z} - (\epsilon_2 - 1)\phi_2 \tag{3.60}$$

$$m_{zy} = \frac{(\epsilon_2 - 1)}{\epsilon_4} \frac{\partial \phi_2}{\partial z} \tag{3.61}$$

$$m_{xy} = \frac{(\epsilon_2 - 1)}{\epsilon_4} \frac{\partial \phi_2}{\partial x} \tag{3.62}$$

where $\epsilon_i, i = 1(1)9$ are given in Appendix, and

$$c_0^2 = \frac{\mu}{\rho}, \beta = \sqrt{\frac{\lambda + 2\mu}{\mu}}, \eta_0 = \frac{\rho c_E c_0^2}{k}, p_l = \left(1 + \frac{{\tau^\alpha}_q}{\alpha!}\frac{\partial^\alpha}{\partial t^\alpha} + \frac{{\tau^{2\alpha}}_q}{2\alpha!}\frac{\partial^{2\alpha}}{\partial t^{2\alpha}}\right), a_w = (1 - a^2 + \epsilon_5).$$

Equations (3.53-3.62) takes the above form, dropping the * for convenience.

3.2.5 Normal Mode Analysis

The decomposition of the solution of the physical variables under consideration has the following form in normal mode:

$$(u, w, \psi, \theta, \phi_2, \sigma_{jk})(x, z, t) = (\bar{u}, \bar{w}, \bar{\psi}, \bar{\theta}, \bar{\phi_2}, \bar{\sigma_{jk}})(x) e^{(st + iqz)}; \tag{3.63}$$

where $\bar{u}, \bar{w}, \bar{\theta}, \bar{\phi_2}, \bar{\sigma_{jk}}$ are the amplitudes of the functions, s is a complex constant, $i = \sqrt{-1}$, and q is the wave numbers in the z-direction.

Using the above equations, we obtain the vector matrix differential equation as

$$\frac{d\overline{z}}{dx} = A\overline{z} \tag{3.64}$$

where

$$\overline{z} = (\bar{u}, \bar{w}, \bar{\phi_2}, \bar{\theta}, \bar{\psi}, \frac{d\bar{u}}{dx}, \frac{d\bar{w}}{dx}, \frac{d\bar{\phi_2}}{dx}, \frac{d\bar{\theta}}{dx}, \frac{d\bar{\psi}}{dx})^T \tag{3.65}$$

$$A = \begin{bmatrix} 0 & 0 & 0 & 0 & 0 & 1 & 0 & 0 & 0 & 0 \\ 0 & 0 & 0 & 0 & 0 & 0 & 1 & 0 & 0 & 0 \\ 0 & 0 & 0 & 0 & 0 & 0 & 0 & 1 & 0 & 0 \\ 0 & 0 & 0 & 0 & 0 & 0 & 0 & 0 & 1 & 0 \\ 0 & 0 & 0 & 0 & 0 & 0 & 0 & 0 & 0 & 1 \\ a_{51} & a_{52} & a_{53} & 0 & 0 & 0 & a_{56} & 0 & a_{58} & a_{59} \\ a_{61} & a_{62} & 0 & a_{64} & 0 & a_{65} & 0 & a_{67} & 0 & 0 \\ a_{71} & 0 & a_{73} & 0 & 0 & 0 & a_{76} & a_{77} & 0 & 0 \\ 0 & a_{82} & 0 & a_{84} & 0 & a_{85} & a_{86} & a_{87} & a_{88} & 0 \\ 0 & a_{92} & 0 & a_{94} & a_{95} & a_{96} & 0 & 0 & 0 & 0 \end{bmatrix} \tag{3.66}$$

and $p_{ls} = \frac{\left(1+\frac{\tau_q{}^{\alpha}}{\alpha!}s^{\alpha}+\frac{\tau_q{}^{2\alpha}}{2\alpha!}s^{2\alpha}\right)}{\left[\lambda_1(1+\frac{\tau_v{}^{\alpha}}{\alpha!}s^{\alpha})+s(1+\frac{\tau_\theta{}^{\alpha}}{\alpha!}s^{\alpha})\right]}$ and All the components of matrix A in equation (3.66) are given in the appendix.

3.2.6 Solution

The following equation represents matrix A's characteristic equation:

$$\det(A - \Lambda I) = 0 \tag{3.67}$$

The eigenvalues of the characteristic equation 3.64 are taken in the form $\Lambda = \pm\Lambda_i$ $(i = 1, 2, 3, 4, 5)$

The eigen vector X corresponds to the eigen value Λ calculated as

$$X = \left[\begin{array}{cccccccccc} \Gamma_1 & \Gamma_2 & \Gamma_3 & \Gamma_4 & \Gamma_5 & \Lambda\Gamma_1 & \Lambda\Gamma_2 & \Lambda\Gamma_3 & \Lambda\Gamma_4 & \Lambda\Gamma_5 \end{array}\right]^T \tag{3.68}$$

where Γ_i $(i, j = 1, 2, 3, 4, 5)$ are given in Appendix. We construct the inverse of the matrix $V = (X_1, X_2, X_3, X_4, X_5, X_6, X_7, X_8, X_9, X_{10}) = (X_{ij})_{10\times 10}, i, j = 1(1)10$ as $V^{-1} = (\omega_{ij})\,,\ \ i,\ j = 1, 2, 3, 4, 5, 6, 7, 8, 9, 10.$

Then the solution of the differential equation (3.67) is [126, 79]

$$\overline{z} = \sum_{j=1}^{10} X_j y_j \tag{3.69}$$

$$y_r = C_r e^{\lambda_r x} \tag{3.70}$$

where C_r is an arbitrary constant that is to be evaluated using initial and boundary conditions. In accordance with our considerations, the medium is assumed to be a half-space medium $(x \geq 0)$. Therefore, the field variables can be expressed in the following final form:

$$u = e^{(st+iqz)}\sum_{j=1}^{5} X_{1j} C_j e^{\Lambda_j x} \tag{3.71}$$

$$w = e^{(st+iqz)}\sum_{j=1}^{5} X_{2j} C_j e^{\Lambda_j x} \tag{3.72}$$

$$\theta = e^{(st+iqz)}\sum_{j=1}^{5} X_{4j} C_j e^{\Lambda_j x} \tag{3.73}$$

$$\phi_2 = e^{(st+iqz)}\sum_{j=1}^{5} X_{3j} C_j e^{\Lambda_j x} \tag{3.74}$$

$$\psi = e^{(st+iqz)} \sum_{j=1}^{5} X_{5j} C_j e^{\Lambda_j x} \tag{3.75}$$

Using equations (3.71-3.75) and simplifying the above equations, we obtain the stress components as follows:

$$\begin{aligned} \sigma_{zz} &= e^{(st+iqz)} \sum_{j=1}^{5} C_j S_{1j}(x) e^{\Lambda_j x}, \\ \sigma_{zx} &= e^{(st+iqz)} \sum_{j=1}^{5} C_j S_{2j}(x) e^{\Lambda_j x}, \end{aligned} \tag{3.76}$$

$$\begin{aligned} \sigma_{xx} &= e^{(st+iqz)} \sum_{j=1}^{5} C_j S_{4j}(x) e^{\Lambda_j x}, \\ \sigma_{xz} &= e^{(st+iqz)} \sum_{j=1}^{5} C_j S_{3j}(x) e^{\Lambda_j x}, \end{aligned} \tag{3.77}$$

$$\begin{aligned} m_{xy} &= e^{(st+iqz)} \sum_{j=1}^{5} C_j S_{6j} e^{\Lambda_j x}, \\ m_{zy} &= e^{(st+iqz)} \sum_{j=1}^{5} C_j S_{5j} e^{\Lambda_j x}, \end{aligned} \tag{3.78}$$

where C_j and S_{ij}(x) (i = 1, 2, 3, 4, 5, 6, 7; j = 1, 2, 3, 4; are given in the Appendix.

3.2.7 Initial and Boundary Conditions

We consider the half-space problem with initial conditions given by $u = v = \phi_2 = \theta = \dot{u} = \dot{v} = \dot{\phi_2} = \dot{\theta} = 0$. at $t = 0$. These initial conditions are employed to solve the preceding equations. The determination of unknown parameters is achieved by applying boundary conditions at $x = 0$, leading to the following set of conditions:

1. $\sigma_{zz} = -p_1 e^{st+iqz}$,
2. $\sigma_{zx} = 0$,
3. $\theta = p_2 e^{st+iqz}$,
4. $m_{xy} = 0$,
5. $\frac{\partial \psi}{\partial x} = 0$.

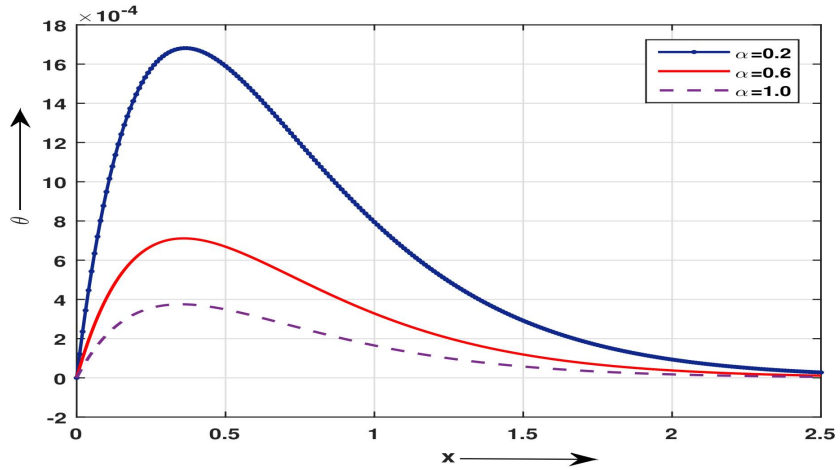

Figure 3.17: Impact of fractional order parameter on temperature distribution at t = 0.1 and z = 1

where p_1, p_2 are arbitrary constants. We can readily ascertain the arbitrary constants $C_j, j = 1(1)5$, in the above equation by employing the inverse matrix method, denoted as

$$\begin{bmatrix} C1 \\ C2 \\ C3 \\ C4 \\ C5 \end{bmatrix} = \begin{bmatrix} S_{11} & S_{12} & S_{13} & S_{14} & S_{15} \\ S_{21} & S_{22} & S_{23} & S_{24} & S_{25} \\ X_{41} & X_{42} & X_{43} & X_{44} & X_{45} \\ S_{61} & S_{62} & S_{63} & S_{64} & S_{65} \\ \Lambda_1 X_{51} & \Lambda_2 X_{52} & \Lambda_3 X_{53} & \Lambda_4 X_{54} & \Lambda_5 X_{55} \end{bmatrix}^{-1} \begin{bmatrix} -p_1 \\ 0 \\ p_2 \\ 0 \\ 0 \end{bmatrix} \tag{3.79}$$

3.2.8 Numerical Results and Discussion

After demonstrating the analytical process earlier, we will now explore a numerical approach to validate the results. For this validation, we selected magnesium as the thermoelastic material, and the relevant parameters are as follows (Abouelregal [11]; Zenkour [161](in SI units)):

$$\begin{gathered} j = 0.2 \times 10^{-19}\ \mathrm{m}^2, \mu = 4.0 \times 10^{10} \mathrm{kg\ m^{-1}s^{-2}}, \lambda = 9.4 \times 10^{10} N/m^2, \varepsilon_0 = 0.3, \\ \rho = 1.74 \times 10^3 \mathrm{kg\ m^{-3}}, T_0 = 293K, k = 1.0 \times 10^{10} \mathrm{kgm^{-1}\ s^{-2}}, \mu_0 = 0.1, \\ \alpha_t = 2.36 \times 10^{-5} \mathrm{K^{-1}}, C_E = 9.623 \times 10^2 \mathrm{Jkg^{-1}K^{-1}}, K = 2.510 \mathrm{Wm^{-1}K^{-1}}, \\ H_0 = 100, \gamma = 0.779 \times 10^{-9} \mathrm{kg\ ms^{-2}}, F_0 = 1, d = 1, \\ q = 3.5,\ s = \omega_0 + i\omega_1, \omega_0 = 2.0, \omega_1 = 0.5. \end{gathered} \tag{3.80}$$

We discuss all graphical representations in view of the TPL model in Figures 3.17-3.20. We consistently set $p_1 = 1$ and $p_2 = 0$ throughout the presentation. In Figure 3.17 the fractional order parameter α has a significant effect on the temperature distribution,

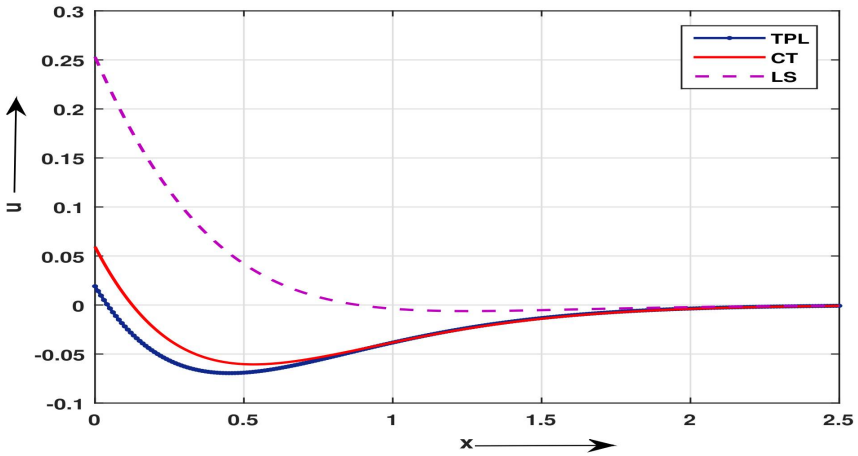

Figure 3.18: Impact of different thermoelasticity theories on u distribution at t = 0.1 and z = 1

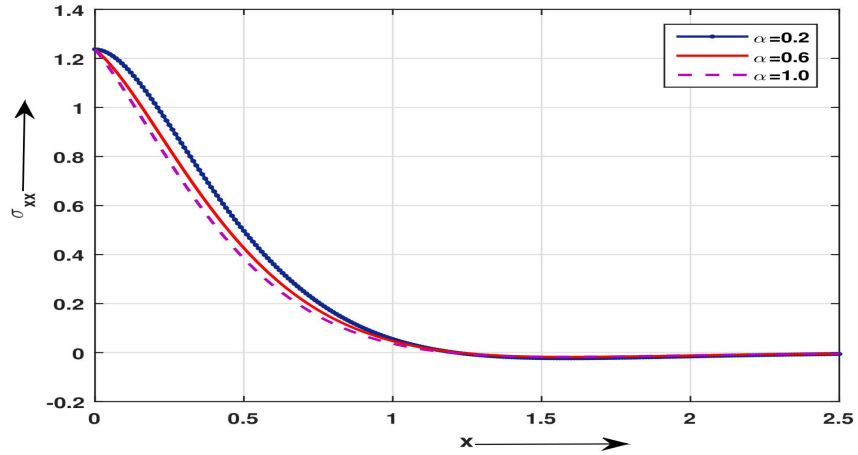

Figure 3.19: Impact of fractional order parameter on σ_{xx} distribution at t=0.1 and z=1

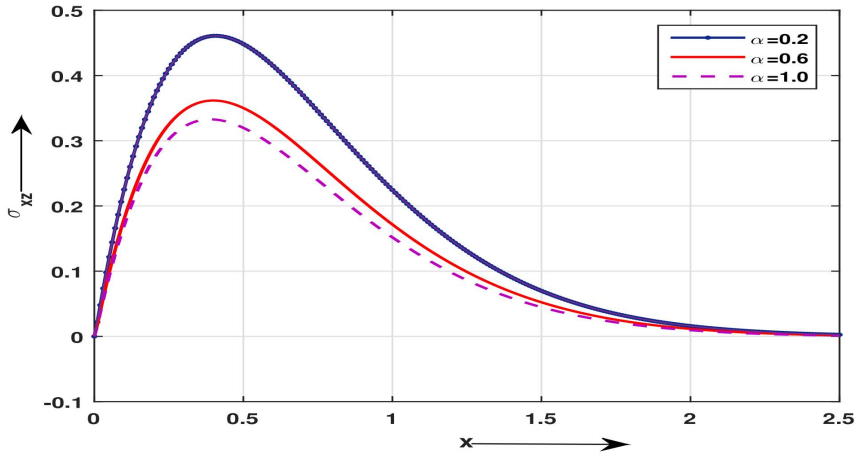

Figure 3.20: Impact of fractional order parameter on σ_{xz} distribution at t = 0.1 and z = 1

where increasing on α causes increasing on and the rate of change of with respect to x also increases when α increases at fixed t = 0.1.

In Figure 3.18, when fractional order $\alpha = 0.6$, time t = 0.1 are fixed and other constants are the same, then the displacement distribution starts with negative values for DPL, LS, and CT theories. The u-distribution up to x = 1.2 for the LS model is greater than for the DPL model and CT model. After x = 1.2, the result is reversed.

In Figure 3.19-3.20, the fractional parameter has significant effects on the stress σ_{xx} , σ_{xy} distribution. Both start at zero initially, which shows that they satisfy the boundary condition. Increasing the fractional parameter α causes decreasing the absolute values of the stresses, and the rate of change of them with respect to x also increases when α increases. For the fixed value of x, the stress σ_{xy} distribution has the lowest value for the fractional parameter $\alpha = 0.2$ in the range $0 \leq x \leq 1.0$. For $x \geq 1.0$, the distribution gradually increases towards zero.

3.2.9 Conclusions

In this work, the effects of the electromagnetic force, fractional order, and phase lag parameters on the temperature distribution, displacement components, and stress components have been studied for a two-dimensional problem in a half-space micropolar thermoelastic medium. The study is conducted within the framework of fractional-order thermoelasticity theory. We found that the fractional order parameter has significant effects on all the studied fields, and the results support the classification of the thermal conductivity of the materials. We compare the displacement distribution(u) using the coupled thermoelasticity theory (CT), the Lord-Shulman (LS) model, and the three-phase-lag (TPL) model. We demonstrate the differences among these theoretical frameworks.

3.2.10 Appendix

$a_{51} = \frac{\epsilon_4 s^2 + a^2 q^2 + \frac{s^2}{\epsilon_1+\epsilon_2}}{1+\epsilon_5}$, $a_{52} = \frac{iq\epsilon_3}{1+\epsilon_5}$, $a_{53} = \frac{iq(a^2-1)-iq\epsilon_5}{1+\epsilon_5}$, $a_{56} = \frac{(1+\nu s)}{(\epsilon_1+\epsilon_2)(1+\epsilon_5)}$, $a_{58} = -b_3$

$a_{61} = \frac{q^2+\epsilon_4 s^2+\epsilon_5 q^2+\frac{s^2}{\epsilon_1+\epsilon_2}}{a^2}$, $a_{62} = \frac{iq(1+\nu s)}{a^2(\epsilon_1+\epsilon_2)}$, $a_{64} = -\frac{iqb_3}{a^2}$, $a_{65} = \frac{iq(a^2-1)-\epsilon_5}{a^2}$, $a_{67} = -\frac{\epsilon_3}{a^2}$

$a_{71} = -iq\epsilon_7$, $a_{73} = q^2 + \epsilon_8 s^2 + 2\epsilon_7$, $a_{77} = \epsilon_7$

$a_{82} = iqp_{ls}\epsilon_9, a_{84} = (p_{ls} + q^2), a_{85} = p_{ls}\epsilon_{10}, a_{86} = p_{ls}\epsilon_9 s,$

$a_{92} = iq\epsilon_{11}$, $a_{93} = 0$, $a_{94} = -\epsilon_{13}$, $a_{95} = q^2 + \epsilon_{14}s^2 + s\epsilon_6 + \epsilon_{12}$, $a_{96} = \epsilon_{11}$

$\epsilon_1 = \frac{\lambda+\mu}{\rho c_0^2}, \epsilon_2 = \frac{\mu+k}{\rho c_0^2}, \epsilon_3 = \frac{k/\rho c_0^2}{(\epsilon_1+\epsilon_2)}, \epsilon_4 = \frac{\epsilon_0\mu_0^2 H_0^2}{\rho(\epsilon_1+\epsilon_2)}, \epsilon_5 = \frac{\mu_0^2 H_0^2}{\rho c_0^2(\epsilon_1+\epsilon_2)}, \epsilon_7 = \frac{kc_0^2}{\gamma\eta_0^2},$

$\epsilon_8 = \frac{\rho J\eta_0^2}{\gamma}, \epsilon_9 = \frac{\beta T_0\gamma_T}{\rho K\eta_0}, \epsilon_{10} = \frac{mT_0\gamma_T}{\rho K\eta_0}$

$\epsilon_6 = \frac{\omega c_0^2}{\beta\eta_0}, \epsilon_{11} = \frac{bc_0^2}{\beta\eta_0^2}\epsilon_{12} = \frac{\epsilon c_0^2}{\beta\eta_0}\epsilon_{13} = \frac{m\rho\ {c_0}^4}{\beta\gamma_T{\eta_0}^2}\epsilon_{14} = \frac{\rho\xi{c_0}^2}{\beta}$

$g_{11} = a_{61} + \Lambda a_{65}, \quad g_{12} = a_{62} - \Lambda^2, \quad g_{13} = a_{64},$

$g_{21} = a_{71}, \quad g_{22} = \Lambda a_{36}, \quad g_{22} = 0,$

$g_{31} = \Lambda a_{85}, \quad g_{32} = a_{82}, \quad g_{33} = a_{84} - \Lambda^2,$

$h_1 = \Lambda a_{67}, \quad h_2 = a_{73} - \Lambda^2, \quad h_3 = 0.$

$\Pi_1 = \frac{(g_{22}g_{33}h_1 - (h_2(g_{12}g_{33} - g_{13}g_{32})))}{(g_{11}g_{22}g_{33} - g_{12}g_{21}g_{33} + g_{13}g_{21}g_{32} - g_{13}g_{22}g_{31})}, \quad \Pi_2 = \frac{(h_2(g_{11}g_{33} - g_{13}g_{31}) - (g_{21}g_{33}h_1))}{(g_{11}g_{22}g_{33} - g_{12}g_{21}g_{33} + g_{13}g_{21}g_{32} - g_{13}g_{22}g_{31})}$

$\Pi_3 = -1, \quad \Pi_4 = \frac{(h_1(g_{21}g_{32} - g_{22}g_{31}) - h_2(g_{11}g_{32} - g_{12}g_{31}))}{(g_{11}g_{22}g_{33} - g_{12}g_{21}g_{33} + g_{13}g_{21}g_{32} - g_{13}g_{22}g_{31})}$

$\Pi_5 = \frac{(g_{22}g_{33}h_1 - (h_2(g_{12}g_{33} - g_{13}g_{32})))}{(g_{11}g_{22}g_{33} - g_{12}g_{21}g_{33} + g_{13}g_{21}g_{32} - g_{13}g_{22}g_{31})}, \quad \Pi_6 = \Lambda\Pi_1$

$\Pi_7 = \Lambda\Pi_2, \quad \Pi_8 = \Lambda\Pi_3$

$\Pi_9 = \Lambda\Pi_4, \quad \Pi_{10} = \Lambda\Pi_5,$

$X_{ij} = j\text{-}th\ element\ of\ \Pi_i, j = 1, 2, 3, 4, 5.$

$S_{1j} = \Lambda_j X_{2j} + iq\epsilon_2 X_{1j} - (\epsilon_2 - 1)X_{3j} \quad S_{2j} = iq(\epsilon_1 + \epsilon_2)X_{2j} + (\epsilon_1 - 1)\Lambda_1 X_{1j} - (1 + s\upsilon)X_{4j}$

$S_{3j} = \epsilon_2\Lambda_1 X_{2j} + iqX_{1j} - (\epsilon_2 - 1)X_{3j} \quad S_{4j} = (\epsilon_1 + \epsilon_2)\Lambda_1 X_{1j} + iq(\epsilon_1 - 1)X_{2j} - (1 + s\upsilon)X_{4j}$

$S_{5j} = \frac{(\epsilon_2 - 1)}{\epsilon_7} iqX_{3j}, \quad S_{6j} = \frac{(\epsilon_2 - 1)}{\epsilon_7}\Lambda_j X_{3j}$

3.3 Problem-5

Dynamic Response of Initially Stressed Microelongated Layer to Gravitational and Electromagnetic Forces

3.3.1 Introduction

The generalized theories of thermoelasticity emerged to address the inherent inconsistency of the infinite speed of heat propagation present in the conventional coupled thermoelasticity theory. This conventional theory(CCTE) is based on the energy equation of parabolic form, relying on Fourier's heat conduction law as established by Biot [20]. Lord and Shulman [85] extended thermal elasticity(LS) theory to isotropic mediums, and Othman [113] applied it to a two-dimensional problem of general linear thermoelasticity. Addressing the challenges of previous theories, Green and Lindsay [46] proposed a general linear thermoelasticity theory based on temperature and frequency considerations. Tzou [146, 145] introduced the dual-phase lag (DPL) model, altering the Fourier law to incorporate phase lags for temperature gradient and heat flux. Several contributions [10, 17, 86] provide valuable insights into the development of elasticity and thermoelasticity theories. Roy Choudhuri [128] introduced the three-phase-lag (TPL) theory, including a third delay time associated with thermal displacement gradient. Quintanilla and Racke [123] further contributed insights into heat conduction models incorporating TPL.

Microstretch continua introduce additional degrees of freedom for elastic bodies, allowing seven degrees of freedom for material particles, including three for displacements, three for microrotations, and one for microstretch. In micro-elongation theory, these particles can undergo volumetric micro-elongation alongside classical medium deformation. Eringen and Şuhubi [39] investigated the effects of microstructure on wave propagations. They extended the generalized thermoelasticity theory proposed by Eringen [37] to incorporate micropolar influences in the new theory. Examples of micro-elongated media include solid–liquid crystals, structural materials with elastic fiber reinforcement, and porous media with gas or non-viscous fluid-filled pores. Despite this, previous works [14, 106, 105, 107] lacked emphasis on crucial factors like electromagnetic force in micro-elongated thermoelasticity.

This study addresses the research gap by investigating the influence of electromagnetic force in the presence of gravitational force on a prestressed micro-elongated thermoelastic layer. A three-phase-lag (TPL) heat conduction equation is employed

for microelongated layer. So, TPL model is employed in conjunction with an elastic layer. The governing equations are introduced, and non-dimensionalization is applied. Normal mode analysis is employed to transform partial differential equations into ordinary ones, and the eigenvalue approach is utilized to solve these equations. The constants in the solutions are determined by the boundary conditions, and the study includes a thorough discussion and graphical representation of the obtained results.

3.3.2 List of symbols

P	Initial pressure
$\varepsilon_{\mathrm{ij}}$	The strain tensor where $\varepsilon_{ij} = \frac{1}{2}\left(u_{i,j} + u_{j,i}\right)$
j_0	Microinertia
$\mathrm{a}_0, \lambda_0, \lambda_1$	Micro-elongational constants
T	Absolute temperature
T_0	Reference temperature
τ_θ	Temperature gradient parameter
τ_q	Heat flux parameter
$\boldsymbol{u}^{\mathrm{e}}$	Displacement vector in an elastic medium
ρ^{e}	Density in an elastic medium
$\lambda^{\mathrm{e}}, \mu^{\mathrm{e}}$	Lame's constants in an elastic medium
k^e	Thermal conductivity in an elastic medium
ρ	Density in micro-elongated medium
$\boldsymbol{u}$	Displacement vector in micro-elongated medium
σ_{ij}	Component of stress tensor for micro-elongated medium
φ	Micro-elongational scalar
k	Thermal conductivity in micro-elongated medium
c_{e}	Specific heat at the constant strain in microelongated medium
λ, μ	Lame's constants in micro-elongated medium
$c_{\mathrm{e}}^{\mathrm{e}}$	Specific heat at the constant strain in an elastic medium
$\alpha_{t_1}, \alpha_{t_2}$	Coefficient of linear thermal expansion where $\beta_0 = (3\lambda + 2\mu)\alpha_{t_1},\ \beta_1 = (3\lambda + 2\mu)\alpha_{t_2}$

3.3.3 Basic Equations and Formulation of the Problem

The fundamental governing equations for micro-elongated thermoelasticity, considering electromagnetic force in the presence of gravitational force on a pre-stressed micro-elongated thermoelastic layer in a TPL model, can be obtained as shown in [14, 106, 128]:

$$\sigma_{ij,j} + F_i + G_i = \rho u_{i,tt}, \tag{3.81}$$

$$a_0\psi_{,ii} + \beta_1 T - \lambda_1\psi - \lambda_0 u_{j,j} = \frac{1}{2}\rho j_0\psi_{,t}, \tag{3.82}$$

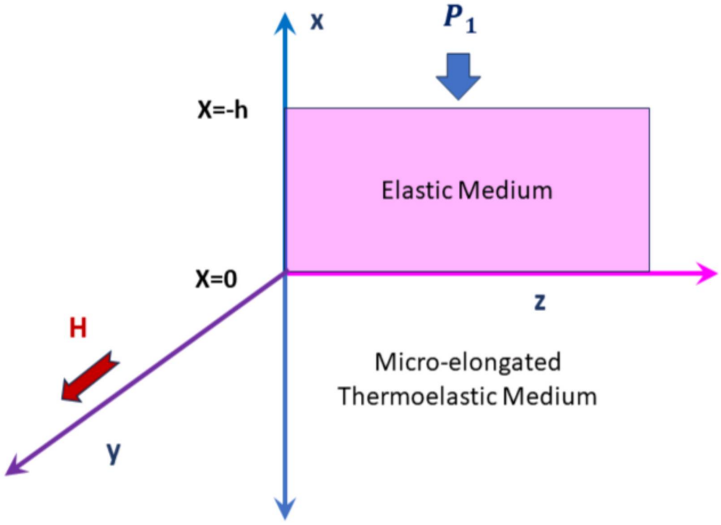

Figure 3.21: Geometry of the problem

$$\begin{aligned}&[K^*\left(1+\tau_\nu\frac{\partial}{\partial t}\right)+K\frac{\partial}{\partial t}\left(1+\tau_\theta\frac{\partial}{\partial t}\right)]T_{,ii}\\&=\left(1+\tau_q\frac{\partial}{\partial t}\right)\left(\rho c_e\frac{\partial T}{\partial t}+\beta_0 T u_{k,k,t}\right)+\beta_1 T_0\psi_{,t},\end{aligned}\tag{3.83}$$

$$\sigma_{ij}=2\mu\varepsilon_{ij}\ -Pw_{ij}+\left(\lambda e-\beta_0 T+\lambda_0\psi-P\right)\delta_{ij},\tag{3.84}$$

where $w_{ij}=\frac{1}{2}\left(u_{j,i}-u_{i,j}\right)$. Here G_i is the force due to gravity and F_i is the Lorentz force, represented as $F_i=\mu_0\left(\vec{J}\times\vec{H}_0\right)_i$. J and F_i can be easily found from Maxwell's equations, which are given below:

$$\begin{aligned}curl\ \vec{h}=\vec{J}+\varepsilon_0\frac{\partial\vec{E}}{\partial t},-\mu_0\frac{\partial\vec{h}}{\partial t}=curl\vec{E},\\div\vec{h}=0,div\vec{E}=0,\\\vec{h}=curl\left(\vec{u}\times\vec{H}_0\right),\vec{E}=-\mu_0\left(\frac{\partial\vec{u}}{\partial t}\times\vec{H}_0\right).\end{aligned}\tag{3.85}$$

Considering the problem in two dimensions in the xz-plane (see Figure 3.21) with a micro-elongated half-space layer, the displacement vector is given by $\vec{u}(x,z,t)=(u,0,w)$, where u and w represent displacements in the x and z directions, respectively. The initial stress, P, and the body force vector, G_i, are defined as follows:

$$G_i=\left(\rho g\frac{\partial w}{\partial x},0,-\rho g\frac{\partial u}{\partial x}\right)$$

$$\vec{H}=\vec{H}_0+\vec{h}(x,y,t),\vec{H}_0=(0,H_0,0)$$
$$(F_x,F_y,F_z)=\mu_0 H_0^2\left(\frac{\partial e}{\partial x}-\varepsilon_0\mu_0\frac{\partial^2 u}{\partial t^2},0,\frac{\partial e}{\partial z}-\varepsilon_0\mu_0\frac{\partial^2 w}{\partial t^2}\right)$$

The equations of motion are given by

$$\mu\nabla^2 u + (\lambda+\mu)e_{,x} - \frac{P}{2}\left(u_{,zz} - w_{,xz}\right) - \beta_0 T_{,x} + \lambda_0\psi_{,x} + \mu_0 H_0^2 e_{,x} \\ -\varepsilon_0{\mu_0}^2 H_0^2 u_{,tt} + g w_{,x} = \rho[u_{,tt} - \Omega^2 u + 2\Omega w_{,t}] \tag{3.86}$$

$$\mu\nabla^2 w + (\lambda+\mu)e_{,z} - \frac{P}{2}\left(w_{,xx} - u_{,xz}\right) - \beta_0 T_{,z} + \lambda_0\psi_{,z} + \mu_0 H_0^2 e_{,z} \\ -\varepsilon_0{\mu_0}^2 H_0^2 u_{,tt} - g u_{,x} = \rho[w_{,tt} - \Omega^2 w - 2\Omega u_{,t}] \tag{3.87}$$

For simplicity, the following non-dimensional variables are utilized:

$$x_i' = \frac{w^*}{c_1}x_i, \quad z' = \frac{w^*}{c_1}z, \quad u_i' = \frac{w^*\rho c_1}{\beta_0 T_0}u_i, \quad u_i^{e'} = \frac{w^*\rho c_1}{\beta_0 T_0}u_i^e, \\ t' = w^* t, \quad \tau_\theta' = w^*\tau_\theta, \quad \tau_q' = w^*\tau_q, \quad \sigma_{ij}' = \frac{\sigma_{ij}}{\beta_0 T_0}, \quad \sigma_{ij}^{e'} = \frac{\sigma_{ij}^e}{\beta_0 T_0}, \\ \psi' = \frac{\lambda_0}{\beta_0 T_0}\psi, \quad T' = \frac{T}{T_0}, \quad P' = \frac{P}{\lambda+2\mu}, \quad P_1' = \frac{P_1}{\beta_0 T_0}, \tag{3.88}$$

where $w^* = \frac{\rho c_1^2 c_e}{k}$, $c_1^2 = \frac{\lambda+2\mu}{\rho}$.

Substituting from equation (3.88) into equations (3.82),(3.83),(3.86) and (3.87), we obtain

$$a_1\nabla^2 u + a_2 e_{,x} + \frac{P}{2}\left(u_{,z,z} - w_{,x,z}\right) - T_{,x} + \psi_{,x} + R_1 e_{,x} + g w_{,x} = \beta^2 u_{,tt} - \Omega^2 u + 2\Omega w_{,t} \tag{3.89}$$

$$a_1\nabla^2 w + a_2 e_{,z} + \frac{P}{2}\left(w_{,x,x} - u_{,x,z}\right) - T_{,z} + \psi_{,z} + R_1 e_{,z} - g u_{,x} = \beta^2 w_{,tt} - \Omega^2 w - 2\Omega u_{,t} \tag{3.90}$$

$$\left(\nabla^2 - a_4\right)\psi + a_3 T - a_5 e = r_5\psi_{,tt} \tag{3.91}$$

$$\left[K_1(1+\tau_v\frac{\partial}{\partial t}) + \frac{\partial}{\partial t}(1+\tau_\theta\frac{\partial}{\partial t})\right]\nabla^2 T = \left(1+\tau_q\frac{\partial}{\partial t} + \frac{\tau_q^2}{2}\frac{\partial^2}{\partial t^2}\right)[r_6 T_{,t} + r_7 e_{,t}] \\ + a_9\psi_{,t}. \tag{3.92}$$

3.3.4 Normal Mode Analysis

The expression for the solution of the identified physical variable can be studied by analyzing its normal modes, represented in the following manner:

$$[u, w, \psi, \theta, \sigma_{ij}, u^e, w^e, \sigma_{ij}^e](x,z,t) = [u^*, w^*\psi^*, \theta^*, \sigma_{ij}^*, u^{e*}, w^{e*}, \sigma_{ij}^{e*}](x)e^{(\omega t + ibz)}, \tag{3.93}$$

where ω is a complex constant, $i = \sqrt{-1}$, and b is the wave number in the z direction.

Using the previously mentioned equations, we obtain the vector matrix differential equation in the following form:

$$\frac{d\xi^*}{dx} = A\xi^* \tag{3.94}$$

where

$$\xi^* = (u^*, w^*, \theta^*, \psi^*, \frac{du^*}{dx}, \frac{dw^*}{dx}, \frac{d\theta^*}{dx}, \frac{d\psi^*}{dx})^T \tag{3.95}$$

Using equation (12) into equations (8)–(11), then we have

$$A = \begin{bmatrix} O_{4\times4} & I_{4\times4} \\ B_{4\times4} & C_{4\times4} \end{bmatrix} \tag{3.96}$$

$$B_{4\times4} = \begin{bmatrix} r_{51} & r_{52} & 0 & 0 \\ r_{61} & r_{62} & r_{63} & r_{64} \\ 0 & r_{72} & r_{73} & r_{74} \\ 0 & r_{82} & r_{83} & r_{84} \end{bmatrix} \quad C_{4\times4} = \begin{bmatrix} 0 & r_{56} & r_{57} & r_{58} \\ r_{65} & 0 & 0 & 0 \\ r_{75} & 0 & 0 & 0 \\ r_{85} & 0 & 0 & 0 \end{bmatrix} \tag{3.97}$$

$$I_{4\times4} = \begin{bmatrix} 1 & 0 & 0 & 0 \\ 0 & 1 & 0 & 0 \\ 0 & 0 & 1 & 0 \\ 0 & 0 & 0 & 1 \end{bmatrix} \quad O_{4\times4} = \begin{bmatrix} 0 & 0 & 0 & 0 \\ 0 & 0 & 0 & 0 \\ 0 & 0 & 0 & 0 \\ 0 & 0 & 0 & 0 \end{bmatrix} \tag{3.98}$$

To find out the solution of the equation (3.94), we use eigen value approach as (Roy and Lahiri[127]). Now the below equation

$$|A - \lambda I| = 0 \tag{3.99}$$

is the characteristic equation of the matrix A while I is the Identity matrix. There are eight eigen values in the form $\lambda = \pm\lambda_i$ $(i = 1, 2, 3, 4)$ of the characteristic equation (3.99). The corresponding eigen vector χ for the eigenvalue Λ obtained as

$$\chi = \begin{bmatrix} \Gamma_1 & \Gamma_2 & \Gamma_3 & \Gamma_4 & \lambda\Gamma_1 & \lambda\Gamma_2 & \lambda\Gamma_3 & \lambda\Gamma_4 \end{bmatrix}^T \tag{3.100}$$

where Γ_i $(i = 1, 2, 3, 4)$ are given in Appendix.

Now the eigenvectors related to the eigen-values $\pm\lambda_j$, $j = 1, 2, 3, 4$ of A are written as

$$\begin{array}{llll} X_1 = (\chi)_{\lambda=\lambda_1}, & X_2 = (\chi)_{\lambda=\lambda_2}, & X_3 = (\chi)_{\lambda=\lambda_3} & X_4 = (\chi)_{\lambda=\lambda_4} \\ X_5 = (\chi)_{\lambda=-\lambda_1}, & X_6 = (\chi)_{\lambda=-\lambda_2}, & X_7 = (\chi)_{\lambda=-\lambda_3}, & X_8 = (\chi)_{\lambda=-\lambda_4}. \end{array} \tag{3.101}$$

We compute the inverse matrix $V^{-1} = (\omega_{ij})$, $i, j = 1(1)8$ of the matrix $V = (X_1, X_2, X_3, X_4, X_5, X_6, X_7, X_8)$. As a result, the solution to the differential equation 3.101 is

$$\xi^* = \sum_{j=1}^{8} X_j y_j \tag{3.102}$$

$$y_p = C_p e^{\lambda_p x} \tag{3.103}$$

where C_p is an arbitrary constant. All the values of C_p can be assessed by using boundary and initial conditions. Here λ_n,$(n = 1, 2, 3, 4)$ are negative roots of the auxiliary equation of equation (3.99).

The general solutions of equation (3.98) bound as $(x \to \infty)$ are given by:

$$(u^*, w^*, T^*, \psi^*)(x) = \sum_{n=1}^{4} (X_{1n}, X_{2n}, X_{3n}, X_{4n}) A_n e^{\lambda_n x}. \tag{3.104}$$

Substituting from equation (3.87) into equation (3.99), and with the help of equation (3.99), we obtain the components of stresses:

$$\sigma^*_{xx}(x) = \sum_{n=1}^{4} S_{5n} A_n e^{\lambda_n x}. \tag{3.105}$$

$$\sigma^*_{xz}(x) = \sum_{n=1}^{4} S_{6n} A_n e^{\lambda_n x}. \tag{3.106}$$

$$\sigma^*_{zz}(x) = \sum_{n=1}^{4} S_{7n} A_n e^{\lambda_n x}. \tag{3.107}$$

where the coefficients $a_i, \delta_i, A, B, C, E$, and S_{in} are obtained in Appendix 1.

The system of governing equations for a general elastic medium is given by [14]:

$$\sigma^e_{ij,j} = \rho^e \ddot{u}^e_i, \tag{3.108}$$

$$\sigma^e_{ij} = \lambda^e u^e_{k,k} \delta_{ij} + \mu^e (u^e_{i,j} + u^e_{j,i}). \tag{3.109}$$

Substituting from equations (3.108) and (3.109) into equation (3.93):

$$(l_3 D^2 - \ell_1) u^{e*} + i b l_2 D w^{e*} = 0, \tag{3.110}$$

$$i b l_2 D u^{e*} + (l_1 D^2 - \ell_2) w^{e*} = 0. \tag{3.111}$$

Therefore, the vector matrix differential equation in the following form:

$$\frac{d\overline{z}}{dx} = E\overline{z} \tag{3.112}$$

where

$$\overline{z} = \left(u^{e*}, w^{e*}, \frac{du^{e*}}{dx}, \frac{dw^{e*}}{dx} \right)^T, \tag{3.113}$$

$$E = \begin{bmatrix} 0 & 0 & 1 & 0 \\ 0 & 0 & 0 & 1 \\ q_{31} & 0 & 0 & q_{34} \\ 0 & q_{42} & q_{43} & 0 \end{bmatrix} \tag{3.114}$$

Now the characteristic equation of the matrix E is

$$|E - mI| = 0 \tag{3.115}$$

where I is the Identity matrix.

There are four eigen values in the form $m = \pm m_i$ $(i = 1, 2, 3, 4)$ of the characteristic equation (3.115). The corresponding eigen vector ζ for the eigenvalue m obtained as

$$\zeta = \begin{bmatrix} x_1 & x_2 & mx_1 & mx_2 \end{bmatrix}^T \tag{3.116}$$

where x_i $(i = 1, 2, 3, 4)$ are given in Appendix. Similar way using eigen value approach, the solutions to equation (3.112) are of the form:

$$u^{e*}(x) = \sum_{n=1}^{4} Y_{1n} B_n e^{m_n x}, \tag{3.117}$$

$$w^{e*}(x) = \sum_{n=1}^{4} Y_{2n} B_n e^{m_n x}. \tag{3.118}$$

Substituting from equations (3.117) and (3.118) into (3.109) and with the help of equations (3.88) and (3.93), we obtain the components of stresses in an elastic medium:

$$\sigma_{xx}^{e*}(x) = \sum_{n=1}^{2} Z_{3n} B_n e^{m_n x}, \tag{3.119}$$

$$\sigma_{zz}^{e*}(x) = \sum_{n=1}^{2} Z_{4n} B_n e^{m_n x}. \tag{3.120}$$

The stress components $\sigma_{xz}^{e*}(x)$ are given by:

$$\sigma_{xz}^{e*}(x) = \sum_{n=1}^{4} Z_{5n} B_n e^{m_n x}. \tag{3.121}$$

where the coefficients l_i, ℓ_i, G, N, and L_{in} are given in Appendix.

3.3.5 Boundary Conditions

$\sigma_{xx} = \sigma_{xx}^{e} - P_1 e^{(\omega t + ibz)} - a_{11} P, \quad \sigma_{xz} = 0$, at $x = -h$

$\sigma_{xx} = \sigma_{xx}^{e} - a_{11} P, \quad \sigma_{xz} = \sigma_{xz}^{e}, \quad u = u^{e}, \quad w = w^{e}, \quad \psi = 0, \quad T = P_2 e^{(\omega t + ibz)}, \quad$ at $\quad x = 0.$

Where P_1 is the magnitude of the mechanical force, and f is a constant. Upon substituting the expressions of the relevant physical quantities into the aforementioned

boundary conditions, we derive the following equations that the coefficients must satisfy:

$$\begin{aligned}
&\sum_{i=1}^{4} A_i S_{5i} e^{-\lambda_i h} - \sum_{i=1}^{4} A_i Z_{3i} e^{-m_i h} = -P_1, && \sum_{i=1}^{4} A_i S_{6i} e^{-\lambda_i h} = 0,\\
&\sum_{i=1}^{4} A_i S_{5i} - \sum_{i=1}^{4} B_i Z_{3i} = 0, && \sum_{i=1}^{4} A_i S_{6i} - \sum_{i=1}^{4} B_i Z_{5i} = 0,\\
&\sum_{i=1}^{4} A_i X_{1i} - \sum_{i=1}^{4} B_i Y_{1i} = 0, && \sum_{i=1}^{4} A_i X_{2i} - \sum_{i=1}^{4} B_i Y_{2i} = 0,\\
&\sum_{i=1}^{4} A_i X_{4i} = 0, && \sum_{i=1}^{4} A_i X_{3i} = P_2,
\end{aligned} \tag{3.122}$$

The utilisation of the expressions of the variables assumed into the boundary mentioned above conditions (3.122) to obtain the equations that are satisfied with the parameters. And hence, eight equations will be obtained.If the matrix inversion method is applied to the eight equations, we obtain the values of the constants $A_n, (n = 1, 2, 3, 4)$ and $B_n, (n = 1, 2, 3, 4)$. So, $C = Vp$ where $C = [A_1, A_2, A_3, A_4, B_1, B_2, B_3, B_4]^T$, $p = [-P_1, 0, 0, 0, 0, 0, 0, P_2]^T$ and V are given in Appendix.

3.3.6 Numerical Results and Discussion

The investigation focuses on an aluminum epoxy-like material with microelongated properties, as detailed in Othman et al. [105]. The material parameters are as follows:

$$\begin{gathered}
\lambda = 7.59 \times 10^{10}\ \text{N/m}^2, \mu = 1.89 \times 10^{10}\ \text{N/m}^2, a_0 = 0.61 \times 10^{-10}\ \text{N}, \rho = 2.19 \times 10^{3}\ \text{kg/m}^3,\\
\beta_0 = \beta_1 = 0.05 \times 10^{5}\ \text{N/m}^2\text{.K}, c_e = 966\ \text{J/kg.K}, K = 252\ \text{J/m.s.K}, j_0 = 0.196 \times 10^{-4}\ \text{m}^2,\\
\lambda_0 = \lambda_1 = 0.37 \times 10^{10}\ \text{N/m}^2, T_0 = 293\text{K}, P = 0.001, \tau_\theta = 1.5 \times 10^{-4}, \tau_q = 9 \times 10^{-4},\\
\omega_0 = -1.77 \times 10^{-4}, \zeta = 3.59 \times 10^{-3}, b = 3, h = 0.001, f = 0.025, \omega = \omega_0 + i\zeta,\\
g = 0.8, P = 1, \Omega = 0.5, \epsilon_0 = 0.1, \mu_0 = 1.
\end{gathered} \tag{3.123}$$

The physical constants for the elastic medium (granite) are taken from Othman et al. [106] and are as follows:

$$\begin{gathered}
\lambda^e = 0.884 \times 10^{10}\ \text{N/m}^2, \mu^e = 1.2667 \times 10^{10}\ \text{N/m}^2,\\
\rho^e = 2.6 \times 10^{3}\ \text{kg/m}^3, c_e^e = 720.7\ \text{J/kg.K},\\
k^e\ = 3.1\ \text{J/m.s.K}.
\end{gathered} \tag{3.124}$$

In this paper, computations are conducted at a dimensionless time $t = 0.3$ over the interval $0 \leq x \leq 1.8$ on the surface $z = 1$. The numerical approach outlined here is employed to analyze the distribution of horizontal displacement u and the micro-elongational scalar ψ within the range $0 \leq x \leq 1.8$. Additionally, stress components σ_{xx} and σ_{xz} are studied versus x to investigate the influence of the electromagnetic term in the model of TPL, considering both its presence and complete absence.

The stress distributions, σ_{xx} and σ_{xz}, with varying values of H_0 are illustrated in figures 3.22 and 3.23, respectively. The displacement (u) distribution with different values of H_0 is depicted in figure 3.24. Additionally, figure 3.25 presents the temperature (T) distribution for various values of H_0.

Furthermore, the displacement (w) distribution is portrayed in figure 3.26, while the microelongation (ψ) distribution is represented in figure 3.27, both with varying values of H_0.

3.3.7 Conclusion

The investigation into the deformation of a thermoelastic medium reveals significant contributions from electromagnetic field, the micro-elongational scalar, and the specified boundary conditions. Notably, as the distance x increases substantially, all examined physical quantities demonstrate a swift convergence to zero. The successful development of analytical solutions for the thermoelastic problem through normal mode analysis underscores the efficacy of this approach.

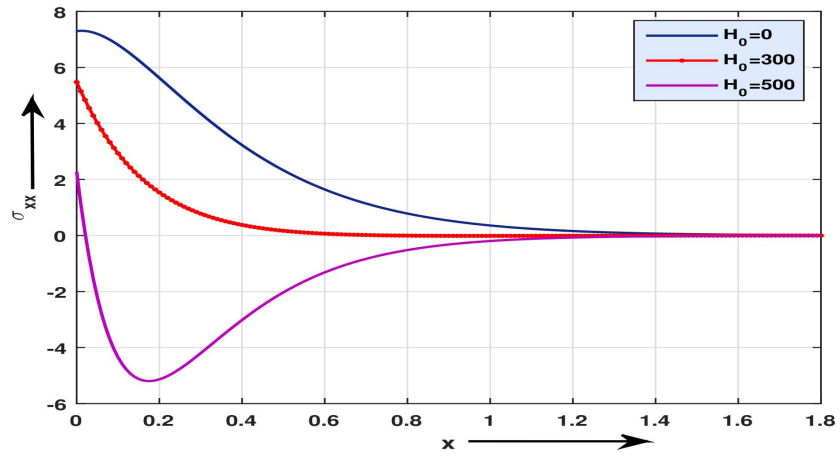

Figure 3.22: The stress σ_{xx} distribution with different values of H_0.

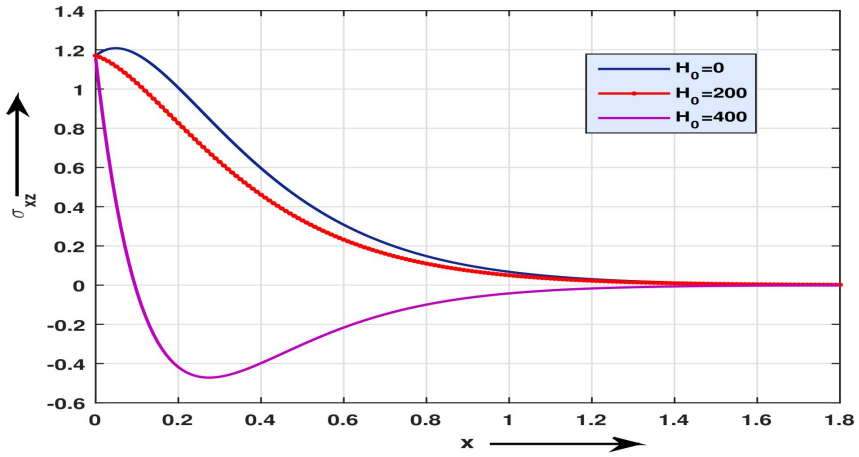

Figure 3.23: The stress σ_{xz}distribution with different values of H_0.

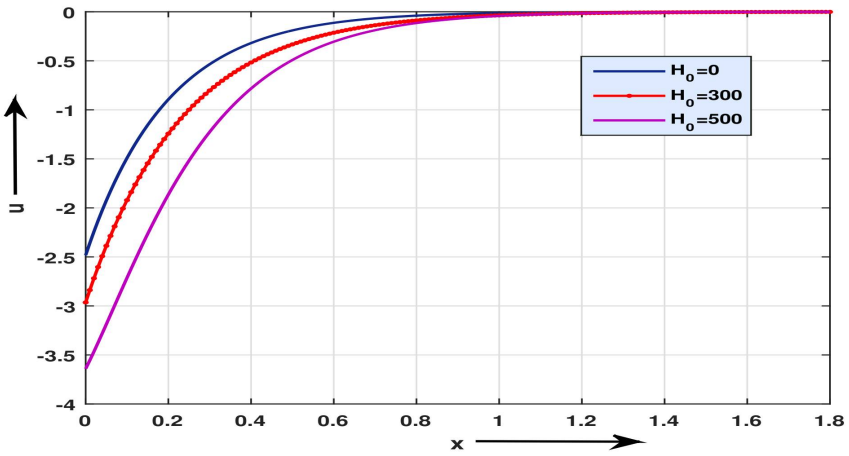

Figure 3.24: Displacement(u) distribution with different values of H_0.

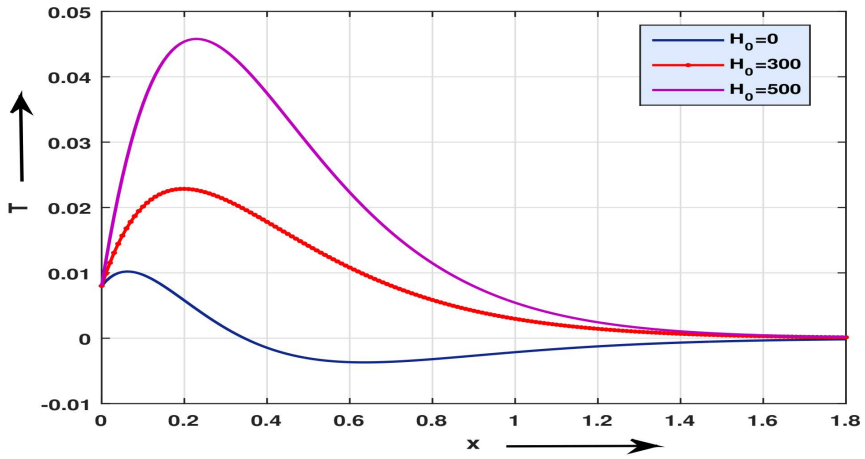

Figure 3.25: The temperature T distribution with different values of H_0.

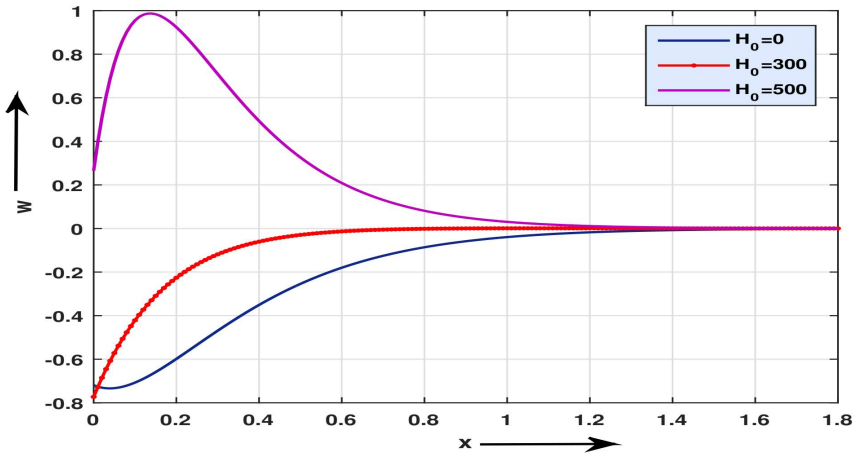

Figure 3.26: Displacement(w) distribution with different values of H_0.

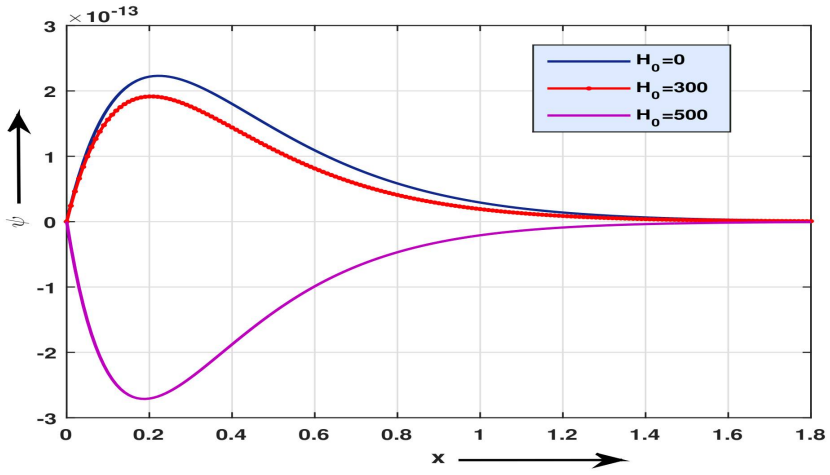

Figure 3.27: The microelongation ψ distribution with different values of H_0.

3.3.8 Appendix

$$a_1 = \frac{\mu}{\rho c_1^2}, a_2 = \frac{\lambda+\mu}{\rho c_1^2}, a_3 = \frac{\beta_1\lambda_0 c_1^2}{a_0\beta_0 w^{*2}},$$
$$a_4 = \frac{\lambda_1 c_1^2}{a_0 w^{*2}}, a_5 = \frac{\lambda_0^2}{a_0\rho w^{*2}}, r_5 = \frac{\rho j_0 c_1^2}{2a_0},$$
$$r_6 = \frac{\rho c_e c_1^2}{k w^*}, r_7 = \frac{\beta_0^2 T_0}{k\rho w^*}, a_9 = \frac{\beta_0\beta_1 T_0 c_1^2}{k\lambda_0 w^*},$$
$$a_{10} = \frac{\lambda}{\rho c_1^2}, a_{11} = \frac{\lambda+2\mu}{\beta_0 T_0}, a_{12} = \frac{\mu+\frac{1}{2}(\lambda+2\mu)P}{\rho c_1^2},$$
$$a_{13} = \frac{\mu-\frac{1}{2}(\lambda+2\mu)P}{\rho c_1^2}, \delta_1 = a_1 + \frac{P}{2},$$
$$l_1 = \frac{\lambda^e+2\mu^e}{\rho^e c_1^{e2}}, l_2 = \frac{\lambda^e+\mu^e}{\rho^2 c_1^{e2}}, l_3 = \frac{\mu^e}{\rho^e c_1^{e2}},$$
$$l_4 = \frac{\lambda^e}{\rho^e c_1^{e2}}, \ell_1 = b^2 l_1 + \omega^2, \ell_2 = l_3 b^2 + \omega^2,$$
$$G = \frac{b^2 l_2^2 - \delta_1 l_1 - \delta_2 l_3}{l_1 l_3}, N = \frac{\delta_1\delta_2}{l_1 l_3},$$

$$r_{51} = \frac{(\beta^2\omega^2 - \Omega^2 + a_1 b^2 - \frac{Pb^2}{2})}{(a_1+a_2+R_1)}, r_{52} = \frac{2\Omega\omega}{(a_1+a_2+R_1)}, r_{56} = \frac{(-iba_2 - ib\frac{P}{2} - ibR_1 - g)}{(a_1+a_2+R_1)},$$
$$r_{57} = \frac{1}{(a_1+a_2+R_1)}, r_{58} = \frac{-1}{(a_1+a_2+R_1)},$$
$$r_{61} = \frac{-2\Omega\omega}{(a_1-\frac{P}{2})}, r_{62} = \frac{(\beta^2\omega^2 - \Omega^2 + a_1 b^2 + a_2 b^2 + R_1 b^2)}{(a_1-\frac{P}{2})}, r_{63} = \frac{ib}{(a_1-\frac{P}{2})}, r_{64} = \frac{-ib}{(a_1-\frac{P}{2})},$$
$$r_{65} = \frac{(g - iba_2 - ib\frac{P}{2} - ibR_1)}{(a_1-\frac{P}{2})}, r_{72} = ib\omega\tau, r_{73} = (a_7\omega\tau + b^2), r_{74} = a_9\omega, r_{75} = a_8\omega\tau,$$
$$r_{82} = iba_5, r_{83} = -a_3, r_{84} = b^2 + a_4 + a_6\omega^2, r_{85} = a_5.$$

$$S_{4n} = ib - a_{10}\lambda_n X_{1n} - X_{2n} + X_{3n},\ S_{5n} = iba_{10} - \lambda_n X_{1n} - X_{2n} + X_{3n},\ S_{6n} = iba_{13}X_{1n} - a_{12}\lambda_n.$$

$$q_{31} = \frac{\omega^2 + b^2 l_3}{l_1}, q_{34} = -\frac{ibl_2}{l_1},$$
$$q_{42} = \frac{\omega^2 + b^2 l_1}{l_3}, q_{43} = \frac{-ibl_2}{l_3},$$
$$x_1 = 1, x_2 = \frac{a_4 - m^2}{ibma_2}, x_3 = mx_1, x_4 = mx_2$$

$$
\begin{aligned}
Y_{1n} &= 1 \\
Y_{2n} &= \frac{m_n^2 - q_{31}}{m_n q_{34}}, \\
Z_{3n} &= ibl_1 + m_n l_4 Y_{2n}, \\
Z_{4n} &= ibl_4 - l_1 m_n Y_{2n}, \\
Z_{5n} &= ibl_3 Y_{2n} + l_3 m_n.
\end{aligned}
$$

V is denoted as

$$
\begin{bmatrix}
S_{51}e^{-\lambda_1 h} & S_{52}e^{-\lambda_2 h} & S_{53}e^{-\lambda_3 h} & S_{54}e^{-\lambda_4 h} & -Z_{31}e^{-m_1 h} & -Z_{32}e^{-m_2 h} & -Z_{33}e^{-m_3 h} & -Z_{34}e^{-m_4 h} \\
S_{61}e^{-\lambda_1 h} & S_{62}e^{-\lambda_2 h} & S_{63}e^{-\lambda_3 h} & S_{64}e^{-\lambda_4 h} & 0 & 0 & 0 & 0 \\
S_{51} & S_{52} & S_{53} & S_{54} & -Z_{31} & -Z_{32} & -Z_{33} & -Z_{34} \\
S_{61} & S_{62} & S_{63} & S_{64} & -Z_{51} & -Z_{52} & -Z_{53} & -Z_{54} \\
X_{11} & X_{12} & X_{13} & X_{14} & -Y_{11} & -Y_{12} & -Y_{13} & -Y_{14} \\
X_{21} & X_{22} & X_{23} & X_{24} & -Y_{21} & -Y_{22} & -Y_{23} & -Y_{24} \\
X_{41} & X_{42} & X_{43} & X_{44} & 0 & 0 & 0 & 0 \\
X_{31} & X_{32} & X_{33} & X_{34} & 0 & 0 & 0 & 0
\end{bmatrix}^{-1}
$$

CHAPTER 4

Generalized Thermoelasticity in Semiconducting Medium

Problems

- Problem-6: ***Photothermal Effect on a Pre-Stressed Rotating Semiconducting Plate with Voids Under Gravitational and Electromagnetic Forces.***
- Problem-7: ***Fractional Thermoelasticity in a Rotating Semiconducting Medium with Effects of Electromagnetic Field, Gravity, Heat Source, and Initial Stress.***

4.1 Problem-6

Photothermal Effect on a Pre-Stressed Rotating Semiconducting Plate with Voids Under Gravitational and Electromagnetic Forces.

4.1.1 Introduction

In recent years, semiconducting materials have found extensive use across various engineering fields due to rapid technological progress. Consequently, researchers are now exploring the study of photothermal effects in semiconducting thermoelastic media. Understanding semiconducting thermoelasticity is crucial for assessing the efficiency and dependability of semiconductor devices in diverse engineering applications, particularly in the swiftly advancing technological environment. Traditional generalized theories of thermoelasticity mainly concentrated on wave propagation in elastic media, often neglecting the complex interaction between coupled plasma and thermal effects.A significant development occurred through the contributions of Lord and Shulman [85], who presented a new model to tackle a crucial problem: the apparent infinite speed of heat transmission, a concept originally introduced by Biot [20]. The novel model, characterized by a heat equation resembling wave dynamics, effectively addressed the issue by guaranteeing finite speeds of propagation for both heat and elastic waves. The exploration of wave propagation in semiconducting media, especially during photothermal processes, has attracted considerable academic and practical attention, with numerous researchers engaging in this area of study. Todorovic [142] explores conditions for neglecting the coupling between these waves and focuses on a semiconductor elastic medium with isotropic and homogeneous thermal and elastic properties. Song et al. [138] presented a coupled approach that involves both generalized thermoelastic and plasma theories. This approach was utilized to investigate the reflection problem at the surface of a semi-infinite semiconducting medium during photothermal processes, as discussed in their work. Their work [138] provides both theoretical and experimental insights into these intricate domains, offering valuable information concerning carrier recombination and transport mechanisms within semiconductor materials. Abo-Dahab and Lotfy [13] explored the two-temperature plane-strain problem within a semiconducting medium, incorporating the photothermal theory. Recent advancements have further enriched this field. This model considered a time-dependent heat source on the surface, all while ensuring the absence of traction under the influence of rotation. Othman and Lotfy [111] delved

into the effects of magnetic fields within a rotational, fiber-reinforced, two-dimensional thermoelastic problem, taking gravitational forces into account. Othman and Song [108] extended their research to study the impact of rotation on the reflection of magnetothermoelastic waves in the presence of temperature fluctuations.

Recent advancements have further enriched this field. Ezzat et al. [40] addressed a three-dimensional problem concerning a homogeneous, isotropic thermoelastic half-space, employing fractional order generalized thermoelasticity. This model considered a time-dependent heat source on the surface, all while ensuring the absence of traction under the influence of rotation. Othman and Lotfy [111] delved into the effects of magnetic fields within a rotational, fiber-reinforced, two-dimensional thermoelastic problem, taking gravitational forces into account. Othman and Song [108] extended their research to study the impact of rotation on the reflection of magnetothermoelastic waves in the presence of temperature fluctuations.

Furthermore, Sarkar and Lahiri [131] explored the influence of gravity fields on plane waves within a fiber-reinforced, two-temperature magneto-thermoelastic medium, all under the Lord–Shulman theory of thermoelasticity. Pal and Kanoria [115] scrutinized the interaction of gravity fields on a transversely isotropic thick plate, utilizing GN-models II and III of generalized thermoelasticity, which considered varying heat sources. The effect of rotation, two-temperature parameters, and voids on magneto-thermoelastic interactions within a homogeneous, isotropic, generalized half-space subject to gravity fields was studied by Deswal and Hooda [32]. In their work, Abd-Alla et al. [5] presented a model of Rayleigh waves on a granular medium within the framework of generalized thermoelasticity, considering the effects of initial stress and gravity fields. Abouelregal and Abo-Dahab [10] examined the induced displacement, temperature, and stress fields in an infinite, nonhomogeneous elastic medium with a spherical cavity, operating within the context of the dual phase-lag (DPL) model. Abo-Dahab and Salama [8] contributed to the field by exploring the reflection and transmission of thermoelastic waves between dissimilar thermoelastic solid half spaces. Their study considered the impact of p-wave interfaces in two solid-liquid media, incorporating initial stress, heat sources, and the influence of a magnetic field.

In the present article, our primary objective is to explore a comprehensive model that investigates the intricate interactions of various factors on an isotropic homogeneous semiconducting plate. The study encompasses the influences of volume fraction, photothermal phenomena, initial stress, electromagnetic fields, gravity, and rotation. All of these elements are studied within the framework of multi-three-phase lag thermoelastic models, and the analysis falls under the broader umbrella of generalized

thermoelasticity. The fundamental governing equations governing this complex problem are presented here. These equations take into account the presence of voids, electromagnetic fields, photothermal effects, initial stresses, gravitational forces, rotational dynamics, and the semiconductor properties of the material. To tackle this multifaceted issue, the research employs the normal mode analysis method to solve partial differential equations under specific boundary conditions. The results obtained from this investigation shed light on the pivotal roles played by photothermal effects, rotation, electromagnetic fields, voids, semiconductor characteristics, initial stresses, gravity, and thermal relaxation times in the phenomenon under scrutiny. The outcomes of this research are presented through analytical expressions and illustrative figures, providing a clear understanding of the impact of external parameters. Moreover, these findings are compared with previous research and practical outcomes. To facilitate a comprehensive overview, tabular data is presented, offering valuable insights for both theoretical developments and practical applications in the realm of semiconducting materials.

4.1.2 Nomenclature

C_E	Specific heat	$\vec{E}$	Components of electric field
e_{ij}	components of strain tensor	γ	$\alpha_T(3\lambda+2\mu)$, Volume coefficient
k	Thermal conductivity	ϵ	$\frac{\gamma}{\rho C_E}$, Dimensionless coupling constant
β	Material constant	τ_0	Relaxation times
T	Temperature	τ_q	Phase lag of heat flux
T_0	Reference temperature	τ_T	Phase lag of temperature gradient
u_i, u, v	Displacement components	β	Ratio of longitudinal to shear wave speed
σ_{ij}	Components of stress tensor	μ_0	Permeability of magnetic field
q_i	Heat flux components	ε_0	Permeability of electric field
c_0	Longitudinal wave speed	N	The carrier density
v_0	Velocity of the heat source	D_E	The carrier diffusion coefficient
α_T	Thermal expansion coefficient	τ	The photo-generated carrier lifetime
δ	Thermal viscosity	θ	$T - T_0$,the thermodynamics temperature
λ , μ	Lame's constants	T	The absolute temperature,
ρ	Density	T_0	Reference temperature
ε_{ijk}	Permutation function	N_0	Carrier concentration
Ω	Angular velocity	κ	Thermal activation coupling parameter
$\alpha, b_v, \omega_v, \zeta$	Void material parameters	m	Coefficient of thermo-void

4.1.3 Basic Equations

In our analysis, we examine a medium that exhibits isotropic and homogeneous semiconductor properties, incorporating the presence of voids. This medium is subject

to a combination of various forces, namely gravitational, and electromagnetic forces, along with the influence of initial stress and rotation. In the scenario where no external heat source is present, the governing equations for this intricate problem can be succinctly articulated as follows:

1. Equation of motion:

$$\sigma_{ji,j} + F_i + G_i = \rho \left[\ddot{u}_i + (\Omega \times (\Omega \times u))_i + (2\Omega \times \dot{u})_i\right] \tag{4.1}$$

Here, G_i represents the gravitational force, and F_i corresponds to the Lorentz force, given as $F_i = \mu_e \left(\vec{J} \times \vec{H}_0\right)_i$. The values of J and F_i can be determined through Maxwell's equations, as presented below:

$$\begin{gathered} \operatorname{curl} \vec{h} = \vec{J} + \varepsilon_0 \frac{\partial \vec{E}}{\partial t}, -\mu_e \frac{\partial \vec{h}}{\partial t} = \operatorname{curl} \vec{E}, \operatorname{div} \vec{h} = 0, \\ \operatorname{div} \vec{E} = 0, \vec{h} = \operatorname{curl}(\vec{u} \times \vec{H}_0,) \; and \; \vec{E} = -\mu_e \left(\frac{\partial \vec{u}}{\partial t} \times \vec{H}_0\right). \end{gathered} \tag{4.2}$$

2. Maxwell's stress equation:

$$\tau_{ij} = \mu_e \left[H_i h_j + H_j h_i - (H_k h_k)\delta_{ij}\right] \tag{4.3}$$

Where τ_{ij} represents Maxwell's stress tensor.

3. Governing equations with plasma, thermoelastic waves, and volume fraction field:

$$D_E N_{,ii} - \frac{N}{\tau} + \kappa T = \frac{\partial N}{\partial t} \tag{4.4}$$

4. Heat conduction equation:

$$\begin{aligned} &[K^*(1 + \sum_{l=1}^{L} \frac{\tau_\nu^l}{l!} \frac{\partial^l}{\partial t^l}) + \epsilon_1 K \frac{\partial}{\partial t}(1 + \sum_{l=1}^{L} \frac{\tau_\theta^l}{l!} \frac{\partial^l}{\partial t^l})]T_{ii} \\ &= (\delta + \tau_0 \frac{\partial}{\partial t} + \sum_{l=1}^{L} \frac{\tau_q^{l+1}}{(l+1)!} \frac{\partial^{l+1}}{\partial t^{l+1}})(\rho C_E \frac{\partial T}{\partial t} + m T_0 \frac{\partial \psi}{\partial t} - \rho Q) \\ &\quad + (\delta + \tau_1 \frac{\partial}{\partial t} + \sum_{l=1}^{L} \frac{\tau_q^{l+1}}{(l+1)!} \frac{\partial^{l+1}}{\partial t^{l+1}}) \gamma_T T_0 \frac{\partial}{\partial t}(e_{kk}) \end{aligned} \tag{4.5}$$

5. Volume fraction field equation:

$$\alpha \psi_{,ii} - b_v u_{i,i} - \zeta \psi - \omega_v \dot{\psi} + mT = \rho \chi \ddot{\psi}_v \tag{4.6}$$

6. Constitutive relations:

$$\begin{aligned}\sigma_{ij} &= [\lambda e - \gamma T - \delta_n N + b_v \psi]\,\delta_{ij} + 2\mu\varepsilon_{ij} - P[\omega_{ij} + \delta_{ij}],\\ \varepsilon_{ij} &= \frac{1}{2}\left(u_{i,j} + u_{j,i}\right), \omega_{ij} = \frac{1}{2}\left(u_{j,i} - u_{i,j}\right), e = u_{i,i}.\end{aligned} \tag{4.7}$$

From equations (4.1) and (4.5), we can derive the following formulation:

$$\begin{aligned}\mu\ u_{i,jj} + (\lambda+\mu)\,u_{j,ji} + \frac{P}{2}(u_{j,ji} - u_{i,jj}) - \gamma T_i - \delta_n N_i + b_v\psi_{,i} + G_i + F_i\\ = \rho\left[\ddot{u}_i + 2\left(\epsilon_{ink}\Omega_n\right)\dot{u}_k + \left(\Omega_i\Omega_k u_k - \Omega_k\Omega_k u_i\right)\right].\end{aligned} \tag{4.8}$$

This set of equations forms the foundation for the comprehensive study of semiconductor behavior under the influence of various physical phenomena, with applications spanning from materials science to electronics and beyond. From the above equations ,we can easily define the different definition of thermoelasticity by changing the parameters.

i. We get Coupled thermoelasticity theory(CTE)[20] model by setting $\tau_\theta = \tau_q = \tau_0$ $=\tau_\nu=\tau_1= 0$ and $\delta = 1$.

ii. Green-Lindsay[46] model(GL) will get if $\tau_\theta = \tau_q = \tau_1 =\tau_\nu= 0$,$\tau_0 > 0$ and $\delta = 1$.

iii. $\tau_\theta =\tau_q=0$,$\tau_0 = \tau_1 > 0$, and $\delta = 1$ represents the Lord-shulman[85] model(LS).

iv. By letting $N = 1$,$\delta = 1$ and $\tau_\nu=0$, $\tau_0 = \tau_1 = \tau_q \geq \tau_\theta$, this represents the simple phase lag(SPL) theory as defined by Tzou[146].

v. By setting $N > 1$,$\tau_0 = \tau_1 = \tau_q$, $\tau_\nu > 0$ and $\tau_\theta > 0$, the definition becomes The refined multiphase thermoelasticity (TPL) theory as defined by Zenkour [160].

vi. This model is confirmed as Bayones et al. [18] if the heat source term and TPL model from heat equation are excluded and $\tau_q = \tau_\theta > 0$, and τ_ν, Q=0, $\delta = 1$.

4.1.4 Problem Formulation

In the xy-plane of two-dimensional space (see figure 4.1), denoted as oxy, various quantities are utilized to represent distinct physical phenomena: $u(x, y, t)$ signifies displacement, reflecting elastic waves; $T(x, y, t)$ represents temperature, indicative of thermal waves; $N(x, y, t)$ expresses carrier density, illustrating plasma waves; and $\psi(x, y, t)$ characterizes the volume fraction field. The occurrence of photothermal voids transport is contingent upon the presence of a non-zero thermal activation coupling parameter denoted as k. The displacement field is formulated as follows:

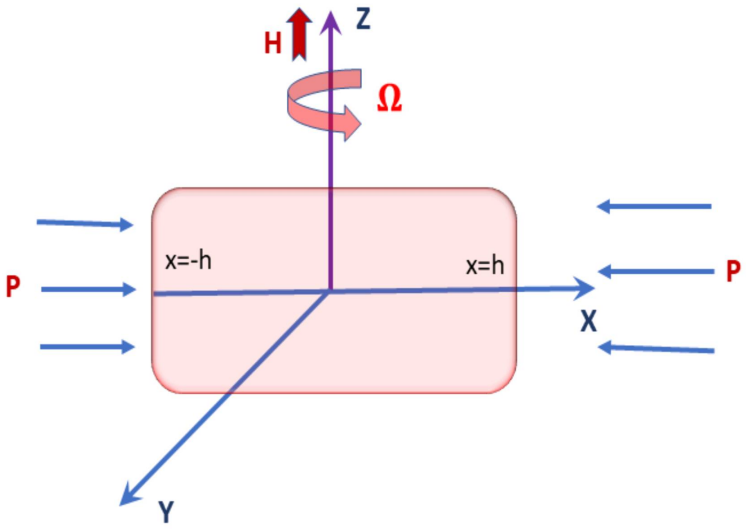

Figure 4.1: Schematic Diagram

$$u = (u_1, u_2, 0)\,, u_1 = u(x, y, t), u_2 = v(x, y, t)$$

and the gravitational force is represented as $G_i = \left(\rho g \frac{\partial v}{\partial y}, -\rho g \frac{\partial u}{\partial y}, 0\right)$. Now, expressing the components of the Lorentz force in the form

$$\vec{H} = \vec{H}_0 + \vec{h}, \quad \vec{H}_0 = (0, 0, H_0)\,,$$

$$(F_x, F_y, F_z) = \mu_e H_0^2 \left(\frac{\partial e}{\partial x} - \varepsilon_0 \mu_e \frac{\partial^2 u}{\partial t^2}, \frac{\partial e}{\partial y} - \varepsilon_0 \mu_e \frac{\partial^2 v}{\partial t^2}, 0\right)$$

where e is the cubical dilatation, given by $e = \frac{\partial u}{\partial x} + \frac{\partial v}{\partial y}$

Maxwell's stress components are then expressed as

$$\tau_{xx} = \tau_{yy} = \mu_e H^2 \left(\frac{\partial u}{\partial x} + \frac{\partial v}{\partial y}\right), \quad \tau_{xy} = 0$$

These equations can be non-dimensionalized using appropriate non-dimensional variables as:

$$\begin{gathered}(x', y', u', v') = \frac{1}{C_T t^*}(x, y, u, v), (t', \tau_0', \tau_\theta') = \frac{1}{t^*}(t, \tau_0, \tau_\theta)\,, \\ (\mathrm{T}', N', \psi') = \frac{1}{(\lambda + 2\mu)}(\gamma \mathrm{T}, \delta_N N, \chi\psi)\,, (\sigma'_{ij}, \tau'_{ij}) = \frac{1}{\mu}(\sigma_{ij}, \tau_{ij})\,, \\ C_T^2 = \frac{\lambda + 2\mu}{\rho}, t^* = \frac{K}{\rho c_e C_T^2}, \Omega = t^*\Omega, g' = \frac{t^*}{C_T} g, \mathrm{P}' = \frac{1}{\mu}\mathrm{P}.\end{gathered} \tag{4.9}$$

Using equation (4.9) into equations (4.1)-(4.8), we obtain

$$\begin{aligned}L_1 \frac{\partial^2 u}{\partial x^2} + R_1 \frac{\partial^2 u}{\partial y^2} + (L_1 - R_1)\frac{\partial^2 v}{\partial x \partial y} - \frac{\partial T}{\partial x} - \frac{\partial N}{\partial x} + \hat{b}\frac{\partial \psi}{\partial x} + g\frac{\partial v}{\partial y} \\ = L_2 \frac{\partial^2 u}{\partial t^2} - \Omega^2 u - 2\Omega \frac{\partial v}{\partial t}\end{aligned} \tag{4.10}$$

$$L_1\frac{\partial^2 v}{\partial y^2}+R_1\frac{\partial^2 v}{\partial x^2}+(L_1-R_1)\frac{\partial^2 u}{\partial x\partial y}-\frac{\partial T}{\partial y}-\frac{\partial N}{\partial y}+\hat{b}\frac{\partial \psi}{\partial y}-g\frac{\partial u}{\partial y} = L_2\frac{\partial^2 v}{\partial t^2}-\Omega^2 v+2\Omega\frac{\partial u}{\partial t} \tag{4.11}$$

$$[p_{l1}\nabla^2-p_{l2}\frac{\partial}{\partial t}]\mathrm{T}-\varepsilon_1 p_{l2}\left(\frac{\partial u}{\partial x}+\frac{\partial v}{\partial y}\right)+\varepsilon_2 N -\varepsilon_4 p_{l2}\psi=0 \tag{4.12}$$

$$[\nabla^2-\frac{Kt^*}{\rho c_e\tau D_E}-\frac{K}{\rho c_e D_E}\frac{\partial}{\partial t}]N+\varepsilon_3\ \mathrm{T}=0 \tag{4.13}$$

$$[\nabla^2-S_2-S_3\frac{\partial}{\partial t}-S_5\frac{\partial^2}{\partial t^2}]\psi-S_1\left(\frac{\partial u}{\partial x}+\frac{\partial v}{\partial y}\right)+S_4\ \mathrm{T}=0 \tag{4.14}$$

$$\begin{aligned}
\sigma_{xx}&=\beta^2\frac{\partial u}{\partial x}+\left(\beta^2-2\right)\frac{\partial v}{\partial y}-\beta^2 T-\beta^2 N+\beta^2\hat{b}\psi-P\\
\sigma_{yy}&=\left(\beta^2-2\right)\frac{\partial u}{\partial x}+\beta^2\frac{\partial v}{\partial y}-\beta^2 T-\beta^2 N+\beta^2\hat{b}\psi-P\\
\sigma_{zz}&=\left(\beta^2-2\right)\left(\frac{\partial u}{\partial x}+\frac{\partial v}{\partial y}\right)-\beta^2 T-\beta^2 N+\beta^2\hat{b}\psi-P\\
\sigma_{xy}&=\left(\frac{\partial u}{\partial y}+\frac{\partial v}{\partial x}\right)-\frac{P}{2}\left(\frac{\partial v}{\partial x}-\frac{\partial u}{\partial y}\right),\sigma_{xz}=\sigma_{yz}=0
\end{aligned} \tag{4.15}$$

where

$$(\varepsilon_1,\varepsilon_2,\varepsilon_3,\varepsilon_4)=\frac{1}{\rho c_e}\left(\frac{\gamma^2\ \mathrm{T}_0 c_e t^*}{K},\frac{\alpha_t E_g t^*}{\tau d_n},\frac{Kkd_n t^*}{\alpha_t D_E},\frac{mT_0\gamma}{\chi},\right),\hat{b}=\frac{b_v}{\chi},\beta^2=\frac{\lambda+2\mu}{\mu},$$

$$(S_1,S_2,S_3,S_4,S_5)=\frac{C_{\mathrm{T}}^2}{\alpha}\left(\frac{b_v t^{*2}\chi^2}{C_{\mathrm{N}}^2\rho},\zeta t^{*2},\omega_v t^*,\frac{mt^{*2}\chi}{\gamma},\rho\chi\right),R_1=\frac{2-\mathrm{P}}{2\beta^2},$$

$$c_A^2=\frac{\mu_e H_0^2}{\rho},c^2=\frac{1}{\varepsilon_0\mu_e},l_{11}=\frac{c_A^2}{C_T^2},l_{12}=\frac{c_A^2}{c^2},L_1=1+l_{11},L_2=1+l_{12}$$

4.1.5 Normal Mode Analysis

The expression characterizing the decomposition of the solution for the considered physical variables follows a specific structure in the normal mode, as depicted by the equation:

$$(u,v,N,T,\psi,\sigma_{ij},\tau_{ij})(x,y,t)=(\bar{u},\bar{v},\bar{N},\bar{T},\bar{\psi},\bar{\sigma_{ij}},\bar{\tau_{ij}})(x)e^{(\omega t+iby)}; \tag{4.16}$$

Here, $\bar{u}(x),\bar{v}(x),\bar{T}(x),\bar{\psi}(x),\bar{\sigma_{jk}}(x),\bar{\tau_{ij}}(x)$ represent the amplitudes of the respective functions. The constant ω is frequency with complex value, i is the imaginary unit, and b signifies the wave numbers in the y-direction.

Utilizing the aforementioned equations, we derive the matrix differential equation in vector form as:

$$\frac{d\overline{\chi}}{dx} = A\overline{\chi} + \overline{R} \tag{4.17}$$

where

$$\overline{\chi} = (\bar{u}, \bar{v}, \bar{\theta}, \bar{N}, \bar{\psi}, \frac{d\bar{u}}{dx}, \frac{d\bar{v}}{dx}, \frac{d\bar{\theta}}{dx}, \frac{d\bar{N}}{dx}, \frac{d\bar{\psi}}{dx})^T \tag{4.18}$$

$$A = \begin{bmatrix} O_{4\times4} & I_{4\times4} \\ B_{4\times4} & C_{4\times4} \end{bmatrix} \tag{4.19}$$

$$B_{4\times4} = \begin{bmatrix} a_{61} & a_{62} & 0 & 0 & 0 \\ a_{71} & a_{72} & a_{73} & a_{74} & a_{75} \\ 0 & a_{82} & a_{83} & a_{84} & a_{85} \\ 0 & 0 & a_{93} & a_{94} & 0 \\ 0 & a_{102} & a_{103} & 0 & a_{105} \end{bmatrix} \quad C_{4\times4} = \begin{bmatrix} 0 & a_{67} & a_{68} & a_{69} & a_{610} \\ a_{76} & 0 & 0 & 0 & 0 \\ a_{86} & 0 & 0 & 0 & 0 \\ 0 & 0 & 0 & 0 & 0 \\ a_{106} & 0 & 0 & 0 & 0 \end{bmatrix}$$

$$I_{4\times4} = \begin{bmatrix} 1 & 0 & 0 & 0 & 0 \\ 0 & 1 & 0 & 0 & 0 \\ 0 & 0 & 1 & 0 & 0 \\ 0 & 0 & 0 & 1 & 0 \\ 0 & 0 & 0 & 0 & 1 \end{bmatrix} \qquad O_{4\times4} = \begin{bmatrix} 0 & 0 & 0 & 0 & 0 \\ 0 & 0 & 0 & 0 & 0 \\ 0 & 0 & 0 & 0 & 0 \\ 0 & 0 & 0 & 0 & 0 \\ 0 & 0 & 0 & 0 & 0 \end{bmatrix}$$

All the components of matrix A in equation (4.19) are given in Appendices.

4.1.6 Solution

To find out the solution of the equation (4.19), we use eigen value approach as (Lahiri et al.[79],Sardar[130]).Now the below equation

$$det(A - \Lambda I) = 0 \tag{4.20}$$

is the characteristic equation of the matrix A while I is the Identity matrix. There are eight eigen values in the form $\Lambda = \pm\Lambda_i$ $(i = 1, 2, 3, 4, 5)$ of the characteristic equation (4.20). The corresponding eigen vector $\underline{X}$ for the eigenvalue Λ obtained as

$$\underline{X} = \begin{bmatrix} \Pi_1 & \Pi_2 & \Pi_3 & \Pi_4 & \Pi_5 & \Lambda\Pi_1 & \Lambda\Pi_2 & \Lambda\Pi_3 & \Lambda\Pi_4 & \Lambda\Pi_5 \end{bmatrix}^T \tag{4.21}$$

where Π_i $(i = 1, 2, 3, 4, 5)$ are given in Appendix. Now the eigenvectors related to the eigen-values $\pm\Lambda_j$, $j = 1, 2, 3, 4$ of A are written as

$$\begin{array}{ll} \Gamma_1 = (\underline{X})_{\Lambda=\Lambda_1}, & \Gamma_6 = (\underline{X})_{\Lambda=-\Lambda_1}, \\ \Gamma_2 = (\underline{X})_{\Lambda=\Lambda_2}, & \Gamma_7 = (\underline{X})_{\Lambda=-\Lambda_2}, \\ \Gamma_3 = (\underline{X})_{\Lambda=\Lambda_3}, & \Gamma_8 = (\underline{X})_{\Lambda=-\Lambda_3}, \\ \Gamma_4 = (\underline{X})_{\Lambda=\Lambda_4}, & \Gamma_9 = (\underline{X})_{\Lambda=-\Lambda_4} \\ \Gamma_5 = (\underline{X})_{\Lambda=\Lambda_5}, & \Gamma_{10} = (\underline{X})_{\Lambda=-\Lambda_5}. \end{array} \tag{4.22}$$

We compute the inverse matrix $V^{-1} = (\omega_{ij})\,,\ i,j = 1(1)10$ of the matrix $V = (\Gamma_1, \Gamma_2, \Gamma_3, \Gamma_4, \Gamma_5, \Gamma_6, \Gamma_7, \Gamma_8, \Gamma_9, \Gamma_{10})$. As a result, the solution to the differential equation (4.20) is

$$\overline{\chi} = \sum_{j=1}^{10} \Gamma_j y_j \tag{4.23}$$

$$y_p = C_p e^{\Lambda_p x} + e^{\Lambda_p x} \int_{-\infty}^{\infty} Q_p e^{-\Lambda_p x}\ and\ Q_p = \sum_{j=1}^{10} \omega_{pj} R_j = \omega_{p8} R_8 \tag{4.24}$$

where C_p is an arbitrary constant. All the values of C_p can be assessed by using boundary and initial conditions. According to our consideration,the medium is taken in plate. So,the field variables can be written in the following final form

$$u = e^{(\omega t + iby)} \sum_{j=1}^{10} X_{1j} (C_j e^{\Lambda_j x} - \frac{Q_j}{\Lambda_j}) \tag{4.25}$$

$$w = e^{(\omega t + iby)} \sum_{j=1}^{10} X_{2j} (C_j e^{\Lambda_j x} - \frac{Q_j}{\Lambda_j}) \tag{4.26}$$

$$N = e^{(\omega t + iby)} \sum_{j=1}^{10} X_{4j} (C_j e^{\Lambda_j x} - \frac{Q_j}{\Lambda_j}) \tag{4.27}$$

$$T = e^{(\omega t + iby)} \sum_{j=1}^{10} X_{3j} (C_j e^{\Lambda_j x} - \frac{Q_j}{\Lambda_j}) \tag{4.28}$$

$$\psi = e^{(\omega t + iby)} \sum_{j=1}^{10} X_{5j} (C_j e^{\Lambda_j x} - \frac{Q_j}{\Lambda_j}) \tag{4.29}$$

Using the above equations (4.25)-(4.29), the simplified stress components are written as-

$$\begin{aligned}
\sigma_{xx} &= e^{(\omega t + iby)} \left(\sum_{j=1}^{10} C_j S_{1j} e^{\Lambda_j x} - M_1 \right) - P, \\
\sigma_{yy} &= e^{(\omega t + iby)} \left(\sum_{j=1}^{10} C_j S_{2j} e^{\Lambda_j x} - M_2 \right) - P, \\
\sigma_{zz} &= e^{(\omega t + iby)} \left(\sum_{j=1}^{10} C_j S_{3j} e^{\Lambda_j x} - M_3 \right) - P, \\
\sigma_{xy} &= e^{(\omega t + iby)} \left(\sum_{j=1}^{10} C_j S_{4j} e^{\Lambda_j x} - M_4 \right), \\
\tau_{xx} &= e^{(\omega t + iby)} \left(\sum_{j=1}^{10} C_j S_{5j} e^{\Lambda_j x} - M_5 \right),
\end{aligned} \tag{4.30}$$

where $X_{1j}, X_{2j}, X_{3j}, X_{4j}, X_{5j}$, S_{ij}, C_j,and M_k (i=1(1)5; k=1(1)5) are given in the Appendix.

4.1.7 Boundary Conditions

The determination of unknown parameters is achieved by applying boundary conditions at $x = \pm h$, leading to the following set of equations:

1. $\sigma_{xx} + \tau_{xx} = -\mathrm{P} - p_1^* e^{\omega t + iby}$,
2. $\sigma_{xy} + \tau_{xy} = 0$,
3. $\theta = p_2^* e^{\omega t + iby}$,
4. $\frac{\partial \psi}{\partial x} = 0$,
5. $D_E \frac{\partial N}{\partial x} = sN$,

where s and p_1^* are arbitrary constants.

Upon substituting the expressions of the relevant physical quantities into the aforementioned boundary conditions, we derive the following equations that the coefficients must satisfy:

$$\begin{aligned}
&\sum_{j=1}^{10} C_j e^{\Lambda_j h}[S_{1j} + S_{5j}] = M_1 + M_5 - {p_1}^*, \quad \sum_{j=1}^{10} C_j e^{-\Lambda_j h}[S_{1j} + S_{5j}] = M_1 + M_5 - {p_1}^*,\\
&\sum_{j=1}^{10} C_j S_{4j} e^{\Lambda_j h} = M_4, \qquad \sum_{j=1}^{10} C_j S_{4j} e^{-\Lambda_j h} = M_4,\\
&\sum_{j=1}^{10} X_{3j}[C_j e^{\Lambda_j h} - \frac{Q_j}{\Lambda_j}] = {p_2}^*, \qquad \sum_{j=1}^{10} X_{3j}[C_j e^{-\Lambda_j h} - \frac{Q_j}{\Lambda_j}] = {p_2}^*,\\
&\sum_{j=1}^{10} X_{5j} C_j \Lambda_j e^{\Lambda_j h} = 0, \qquad \sum_{j=1}^{10} X_{5j} C_j \Lambda_j e^{-\Lambda_j h} = 0,\\
&\sum_{j=1}^{10} (\nu - \Lambda_j) C_j X_{4j} e^{\Lambda_j h} = 0, \qquad \sum_{j=1}^{10} (\nu - \Lambda_j) C_j X_{4j} e^{-\Lambda_j h} = 0.
\end{aligned} \tag{4.31}$$

By solving the ten equations, we obtain the values of the constants C_i for $i = 1(1)10$.

4.1.8 Numerical Results and Discussion

In this investigation, we present a numerical illustration aimed at deriving mathematical outcomes for various physical parameters. The characterization of these quantities hinges on the assumptions outlined in the relevant literature. To conduct our numerical analysis, we have employed silicon as the material of interest, leveraging its specific physical constants as detailed in the works of Othman et al.[113] and Bayones et al.[18]. So, the constants are

$\lambda = 3.64 \times 10^{10}\text{Nm}^{-2}, \mu = 5.46 \times 10^{10}\text{kgm}^{-1}\ \text{s}^{-2}, \rho = 2.33 \times 10^{3}\text{kgm}^{-3}, K = 150\text{wm}^{-1}\text{k}^{-1},$
$s = 2\ \text{ms}^{-1}, \text{f}_1^* = 1,\ \text{d}_\text{n} = -9 \times 10^{-31}\ \text{m}^3, D_E = 2.5 \times 10^{-3}\ \text{m}^2\ \text{s}^{-1}, E_g = 1.12\text{eV}, y = 1.5,$
$t = 3 \times 10^{-5}, \alpha_t = 3 \times 10^{-6}\text{k}^{-1},\ \text{N}_0 = 300K, \zeta = 0.35, \omega_0 = 1.5, \omega = \omega_0 + i\zeta, c_e = 695,$
$\tau = 5 \times 10^{-5},\ , b = 1.2, i = \sqrt{-1}, 0 \leq x \leq 4.5, Q = 0.6.$

4.1.9 Graphical Discussion

Here $L = 5$ taken in throughout discussion for RTPL. The distribution of N with various definitions of thermoelasticity is presented in Figure 4.2. Initial begins with negative value for all definition of thermoelasticity. Figure 4.3 illustrates the σ_{xx} distribution for different time values. As time increase, the value of this distribution gets higher positive value at both boundary. The distribution of stress σ_{xy} with varying initial stress is shown in Figure 4.4. The distribution of stress σ_{xx} with different gravity values is depicted in Figure 4.5. Figure 4.6 displays the stress σ_{xy} distribution with varying gravity values.

The temperature (T) distribution with different initial stress values is visualized in Figure 4.7. Figure 4.8 showcases the temperature (T) distribution with various definitions of thermoelasticity. The u-distribution with different gravity values is illustrated in Figure 4.9. Finally, Figure 4.10 presents the u-distribution with varying initial stress values. All graphs satisfy both the boundary and initial conditions.

4.1.10 Conclusion

In conclusion, our investigation into the thermoelastic behavior of an isotropic homogeneous semiconducting plate, under the influence of various interacting factors, has provided valuable insights. The comprehensive model considered volume fraction, photothermal phenomena, initial stress, electromagnetic fields, gravity, and rotation, within the framework of multi-three-phase lag thermoelastic models falling under generalized thermoelasticity.

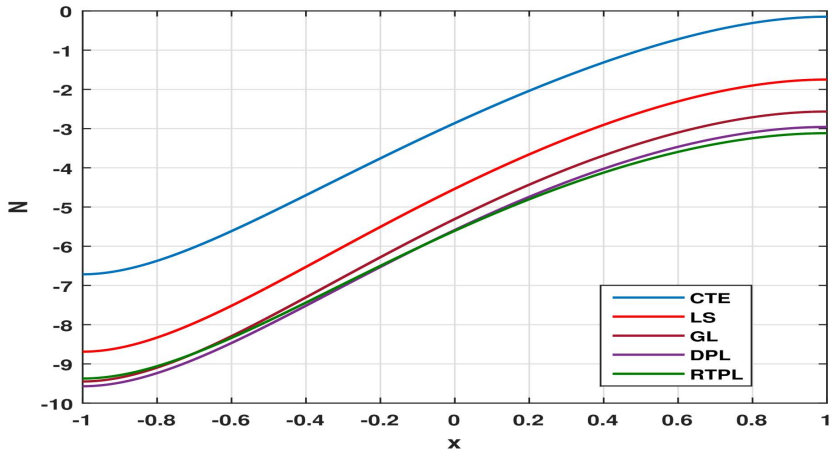

Figure 4.2: The N-distribution with different definition of thermoelasticity.

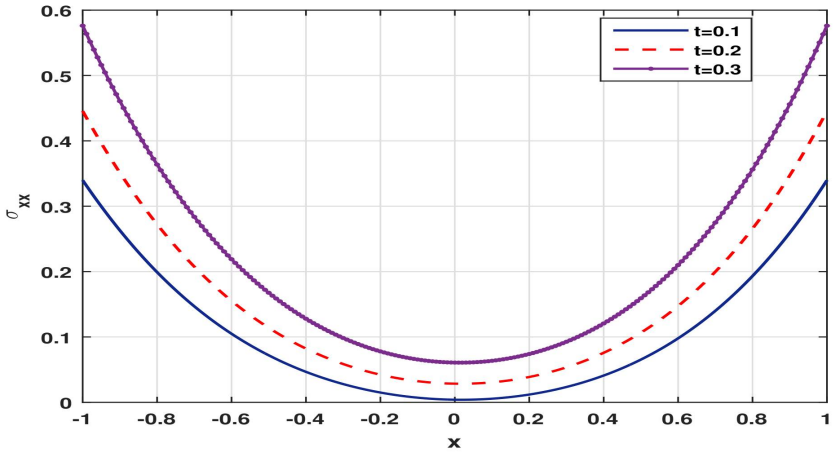

Figure 4.3: The σ_{xx}-distribution with different value of time.

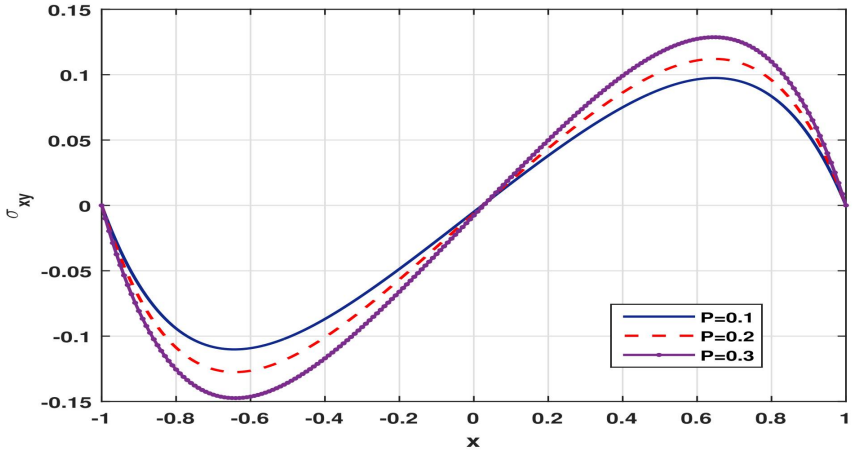

Figure 4.4: The stress σ_{xy} distribution with different value initial stress.

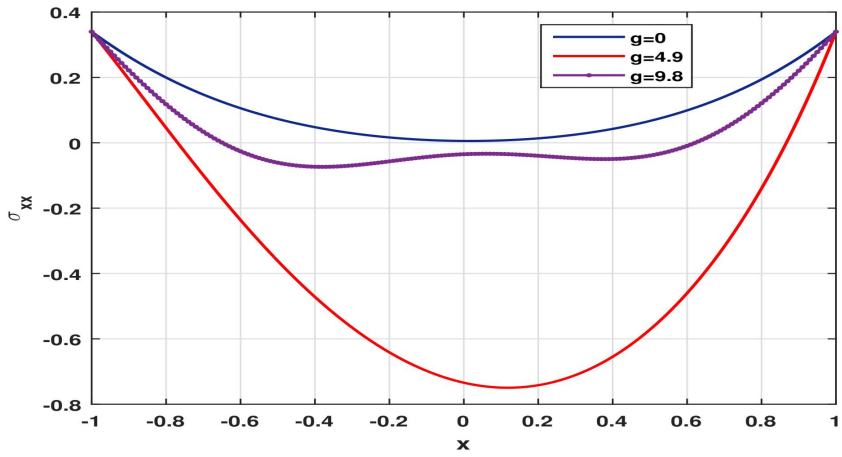

Figure 4.5: The stress σ_{xx} distribution with different value gravity.

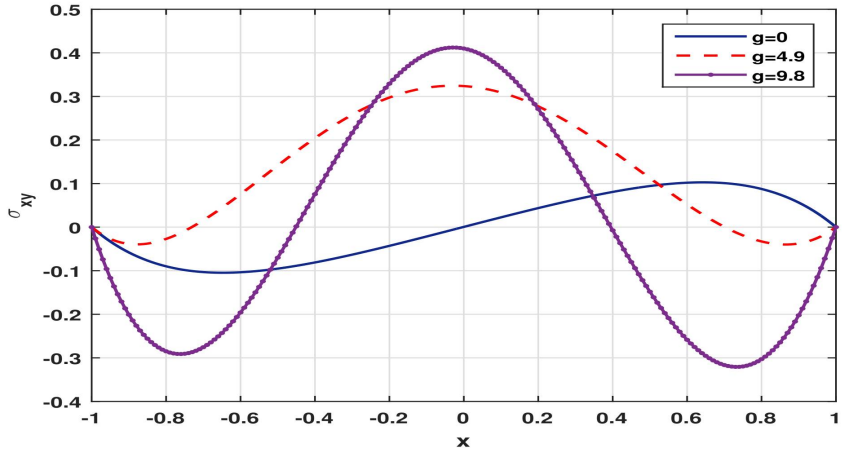

Figure 4.6: The stress σ_{xy} distribution with different value gravity.

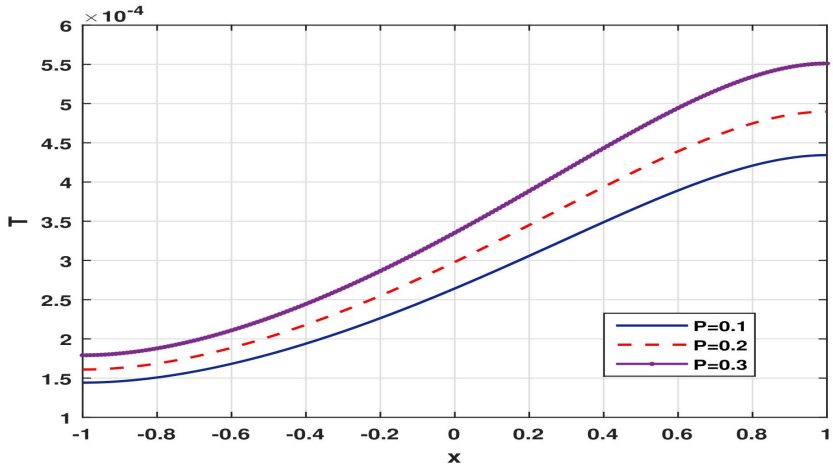

Figure 4.7: The temperature(T) distribution with different value of initial stress.

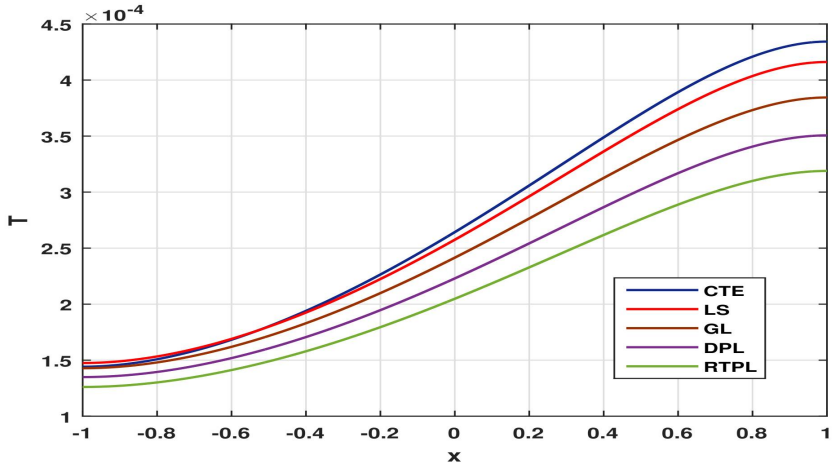

Figure 4.8: The temperature(T) distribution with different definition of thermoelasticity.

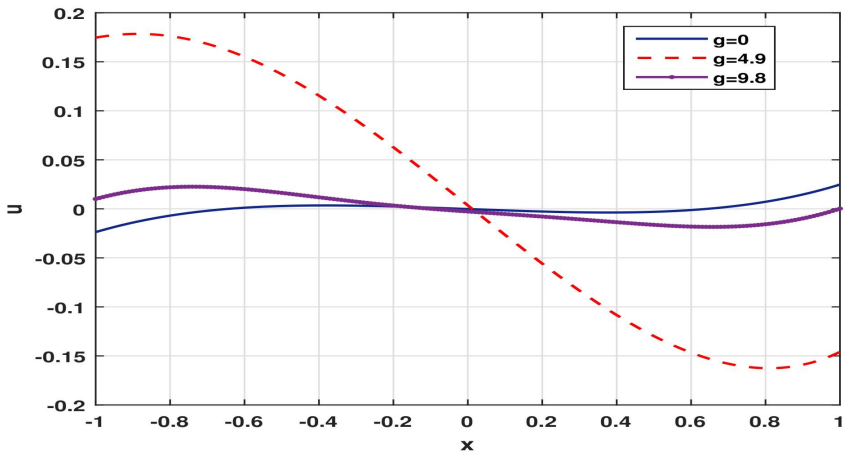

Figure 4.9: The u-distribution with different value of gravity.

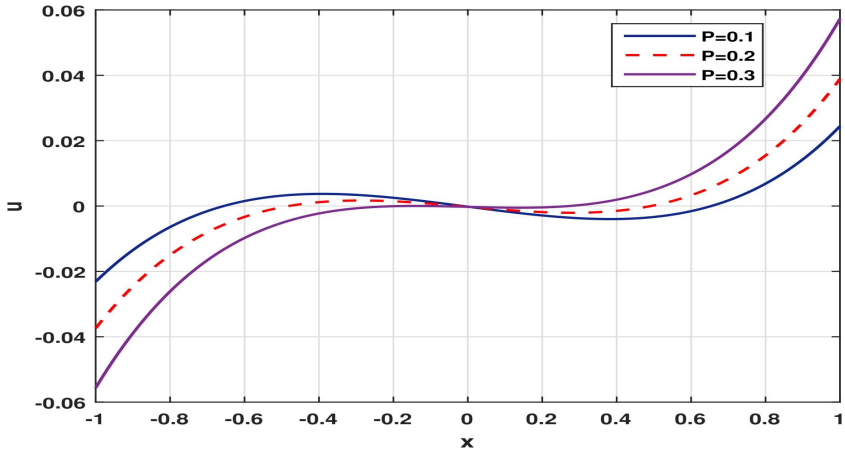

Figure 4.10: The u-distribution with different value of initial stress.

The governing equations, accounting for voids, electromagnetic fields, photothermal effects, initial stresses, gravitational forces, rotational dynamics, and semiconductor properties, were solved using the normal mode analysis method. The results highlighted the significant roles played by photothermal effects, voids, semiconductor characteristics, initial stresses, and gravity in the studied phenomenon.

Through analytical expressions, illustrative figures, and comparative analyses, we gained a nuanced understanding of the impact of these external parameters.

4.1.11 Appendix

$$a_{61} = \frac{b^2R_1 + L_2\omega^2 - \Omega^2}{L_1}, a_{62} = \frac{-(ibg + 2\Omega\omega)}{L_1}, a_{67} = \frac{-ib(L_1 - R_1)}{L_1},$$

$$a_{68} = \frac{1}{L_1}, a_{69} = \frac{1}{L_1}, a_{610} = -\frac{\hat{b}}{L_1},$$

$$a_{71} = \frac{(ibg + 2\Omega\omega)}{R_1}, a_{72} = \frac{b^2L_1 + L_2\omega^2 - \Omega^2}{R_1}, a_{73} = \frac{ib}{R_1}, a_{74} = \frac{ib}{R_1}, a_{75} = \frac{-ib\hat{b}}{R_1},$$

$$a_{76} = \frac{-ib(L_1 - R_1)}{R_1},$$

$$a_{82} = ib\epsilon_1 p_l, a_{83} = b^2 + \omega p_l, a_{84} = \epsilon_2 p_l, a_{85} = \epsilon_1 p_l \omega,$$

$$a_{93} = -\varepsilon_3, a_{94} = (b^2 + l_1 + l_2\omega),$$

$$a_{102} = ibS_1, a_{103} = -S_5, a_{105} = b^2 + S_2 + S_3\omega + S_4\omega^2, a_{106} = S_1.$$

$$p_{l1} = [K_1(1 + \sum_{l=1}^{L} \frac{\tau_\nu^l}{l!}\frac{\partial^l}{\partial t^l}) + \epsilon_1\frac{\partial}{\partial t}(1 + \sum_{l=1}^{L} \frac{\tau_\theta^l}{l!}\frac{\partial^l}{\partial t^l})], p_{l2} = (\delta + \tau_1\frac{\partial}{\partial t} + \sum_{n=1}^{L} \frac{\tau_q^{n+1}}{(n+1)!}\frac{\partial^{n+1}}{\partial t^{n+1}}),$$

$$p_l = \frac{(\delta + \tau_0\omega + \sum_{n=1}^{L} \frac{\tau_q^{n+1}}{(n+1)!}\omega^{n+1})}{[K_1(1 + \sum_{l=1}^{L} \frac{\tau_\nu^l}{l!}\omega^l) + \epsilon_1\frac{\partial}{\partial t}(1 + \sum_{l=1}^{L} \frac{\tau_\theta^l}{l!}\omega^l)]}.$$

$$a_1 = L_1b^2 + L_2\omega^2 - \Omega^2, a_2 = \varepsilon_1\omega P_l, a_3 = \Lambda_1 b^2 + \omega P_l, a_5 = 2\Omega\omega + ibg,$$

$$a_{55} = b^2 + S_2 + S_3\omega + S_5\omega^2, a_6 = \varepsilon_4\omega P_l, l_1 = \frac{Kt^*}{\rho c_e \tau D_E}, l_2 = \frac{K\omega}{\rho c_e D_E},$$

$$m^2 = R_1b^2 + L_2\omega^2 - \Omega^2, a_4 = a_{94},$$

$$\mho_{1n} = \left(\Lambda_n^2 - b^2\right), \mho_{2n} = \left(\Lambda_n^2 - a_5\right), \mho_{3n} = \left(\Lambda_n^2 - a_3\right), \mho_{4n} = \left(J_1\Lambda_n^2 - a_1\right),$$
$$\mho_{5n} = \left(\Lambda_n^2 - a_4\right), \mho_{6n} = \left(\Lambda_1\Lambda_n^2 - a_3\right), \mho_{7n} = \left(\Lambda_n^2 - a_{55}\right), X_{1n} = 1, X_{2n} = \frac{-a_5}{\Gamma_1\Lambda_n^2 - m^2},$$
$$X_{3n} = \frac{\left[a_6\mho_4 - a_2 b\mho_1 - a_5 a_6 X_{2n}\right]\mho_5}{\varepsilon_3\left(\varepsilon_2\hat{b} - a_6\right) - \left[\mho_6\hat{b} - a_6\right]\mho_5}, X_{4n} = \frac{\varepsilon_3 X_{3n}}{\mho_{5n}}, X_{5n} = \frac{S_4 X_{3n} + S_1\mho_{1n}}{\mho_{7n}},$$
$$S_{5n} = \frac{c_A^2}{\mu}\mho_{1n},$$
$$S_{1n} = \beta^2\left(\Lambda_n^2 - b^2 - X_{3n} - X_{4n} + \hat{b}X_{5n}\right) + 2b^2 - 2ib\Lambda_n X_{2n},$$
$$S_{2n} = \beta^2\left(\Lambda_n^2 - b^2 - X_{3n} - X_{4n} + \hat{b}X_{5n}\right) - 2\left(\Lambda_n^2 - ib\Lambda_n X_{2n}\right),$$
$$S_{4n} = ibX_{1n} - \Lambda_n X_{2n} + \frac{\mathrm{P}}{2}\left(\Lambda_n X_{2n} + ibX_{1n}\right),$$

$$M_1 = \sum_{j=1}^{10}\frac{Q_j}{\Lambda_j}\left(ib(\beta^2 - 2)X_{2j} - \beta^2(X_{3n} + X_{4n} - \hat{b}X_{5n})\right),$$
$$M_2 = \sum_{j=1}^{10}\frac{Q_j}{\Lambda_j}(ib\beta^2 X_{2j} - \beta^2(X_{3n} + X_{4n} - \hat{b}X_{5n})),$$
$$M_3 = \sum_{j=1}^{10}\frac{Q_j}{\Lambda_j}\left(ib\beta^2(X_{1j} + X_{2j}) - \beta^2(X_{3n} + X_{4n} - \hat{b}X_{5n})\right),$$
$$M_4 = \sum_{j=1}^{10}\frac{Q_j}{\Lambda_j}(ib(1 + \frac{P}{2})X_{1j}),$$
$$M_5 = \sum_{j=1}^{10}\frac{Q_j}{\Lambda_j}(ib\frac{c_A^2}{\mu}X_{2j}).$$

4.2 Problem-7

Fractional Thermoelasticity in a Rotating Semiconducting Medium with Effects of Electromagnetic Field, Gravity, Heat Source, and Initial Stress.

4.2.1 Introduction

A wide range of thermoelastic applications have been influenced by photothermal effects in recent years. Thus, researchers have shown keen interest in exploring this field. There has been investigation into both the thermal and non-thermal effects of photothermal radiation, taking external factors into account such as laser effects and electromagnetic fields. Among others, Lord and Shulman [85] examined the effects of single relaxation times on wave velocities of various kinds. According to various laboratory studies, this characteristic time is crucial in thermal conductivity equations. According to Hetnarski and Ignaczak [57], generalized thermoelasticity affects displacements, temperatures, and stresses with variation in experimental time. They compared different times to determine velocities in their examination.

The exploration of thermoelastic models has evolved with the incorporation of fractional calculus. Hamza et al. [54] introduced memory time effect over electromagnetic force in a fractional order thermoelastic medium. Magin and Royston [89] introduced a pioneering model that utilized fractional derivatives of deformation to characterize material behavior. Here, the zero-order derivative corresponds to a Hookean solid, while the first order is associated with a Newtonian fluid. Thermoelastic and thermo-viscoelastic materials fall within an intermediate range, featuring a fractional-order parameter between zero and one. Another noteworthy contribution comes from Youssef [153], who developed a generalized thermoelasticity theory dependent on strain with a fractional-order derivative. This model presented a modification to the Duhamel-Neumann [34] stress-strain relation. Youssef also applied thermoelasticity with fractional-order strain to a one-dimensional half-space within the frameworks of Biot [20], Lord-Shulman [85], Green-Lindsay [46], and Green-Naghdi [50] type II models. Meanwhile, Song et al. [138] conducted a study on the reflection of photothermal waves in a semiconducting medium. Hobiny and Abbas[58] discusses effect of fractional order thermoelasticity in semiconducting plane. Abbas et al. [4] developed a photo-thermal effect in view of DPL model. Bayones et al. [18] studied

the effects of rotation, electromagnetic field, initial stress in a semiconducting medium with void.

We present a fractional thermoelasticity for the thermoelastic photothermal response of a rotating semiconducting half-space medium. The semiconducting medium is subjected to an internal heat source. The propagation of photothermal waves in a prestressed semiconducting half-space with a gravity effect has been investigated. The normal mode analysis precisely resolved all coupled photo-thermoelastic equations. The eigenvalue approach is adopted to derive the analytical solution of the main variables of the medium. Temperature, horizontal and vertical displacements, stresses, and carrier density were all measured. The dependence of all field variables on the internal heat source, initial stress, rotation, electromagnetic field, fractional order parameter, and inclusion of gravity is demonstrated. The results are graphed to serve as benchmarks for future comparisons, and additional results are shown to demonstrate the physical meaning of the phenomenon.

4.2.2 Nomenclature

C_E	Specific heat	δ	Thermal viscosity
e_{ij}	Components of strain tensor	λ	Lame's constants
K	Thermal conductivity	γ	$\alpha_T(3\lambda+2\mu)$ Volume coefficient
β	Material constant		of thermal expansion
T	Temperature	Ω	Angular velocity
T_0	Reference temperature	$\vec{E}$	Components of electric field
u_i	Displacement components	ρ	Density
q_i	Heat flux components	τ_0	Relaxation times
c_0	Longitudinal wave speed	σ_{ij}	Components of stress tensor
v_0	Velocity of the heat source	τ_0	Relaxation time parameter
α_T	Thermal expansion coefficient	μ_0	Permeability of magnetic field
P	Initial stress	ε_0	Permeability of electric field
ϑ	$\frac{sC_\theta\eta}{D_E}$	g	Gravity

4.2.3 Basic Equatons

Following Kilany et al. [73] and Youssef [153], we consider a homogeneous thermoelastic semiconducting medium governed by the following equations:

1. Equation of motion:

$$\sigma_{ij,j} + F_i + G_i = \rho[\ddot{u}_i + (\Omega \times (\Omega \times u))_i + (2\Omega \times \dot{u})_i] \tag{4.32}$$

where, G_i is the force due to gravity and F_i is the Lorentz force, represented as $F_i = \mu_0 \left(\vec{J} \times \vec{H}_0\right)_i$. J and F_i can be found easily from Maxwell's equation which are given below

$$\begin{gathered} curl\ \vec{h} = \vec{J} + \varepsilon_0 \frac{\partial \vec{E}}{\partial t}, -\mu_0 \frac{\partial^\beta \vec{h}}{\partial t^\beta} = curl\vec{E}, \\ div\vec{h} = 0, div\vec{E} = 0 \\ \vec{h} = curl\left(\vec{u} \times \vec{H}_0\right), \vec{E} = -\mu_0 \left(\frac{\partial \vec{u}}{\partial t} \times \vec{H}_0\right) \end{gathered} \tag{4.33}$$

where

$$\frac{\partial^\alpha}{\partial t^\alpha} f(x,t) = \begin{cases} f(x,t) - f(x,0), & \text{when } \alpha \to 0, \\ I^{1-\alpha} \frac{\partial f(x,t)}{\partial t}, & \text{when } 0 < \alpha < 1, \\ \frac{\partial f(x,t)}{\partial t}, & \text{when } \alpha = 1. \end{cases} \tag{4.34}$$

In the above definition, the Riemann-Liouville fractional integral operator I^α is defined as $I^\alpha f(t) = \frac{1}{\Gamma(\alpha)} \int_0^t (t-s)^{\alpha-1} f(s)\, ds$.

2. Maxwell's stress equation:

$$\tau_{ij} = \mu_0 \left[H_i h_j + H_j h_i - \left(\vec{H}_k \cdot \overrightarrow{h_k}\right) \delta_{ij}\right], i, j = 1, 2, 3 \tag{4.35}$$

where τ_{ij} is Maxwell's stress tensor.

3. The equation of coupled plasma transport:

$$D_E \nabla^2 N - \frac{N}{\tau} + k\tau = \frac{\partial N}{\partial t}. \tag{4.36}$$

4. Heat conduction equation:

$$KI^{\alpha-1} \nabla^2 T + \frac{E_g}{\tau} N = \left(1 + \tau_o \frac{\partial}{\partial t}\right) (\gamma T_o \dot{e} + \rho c_e \dot{T} - \rho Q) \tag{4.37}$$

5. The constitutive relations:

$$\sigma_{ij} = 2\mu \varepsilon_{ij} + [\lambda e - \gamma \mathrm{T} - \delta_n N - \mathrm{P}]\, \delta_{ij} - \mathrm{P}\omega_{ij} \tag{4.38}$$

$$\varepsilon_{ij} = \frac{1}{2}\left(u_{i,j} + u_{j,i}\right), \omega_{ij} = \frac{1}{2}\left(u_{j,i} - u_{i,j}\right), e = u_{i,i}, i, j = 1, 2, 3 \tag{4.39}$$

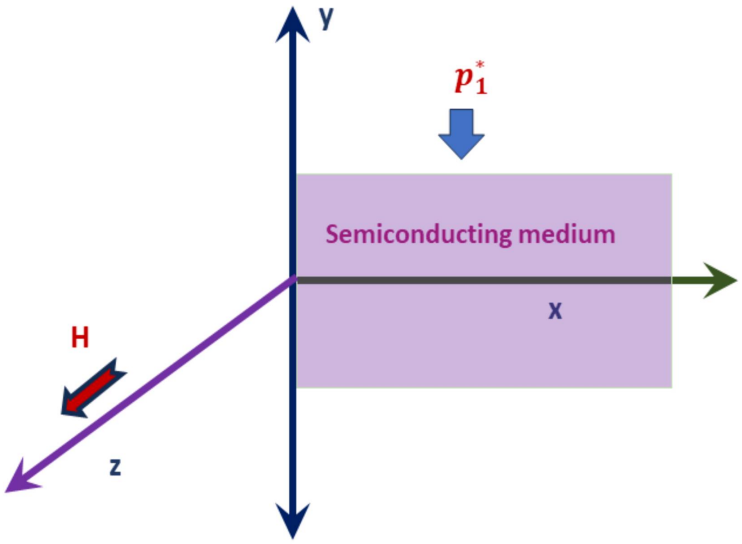

Figure 4.11: Schematic Diagram

4.2.4 Formulation of the Problem

In two dimensions (see figure 4.11) oxy (xy-plane), the quantities $u(x,y,t), T(x,y,t), N(x,y,t)$ express the displacement (elastic waves), temperature (thermal waves), carrier density (plasma waves) respectively. The displacement is

$$u = (u_1, u_2, 0)\,, u_1 = u(x,y,t), u_2 = v(x,y,t).$$

Therefore, equation of motion becomes,

$$\begin{aligned}\left(\mu - \frac{\mathrm{P}}{2}\right)\nabla^2 u_i + \left(\lambda + \mu + \frac{\mathrm{P}}{2}\right)\nabla e - \gamma\nabla T - \delta_n \nabla N + G_i + F_i \\ = \rho\left[\ddot{u}_i + \{\Omega \times \Omega \times u\}_i + (2 \times \Omega \times \dot{u})_i\right]\end{aligned} \tag{4.40}$$

where

$$G_i = \left(\rho g\frac{\partial v}{\partial x}, -\rho g\frac{\partial u}{\partial x}, 0\right)$$

$$\vec{H} = \vec{H}_0 + \vec{h}(x,y,t), \vec{H}_0 = (0,0,H_0)$$

$$J = (\frac{\partial h}{\partial x} - \epsilon_0\frac{\partial E}{\partial t}, \frac{\partial h}{\partial y} - \epsilon_0\frac{\partial E}{\partial t}, 0)$$

$$h = (0, 0, -\left(\frac{H_0\beta!}{\tau^{\beta-1}}\right)\frac{\partial^{1-\beta}}{\partial t^{1-\beta}}e)$$

$$E = (-\mu_0 H_0\frac{\partial u}{\partial t}, -\mu_0 H_0\frac{\partial v}{\partial t}, 0)$$

$$(F_x, F_y, F_z) = \mu_e H_0^2\left(\beta!\tau^{\beta-1}\frac{\partial^{1-\beta}}{\partial t^{1-\beta}}\frac{\partial e}{\partial x} - \varepsilon_0\mu_e\frac{\partial^2 u}{\partial t^2}, \beta!\tau^{\beta-1}\frac{\partial^{1-\beta}}{\partial t^{1-\beta}}\frac{\partial e}{\partial y} - \varepsilon_0\mu_e\frac{\partial^2 v}{\partial t^2}, 0\right)$$

By using the following non-dimensional variables to the above equations

$$\begin{gathered}(x', y', u', v') = \frac{1}{c_\theta \eta}(x, y, u, v), (t', \tau', \tau_0', \tau'_\theta) = \frac{1}{\eta}\left(t, \tau, \tau_0, \tau_\theta\right), \\ (\mathrm{T}', N') = \frac{1}{(\lambda + 2\mu)}\left(\gamma \mathrm{T}, \delta_N N\right), (\sigma'_{ij}, \tau'_{ij}) = \frac{1}{\mu}\left(\sigma_{ij}, \tau_{ij}\right), \\ c_\theta^2 = \frac{\lambda + 2\mu}{\rho}, \eta = \frac{K}{\rho c_e c_\theta^2}, (Q^*, \Omega) = \eta(Q, \Omega), g' = \frac{\eta}{c_\theta} g, \mathrm{P}' = \frac{1}{\mu}\mathrm{P}.\end{gathered} \tag{4.41}$$

Using equation (4.41) into equations (4.32)-(4.40) we obtain

$$\begin{gathered}J_1 u_{,xx} + \Gamma_1 u_{,yy} + (J_1 - \Gamma_1) v_{,xy} - T_{,x} - N_{,x} + g v_{,x} = J_2 u_{,tt} - \Omega^2 u - 2\Omega v_{,t} \\ J_1 v_{,yy} + \Gamma_1 v_{,xx} + (J_1 - \Gamma_1) u_{,xy} - T_{,y} - N_{,y} - g u_{,x} = J_2 v_{,tt} - \Omega^2 v - 2\Omega u_{,t} \\ \nabla^2 \mathrm{T} - \varepsilon_1 (1 + \tau_o \frac{\partial}{\partial t})(u_{,x} + v_{,y}) + \varepsilon_2 N + \varepsilon (1 + \tau_0 \frac{\partial^\alpha}{\partial t^\alpha}) T = (1 + \tau_0 \frac{\partial^\alpha}{\partial t^\alpha}) Q \\ [\nabla^2 - \frac{K\eta}{\rho c_e \tau D_E} - \frac{K}{\rho c_e D_E}\frac{\partial}{\partial t}] N + \varepsilon_3 \ \mathrm{T} = 0\end{gathered} \tag{4.42}$$

$$\begin{gathered}\sigma_{xx} = \beta^2 u_{,x} + \left(\beta^2 - 2\right) v_{,y} - \beta^2 T - \beta^2 N - P \\ \sigma_{xy} = u_{,y} + v_{,x} - \frac{P}{2}\left(v_{,x} - u_y\right).\end{gathered} \tag{4.43}$$

where

$$\begin{gathered}(\varepsilon_1, \varepsilon_2, \varepsilon_3, \varepsilon_4) = \frac{1}{\rho c_e}\left(\frac{\gamma^2 \ \mathrm{T}_0 c_e \eta}{K}, \frac{\alpha_t E_g \eta}{\tau d_n}, \frac{K k d_n \eta}{\alpha_t D_E}, \frac{\gamma T_0}{K}\right), \beta^2 = \frac{\lambda + 2\mu}{\mu}, \\ \Gamma_1 = \frac{2 - \mathrm{P}}{2\beta^2}, c_A^2 = \mu_e H_0^2, c^2 = \frac{1}{\varepsilon_0 \mu_e}, \\ R_H = \frac{c_A^2}{C_{\mathrm{N}}^2}, \alpha^* = \frac{c_A^2}{c^2}, J_1 = (1 + \beta! \tau^{\beta - 1} \frac{\partial^{1-\beta}}{\partial t^{1-\beta}}) R_H, J_2 = 1 + \alpha^*.\end{gathered}$$

4.2.5 Solution Procedure

The solution of the considered physical variables decomposes in the normal mode as

$$(u, v, N, T, \sigma_{ij}, \tau_{ij})(x, y, t) = (\bar{u}, \bar{v}, \bar{N}, \bar{T}, \bar{\sigma_{ij}}, \bar{\tau_{ij}})(x) e^{(\omega t + iby)}; \tag{4.44}$$

where $\bar{u}(x), \bar{v}(x), \bar{T}(x), \bar{\sigma_{jk}}(x), \bar{\tau_{ij}}(x)$ are amplitudes, ω is a complex constant, $i = \sqrt{-1}$, and b is the wave number in the y-direction.

Using the above equations, we obtain the vector matrix differential equation

$$\frac{d\overline{\chi}}{dx} = A\overline{\chi} + \overline{f}, \tag{4.45}$$

where

$$\overline{\chi} = (\bar{u}, \bar{v}, \bar{T}, \bar{N}, \frac{d\bar{u}}{dx}, \frac{d\bar{v}}{dx}, \frac{d\bar{\theta}}{dx}, \frac{d\bar{N}}{dx})^T, \tag{4.46}$$

$$A = \begin{bmatrix} O_{4\times4} & I_{4\times4} \\ B_{4\times4} & C_{4\times4} \end{bmatrix}, \quad and \quad \overline{f} = (0,0,0,0,0,0,R_7,0)^T. \tag{4.47}$$

Now

$$B_{4\times4} = \begin{bmatrix} a_{51} & a_{52} & 0 & 0 \\ a_{61} & a_{62} & a_{63} & a_{64} \\ 0 & a_{72} & a_{73} & a_{74} \\ 0 & 0 & a_{83} & a_{84} \end{bmatrix}, \quad C_{4\times4} = \begin{bmatrix} 0 & a_{56} & a_{57} & a_{58} \\ a_{65} & 0 & 0 & 0 \\ a_{75} & 0 & 0 & 0 \\ 0 & 0 & 0 & 0 \end{bmatrix}, \tag{4.48}$$
$$I_{4\times4} = \text{Identity Matrix}, \quad O_{4\times4} = \text{Zero Matrix}.$$

To find the solution of the equation (4.45), we use the eigenvalue approach as described by Das et al. [31]. Now the below equation

$$det(A - \Lambda I) = 0 \tag{4.49}$$

is the characteristic equation of the matrix A while I is the Identity matrix. There are eight eigen values in the form $\Lambda = \pm\Lambda_i$ $(i = 1,2,3,4,5)$ of the characteristic equation (4.49). The corresponding eigen vector $\underline{X}$ for the eigenvalue Λ obtained as

$$\underline{X} = \begin{bmatrix} \Pi_1 & \Pi_2 & \Pi_3 & \Pi_4 & \Lambda\Pi_1 & \Lambda\Pi_2 & \Lambda\Pi_3 & \Lambda\Pi_4 \end{bmatrix}^T \tag{4.50}$$

where Π_i $(i = 1,2,3,4)$ are given in Appendix.

Now the eigenvectors related to the eigen-values $\pm\Lambda_j$, $j = 1,2,3,4$ of A are written as

$$\begin{array}{llll} \Gamma_1 = (\underline{X})_{\Lambda=\Lambda_1}, & \Gamma_2 = (\underline{X})_{\Lambda=\Lambda_2}, & \Gamma_3 = (\underline{X})_{\Lambda=\Lambda_3} & \Gamma_4 = (\underline{X})_{\Lambda=\Lambda_4} \\ \Gamma_5 = (\underline{X})_{\Lambda=-\Lambda_1}, & \Gamma_6 = (\underline{X})_{\Lambda=-\Lambda_2}, & \Gamma_7 = (\underline{X})_{\Lambda=-\Lambda_3}, & \Gamma_8 = (\underline{X})_{\Lambda=-\Lambda_4}. \end{array} \tag{4.51}$$

We compute the inverse matrix $V^{-1} = (\omega_{ij})$, $i,j = 1(1)8$ of the matrix $V = (\Gamma_1,\Gamma_2,\Gamma_3,\Gamma_4,\Gamma_5,\Gamma_6,\Gamma_7,\Gamma_8)$. As a result, the solution to the differential equation (4.51) is

$$\overline{Y} = \sum_{j=1}^{8} \Gamma_j y_j \tag{4.52}$$

$$y_p = C_p e^{\Lambda_p x} + e^{\Lambda_p x} \int_{-\infty}^{\infty} Q_p e^{-\Lambda_p x} \; and \; Q_p = \sum_{j=1}^{8} \omega_{pj} R_j = \omega_{p7} R_7 \tag{4.53}$$

where C_p is an arbitrary constant. All the values of C_p can be assessed by using

boundary and initial conditions. Therefore the final results are given below,

$$\begin{aligned} u &= e^{(\omega t+iqy)}\sum_{j=1}^{4} X_{1j}(C_j e^{\Lambda_j x} - \frac{Q_j}{\Lambda_j}), \\ v &= e^{(\omega t+iqy)}\sum_{j=1}^{4} X_{2j}(C_j e^{\Lambda_j x} - \frac{Q_j}{\Lambda_j}) \\ T &= e^{(\omega t+iby)}\sum_{j=1}^{4} X_{3j}(C_j e^{\Lambda_j x} - \frac{Q_j}{\Lambda_j}) \\ N &= e^{(\omega t+iby)}\sum_{j=1}^{4} X_{4j}(C_j e^{\Lambda_j x} - \frac{Q_j}{\Lambda_j}) \end{aligned} \tag{4.54}$$

where the real part of $\Lambda_j < 0, j = 1(1)4$. Using the above equations (4.54), the simplified stress components are written as:

$$\begin{aligned} \sigma_{xx} &= e^{(\omega t+iby)}\left(\sum_{j=1}^{4} C_j S_{1j} e^{\Lambda_j x} - M_1\right) - P, \\ \sigma_{xy} &= e^{(\omega t+iby)}\left(\sum_{j=1}^{4} C_j S_{2j} e^{\Lambda_j x} - M_2\right), \\ \tau_{xx} &= e^{(\omega t+iby)}\left(\sum_{j=1}^{4} C_j S'_{1j} e^{\Lambda_j x} - M_3\right) \\ \sigma_{yy} &= e^{(\omega t+iby)}\left(\sum_{j=1}^{4} C_j S_{4j} e^{\Lambda_j x} - M_4\right) - P, \end{aligned} \tag{4.55}$$

where $S_{ij}, S'_{ij}, M_i, i, j = 1(1)4$ are given in Appendix.

4.2.6 Boundary Conditions

The determination of unknown parameters is achieved by applying boundary conditions at $x = 0$, expressed as:

$$\sigma_{xx} + \tau_{xx} = -\mathrm{P} - p_1^* e^{\omega t+iby},\ \sigma_{xy} + \tau_{xy} \ = 0,\ \frac{\partial \mathrm{T}}{\partial x} = 0,\ D_E \frac{\partial N}{\partial x} \ = sN, \tag{4.56}$$

where s and p_1^* are arbitrary constants. These conditions help determine the values of the unknown parameters under consideration. Therefore using above equation (4.56), we get the unknown parameters as:

$$\begin{pmatrix} C_1 \\ C_2 \\ C_3 \\ C_4 \end{pmatrix} = \begin{pmatrix} H_{11} & H_{12} & H_{13} & H_{14} \\ H_{21} & H_{22} & H_{23} & H_{24} \\ \Lambda_1 X_{31} & \Lambda_2 X_{32} & \Lambda_3 X_{33} & \Lambda_4 X_{34} \\ s_1 S_{41} & s_2 S_{42} & s_3 S_{43} & s_4 S_{44} \end{pmatrix}^{-1} \begin{pmatrix} M_1 + M_3 - p_1^* \\ M_2 \\ 0 \\ \vartheta M_5 \end{pmatrix}$$

where $s_i = (\vartheta - \Lambda_i)\,, H_{1i} = S_{1i} + S'_{1i}, H_{2i} = S_{2i}\ \ i = 1(1)4$ and M_5 given in Appendix.

4.2.7 Numerical Discussion

We consider a numerical example in which to find mathematical results for the different physical quantities whose behavior is to be determined primarily on the assumptions cited in the matter. Therefore, numerical calculations have been made using silicon material which has the physical constants as follows Othman et al. [113]:

$$\lambda = 3.64 \times 10^{10}\mathrm{Nm}^{-2}, \mu = 5.46 \times 10^{10}\mathrm{kgm}^{-1}\ \mathrm{s}^{-2}, \rho = 2.33 \times 10^{3}\mathrm{kgm}^{-3},$$
$$K = 150\mathrm{wm}^{-1}\mathrm{k}^{-1}, s = 2\ \mathrm{ms}^{-1}, \mathrm{p}_1^* = 1,\ \mathrm{d_n} = -9 \times 10^{-31}\ \mathrm{m}^3,$$
$$D_E = 2.5 \times 10^{-3}\ \mathrm{m}^2\ \mathrm{s}^{-1}, E_g = 1.12\mathrm{eV}, y = 1.5, \alpha = 0.6,$$
$$t = 3 \times 10^{-5}, \alpha_t = 3 \times 10^{-6}\mathrm{k}^{-1},\ \mathrm{N}_0 = 300K, \zeta = 0.35, \omega_0 = 1.5,$$
$$\omega = \omega_0 + i\zeta, c_e = 695, \tau = 5 \times 10^{-5}, b = 1.2, i = \sqrt{-1}, Q = 0.5.$$

4.2.8 Graphical Discussion

We discuss all graphical representations in the context of fractional thermoelasticity with a memory parameter of $\beta = 0.9$, as depicted in Figures 4.12-4.15. Throughout the presentation, we maintain a constant value of $p_1 = 1$.

In Figure 4.12, the initial stress parameter P noticeably influences the u-distribution, with an increase in P leading to a decrease in u. Additionally, as α increases, while keeping t fixed at 0.1, the u-distribution also increases.

Figure 4.13 illustrates the v-displacement distribution for a fixed fractional order $\alpha = 0.6$ and time $t = 0.1$, with varying Ω. The v-distribution exhibits positive values up to $x = 0.8$, followed by a decrease and subsequent reversal in results after $x = 1.2$. Figures 4.14-4.15 demonstrate the significant impact of the rotational parameter on the stress distributions σ_{xx} and σ_{xy}. σ_{xy}-stress distribution initiate from zero, satisfying the boundary conditions. All figures satisfy boundary condition.

4.2.9 Conclusion

In this study, we investigate the impact of electromagnetic force, fractional order, gravity, initial stress, and heat source on displacement and stress components in a two-dimensional problem within a half-space semiconducting thermoelastic medium. The examination is conducted using the framework of fractional-order thermoelasticity theory with memory effect on electromagnetic field. Our findings indicate that initial stress and angular velocity exert substantial effects on all the analyzed fields. The investigation is conducted within the three-phase-lag(TPL) model.

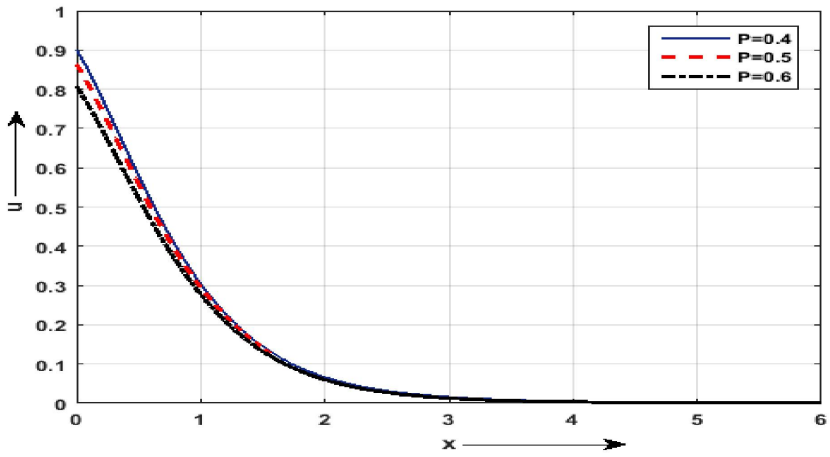

Figure 4.12: u distribution vs x axis.

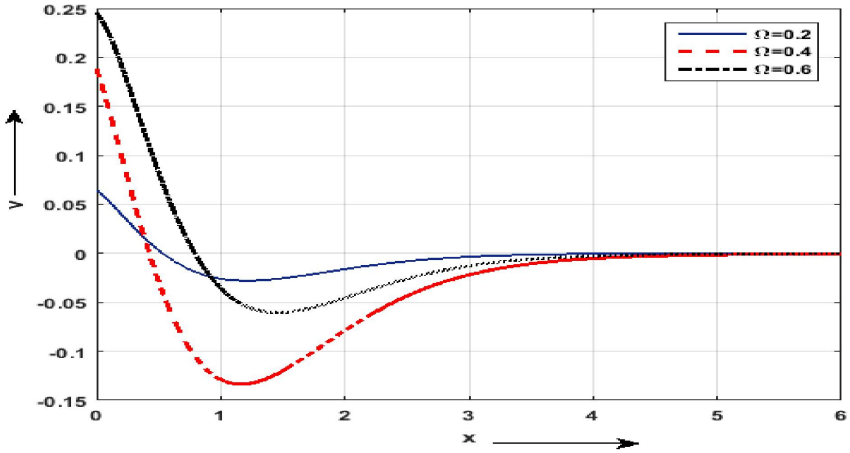

Figure 4.13: v distribution vs x axis.

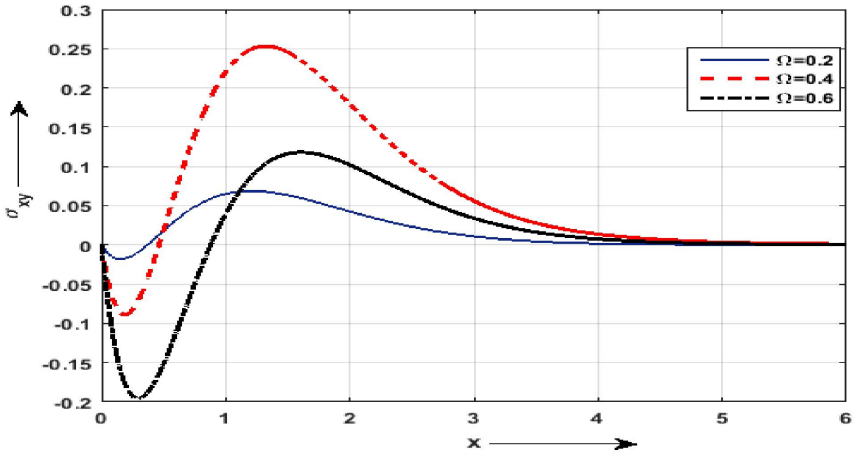

Figure 4.14: σ_{xy} distribution vs x axis at $\alpha = 0.5$.

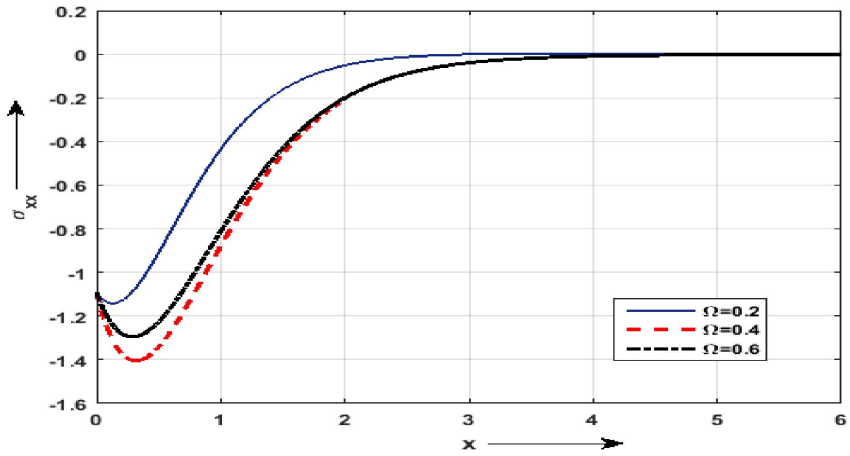

Figure 4.15: σ_{xx} distribution vs x axis at $\alpha = 0.5$.

4.2.10 Appendix

$$J_{1\omega} = (1 + \beta!\tau^{\beta-1}\omega^{1-\beta})R_H, a_{51} = \frac{b^2\Gamma_1 + J_2\omega^2 - \Omega^2}{J_1}, a_{52} = \frac{-2\Omega\omega}{J_{1\omega}},$$

$$a_{56} = \frac{-ib(J_{1\omega} - \Gamma_1 + g)}{J_{1\omega}}, a_{57} = \frac{1}{J_{1\omega}}, a_{58} = \frac{1}{J_{1\omega}},$$

$$a_{61} = \frac{2\Omega\omega}{\Gamma_1}, a_{62} = \frac{b^2 J_{1\omega} + J_2\omega^2 - \Omega^2}{\Gamma_1}, a_{63} = \frac{ib}{\Gamma_1}, a_{64} = \frac{ib}{\Gamma_1}, a_{65} = \frac{g}{\Gamma_1},$$

$$a_{72} = ib\varepsilon_1 p_l, a_{73} = b^2 + \omega p_l, a_{74} = \varepsilon_2 p_l, a_{75} = \varepsilon_1 p_l\omega$$

$$a_{83} = -\varepsilon_3, a_{84} = (b^2 + l_1 + l_2\omega)$$

$$a_1 = J_{1\omega}b^2 + J_2\omega^2 - \Omega^2, a_2 = \varepsilon_1\omega P_l, a_3 = \Lambda_1 b^2 + \omega P_l, a_5 = 2\Omega\omega + ibg,$$

$$a_{55} = b^2 + S_2 + S_3\omega + S_5\omega^2, a_6 = \varepsilon_4\omega P_l, l_1 = \frac{Kt^*}{\rho c_e \tau D_E}, l_2 = \frac{K\omega}{\rho c_e D_E},$$

$$a_4 = a_{94}, P_l = (1 + \tau_0\omega^\alpha)$$

$$\mho_{1n} = \left(\Lambda_n^2 - b^2\right), \mho_{2n} = \left(\Lambda_n^2 - a_5\right), \mho_{3n} = \left(\Lambda_n^2 - a_3\right), \mho_{4n} = \left(J_1\Lambda_n^2 - a_1\right),$$

$$\mho_{5n} = \left(\Lambda_n^2 - a_4\right), \mho_{6n} = \left(\Lambda_1\Lambda_n^2 - a_3\right), \mho_{7n} = \left(\Lambda_n^2 - a_{55}\right), X_{1n} = 1, X_{2n} = \frac{-a_5}{\Gamma_1\Lambda_n^2 - m^2},$$

$$X_{3n} = \frac{\left[a_6\mho_4 - a_2 b\mho_1 - a_5 a_6 X_{2n}\right]\mho_5}{\varepsilon_3\left(\varepsilon_2\hat{b} - a_6\right) - \left[\mho_6\hat{b} - a_6\right]\mho_5}, X_{4n} = \frac{\varepsilon_3 X_{3n}}{\mho_{5n}},$$

$$S'_{1n} = \frac{c_A^2}{\mu}\mho_{1n}, S_{1n} = \beta^2\left(\Lambda_n^2 - b^2 - X_{3n} - X_{4n}\right) + 2b^2 - 2ib\Lambda_n X_{2n},$$

$$S_{4n} = \beta^2\left(\Lambda_n^2 - b^2 - X_{3n} - X_{4n}\right) - 2\left(\Lambda_n^2 - ib\Lambda_n X_{2n}\right),$$

$$S_{2n} = ibX_{1n} - \Lambda_n X_{2n} + \frac{\mathrm{P}}{2}\left(\Lambda_n X_{2n} + ibX_{1n}\right),$$

$$M_1 = \sum_{j=1}^{8} \frac{Q_j}{\Lambda_j} \left(ib(\beta^2 - 2)X_{2j} - \beta^2(X_{3n} + X_{4n}) \right),$$

$$M_2 = \sum_{j=1}^{8} \frac{Q_j}{\Lambda_j} (ib(1 + \frac{P}{2})X_{1j}),$$

$$M_3 = \sum_{j=1}^{8} \frac{Q_j}{\Lambda_j} (ib\frac{c_A^2}{\mu}X_{2j}),$$

$$M_4 = \sum_{j=1}^{8} \frac{Q_j}{\Lambda_j} (ib\beta^2 X_{2j} - \beta^2(X_{3n} + X_{4n})),$$

$$M_5 = \sum_{j=1}^{8} \vartheta \frac{X_{4j}Q_j}{\Lambda_j}.$$

Bibliography

[1] Abbas, I., and Othman, M. Effect of rotation on plane waves at the free surface of a fiber-reinforced thermoelastic half-space using the finite element method. *Meccanica 46* (2011), 413–421.

[2] Abbas, I., and Youssef, H. M. Two-dimensional fractional order generalized thermoelastic porous material. *Latin American Journal of Solids and Structures 12* (2015), 1415–1431.

[3] Abbas, I. A. Generalized magnetothermoelasticity in a fiber-reinforced anisotropic half-space. *International Journal of Thermophysics 32*, 5 (2011), 1071–1085.

[4] Abbas, I. A., Alzahrani, F. S., and Elaiw, A. A dpl model of photothermal interaction in a semiconductor material. *Waves in Random and Complex Media 29*, 2 (2019), 328–343.

[5] Abd-Alla, A. M., Abo-Dahab, S. M., Hammad, H. A., and Mahmoud, S. R. On generalized magnetothermoelastic rayleigh waves in a granular medium under influence of gravity field and initial stress. *Journal of Vibration and Control 17* (2011), 115–128.

[6] Abel, N. H., Sylow, L., and Lie, S. *Solution de quelques problèmes à l'aide d'intégrales définies*. 2012.

[7] Abo-Dahab, S. M., Abd-Alla, A. M., Ahmed, S. M., and Rashid, M. M. Effect of magnetic field and three-phase-lag in a rotating micropolar thermo-viscoelastic half-space homogeneous isotropic material. *Waves in Random and Complex Media* (2019).

[8] Abo-Dahab, S. M., and Salama, M. M. A plane magnetothermoelastic waves reflection and transmission between two solid media with external heat sources and initial stress. *Journal of Thermal Stresses 37* (2014), 1124–1151.

[9] Abouelregal, A. E. A novel generalized thermoelasticity with higher-order time-derivatives and three-phase lags. *Multidiscipline Modeling in Materials and Structures 16*, 4 (2020), 689–711.

[10] Abouelregal, A. E., and Abo-Dahab, S. M. Dual phase lag model of magneto-thermoelasticity infinite nonhomogeneous solid having a spherical cavity. *Journal of Thermal Stresses 35*, 9 (2012), 820–841.

[11] Abouelregal, A. E., Khalil, K. M., and Mohammed, F. A. e. a. A generalized heat conduction model of higher-order time derivatives and three-phase-lags for non-simple thermoelastic materials. *Sci Rep 10* (2020), 13625.

[12] Abouelregal, A. E., Marin, M., and Alsharari, F. Thermoelastic plane waves in materials with a microstructure based on micropolar thermoelasticity with two temperature and higher order time derivatives. *Mathematics 10*, 9 (2022), 1552.

[13] Abo-Dahab, S. M., and Lotfy, K. Two-temperature plane strain problem in a semiconducting medium under photothermal theory. *Waves in Random and Complex Media 27* (2017), 67–91.

[14] Ailawalia, P., and Sachdeva, S. K. Plane strain deformation in thermoelastic microelongated solid. *Civil and Environmental Research 7*, 2 (2015), 92–98.

[15] Alzahrani, F. S., and Abbas, I. A. Generalized photo-thermo-elastic interaction in a semiconductor plate with two relaxation times. *Thin-Walled Structures 129* (2018), 342–348.

[16] Aouadi, M. Eigenvalue approach to linear micropolar thermoelasticity under distributed loading. *Journal of Thermal Stresses 30*, 5 (2007), 421–440.

[17] Askarizadeh, H., and Ahmadikia, H. Dual-phase-lag heat conduction in finite slabs with arbitrary time-dependent boundary heat flux. *Heat Transfer Engineering 37*, 12 (2016), 1038–1049.

[18] Bayones, F. S., Kilany, A. A., Abouelregal, A. E., and Abo-Dahab, S. M. A rotational gravitational stressed and voids effect on an electromagnetic photothermal semiconductor medium under three models of thermoelasticity. *Mechanics Based Design of Structures and Machines 51*, 2 (2023), 1115–1141.

[19] Bellman, R., Kalaba, R. E., and Lockett, J. Numerical inversion of the laplace transform.

[20] Biot, M. A. Thermoelasticity and irreversible thermodynamics. *Journal of Applied Physics 27* (1956), 240–253.

[21] Biswas, S. Modeling of memory-dependent derivatives in orthotropic medium with three-phase-lag model under the effect of magnetic field. *Mechanics Based Design of Structures and Machines 47*, 3 (2019), 302–318.

[22] Boley, B. A., and Weiner, J. H. *Theory of Thermal Stresses*. John Wiley, New York, 1960.

[23] Caputo, M. Linear models of dissipation whose q is almost frequency independent ii. *Geophysical Journal International 13*, 5 (1967), 529–539.

[24] Cattaneo, C. *Ahi del Seminario Mathematico e Fisico della Universita di Modena*, vol. 3. 1948.

[25] Cattaneo, C. Sur une forme de l'equation de la chaleur elinant le paradoxe d'une propagation instantance. *Comptes Rendus de l'Academie des Sciences Paris 247* (1958), 431–433.

[26] Cauchy, A. L. Memoire sur les systems isotropes de points materials. *Mém. Acad. Sci., Paris 22* (1850), 615–654. Oeuvres, Vol. 2 (1), pp. 351–386.

[27] Chadwick, P. *Thermoelasticity, the Dynamic Theory in Progress in Solid Mechanics*, vol. 1. 1960.

[28] Chandrasekharaiah, D. S. Thermoelasticity with second sound: A review. *Applied Mechanics Reviews 39*, 3 (1986), 355–376.

[29] Chandrasekharaiah, D. S. Hyperbolic thermoelasticity: A review of recent literature. *Applied Mechanics Reviews 21*, 12 (1998), 705–729.

[30] Das, B. *Problems and Solutions in Thermoelasticity and Magnetothermoelasticity*. Springer Science and Business Media LLC, 2017.

[31] Das, B., and Lahiri, A. Generalized magnetothermoelasticity for isotropic media. *Journal of Thermal Stresses 38* (2015), 210–228.

[32] Deswal, S., and Hooda, N. A two-dimensional problem for a rotating magneto-thermoelastic half-space with voids and gravity in a two-temperature generalized thermoelasticity theory. *Journal of Mechanics 31*, 6 (2015), 639–651.

[33] Dhaliwal, R. S., and Sherief, H. H. Generalized thermoelasticity for anisotropic media. *Quarterly of Applied Mathematics 33*, 1 (1980), 1–8.

[34] Duhamel, J. Second memories sur les phenomes thermomechanics. *J. De I'E Cole Polytech. 15* (1837), 1–15.

[35] Eringen, A. Linear theory of micropolar elasticity. *J. Math. Mech. 15* (1966), 909–923.

[36] Eringen, A. A unified theory of thermomechanical materials. *Int. J. Eng. Sci. 4* (1966), 179–202.

[37] Eringen, A. *Theory of micropolar elasticity*, vol. II. New York, 1968.

[38] Eringen, A. C. Linear theory of micropolar elasticity. ONR Technical Report 29, School of Aeronautics, Aeronautics and Engineering Science, Purdue University, 1965.

[39] Eringen, A. C., and Suhubi, E. S. Non-linear theory of micro-elastic solids I. *International Journal of Engineering Science 2* (1964), 189–203.

[40] Ezzat, M. A. Thermoelectric mhd non-newtonian fluid with fractional derivative heat transfer. *Physica B 405* (2010), 88–94.

[41] Ezzat, M. A., and El-Karaman, A. S. Fractional order heat conduction law in magneto-thermoelasticity involving two temperatures. *Z. Angew. Math. Phys. 62* (2011), 937–952.

[42] Ezzat, M. A., and El-Karaman, A. S. Fractional thermoelectric viscoelastic materials. *Appl. Polym. Sci. 124* (2012), 2187–2199.

[43] Galileo. *Discoursi e Dimostrazioni Matematiche.* Leiden, 1638.

[44] Ghosh, D. *Comparative Study Of Some Problems Of Thermoelasticity.* PhD thesis, Jadavpur University, India, 2020.

[45] Ghosh, D., and Lahiri, A. A study on the generalized thermoelastic problem for an anisotropic medium. *Journal of Heat Transfer 140*, 9 (2018), 094501.

[46] Green, A. A note in linear. *Mathematika 19* (1972), 69–75.

[47] Green, A., and Laws, N. On the entropy production inequality. *Arch. Rat. Mech. Anal. 45* (1972), 47–53.

[48] Green, A., and Lindsay, K. Thermoelasticity. *Journal of Elasticity 2* (1972), 1–7.

[49] Green, A., and Naghdi, P. A re-examination of the basic postulates of thermomechanics. *Proc. Roy. Soc. London Ser. A. 432* (1991), 171–194.

[50] Green, A., and Naghdi, P. On undamped heat waves in an elastic solid. *Journal of Thermal Stresses 15* (1992), 253–264.

[51] Green, A., and Naghdi, P. Thermoelasticity without energy dissipation. *J. Elasticity 31* (1993), 189–208.

[52] Gurtin, M., and Pipkin, A. A general theory of heat conduction with finite wave speeds. *Arch. Rat. Mech. Anal. 31* (1968), 113–126.

[53] Hamza, F., Abd El-Latief, A. M., and Abdou, M. 1d applications on fractional generalized thermoelasticity associated with two relaxation times. *Mechanics of Advanced Materials and Structures 23*, 6 (2016), 689–703.

[54] Hamza, F., Abd El-Latief, A. M., and Fayik, M. Memory time effect on electromagnetic-thermoelastic materials. *Journal of Electromagnetic Waves and Applications* (2015).

[55] Hamza, F., Abdou, M., and Abd El-Latief, A. M. Generalized fractional thermoelasticity associated with two relaxation times. *Journal of Thermal Stresses 37*, 9 (2014), 1080–1098.

[56] Hetnarski, R. Coupled one-dimensional thermal shock problems for small times. *Arch. Mech. Stos. 13* (1961), 295–306.

[57] Hetnarski, R. B. Solution of the coupled problem of thermoelasticity in the forms of series of functions. *Arch. Mech. 16* (1964), 919–941.

[58] Hobiny, A., and Abbas, I. Fractional order gn model on photo-thermal interaction in a semiconductor plane. *Silicon 12*, 8 (2020), 1957–1964.

[59] Hooke, R. *De Potentia Restitutiva*. 1678.

[60] Iesăn, D. *Thermoelastic Models of Continua*. Kluwer Academic, Dordrecht, 2004.

[61] Ignaczak, J., and Ostoja-Starzewski, M. *Thermoelasticity with Finite Wave Speeds*. Oxford University Press, New York, 2010.

[62] Jeffreys, H. State-space approach of two-temperature generalized thermoelasticity of a one-dimensional problem. *Int. J. Solids Struct. 44* (1930), 1550–1562.

[63] Johns, D. *Thermal stress analysis*. Pergamon Press, Oxford, 1965.

[64] Jumarie, G. Derivation and solutions of some fractional black–scholes equations in coarse-grained space and time application to merton's optimal portfolio. *Comput. Math. Appl. 59* (2010), 1142–1164.

[65] Kaliski, S. Waves equation of thermoelasticity. *Bull. Acad. Polon Sci., Ser. Sci. Techn. 13* (1965), 253–260.

[66] Kaliski, S., and Michalec, J. The resonance amplification of a magnetoelastic wave radiated from a cylindrical cavity. *Proc. Vibr. Prob 10* (1963), 159–169.

[67] Kaliski, S., and Nowacki, W. Combined elastic and electromagnetic waves produced by thermal shock. *Bull. Acad. Polon Sci., Ser. Sci. Techn. 10* (1962), 159–169.

[68] Kaliski, S., and Petykiewicz, J. Equation of motion coupled with the field of temperature in a magnetic. *Journal of Engineering Science 7* (1959), 437–445.

[69] Kar, A., and Kanoria, M. Thermoelastic interaction with energy dissipation in a transversely isotropic thin circular disc. *European J. Mech. A/Solids 26* (2006), 969–981.

[70] Kar, A., and Kanoria, M. Thermoelastic interaction with energy dissipation in an infinitely extended thin plate containing a circular hole. *Far East J. Appl. Math. 24* (2006), 201–217.

[71] Kar, A., and Kanoria, M. Thermoelastic interaction with energy dissipation in an unbounded body with a spherical hole. *Int. J. Solids and Structures 44* (2007), 2961–2971.

[72] Keshavan, H. *Some wave propagation problems in generalized thermoelasticity.* PhD thesis, Bangalore University, Bangalore, 1993.

[73] Kilany, A. A., Abo-Dahab, S. M., Abd-Alla, A. M., and Abdalla, A. N. Photothermal and void effect of a semiconductor rotational medium based on lord–shulman theory. *Mechanics Based Design of Structures and Machines* (2020).

[74] Kimmich, R. Strange kinetics, porous media and nmr. *Chem Phys 284* (2002), 243–285.

[75] Kirchhoff, G. Uber die gleichungen des gleichgewichts einer elastischen körpers bei nicht unendlich kleinen verschiebungen seiner teile. *Sitzgsber. Akad. Wiss. Wien. 9* (1852), 762–773.

[76] Kovalenko, A. *Thermoelasticity.* Wolters Noordhoff, Groningen, 1969.

[77] Kumar, R., and Deswal, S. Steady state response of a generalized thermoelastic half-space to moving mechanical/thermal loads. *Indian Journal of Pure and Applied Mathematics 4* (2000), 449–465.

[78] Lahiri, A., and Das, B. Eigenvalue approach to generalized thermoelastic interactions in an unbounded body with circular cylindrical hole without energy dissipation. *Int. Jour. of Appld. Mechanics and Engineering 13*, 4 (2008), 939–953.

[79] Lahiri, A., Das, N., Sarkar, S., and Das, M. Matrix method of solution of coupled differential equations and it's application to generalized thermoelasticity. *Bull.Cal.Math.Soc 101*, 6 (2009), 571–590.

[80] Lamé, G. *Lecons sur la théorie mathématique de l'Elasticité des corps solides.* Gautheir-Villars, Paris, 1852.

[81] Lebon, G., and Lambermont, J. A consistent thermodynamic formulation of the field equations for elastic bodies removing the paradox of infinite speed of propagation of thermal signals. *J. de Mechanique 15* (1976), 579–594.

[82] Lessen, M. Thermoelasticity and thermal shock. *J. Mech. Phys. Solids 5* (1956), 57–61.

[83] Lessen, M., and Duke, C. On the motion of elastic thermally conducting solids. In *Proc. First Midwest Conference on Mechanics of Solids* (1953).

[84] Liouville, J. Sur le calcul des differentielles a indices quelconques. *J. Ecole Polytechn. 13* (1832), 1–69.

[85] Lord, H. W., and Shulman, Y. A. A generalized dynamical theory of thermoelasticity. *Journal of the Mechanics and Physics of Solids 15*, 5 (1967), 299–309.

[86] Lotfy, K. Photothermal waves for two temperatures with a semiconducting medium under using a dual-phase-lag model and hydrostatic initial stress. *Waves in Random and Complex Media 27*, 3 (2017), 482–501.

[87] Love, A. *Treatise on the Mathematical Theory of Elasticity.* Oxford, 1927.

[88] Lykov, A. Application of methods of thermodynamics of irreversible process to investigation of heat and mass exchange. *J. Engng. Phy. 9* (1965), 287–304.

[89] Magin, R., and Royston, T. Fractional-order elastic models of cartilage: A multi-scale approach. *Communications in Nonlinear Science and Numerical Simulation 15* (2010), 657–664.

[90] Maxwell, J. On the dynamic theory of gases. *Phil. Trans. Roy. Soc., London 157* (1867), 49–88.

[91] Mitra, K., Kumar, S., Vedevarz, A., and Moallemi, M. K. Experimental evidence of hyperbolic heat conduction in processed meat. *ASME Journal of Heat Transfer 117*, 3 (August 1995), 568–573.

[92] Mitra, R. *Eigenvalue Approach to Some Problems of Generalized Thermoelasticity.* PhD thesis, Jadavpur University, India, 2020.

[93] Mittal, G., and Kulkarni, V. Dynamic model of fractional thermoelasticity due to ramp-type heating with two relaxation times. *Sādhanā 44* (2019).

[94] Mukhopadhyay, S. Thermoelastic interaction without energy dissipation in an unbounded medium with a spherical cavity due to a thermal shock at the boundary. *Journal of Thermal Stresses 25*, 9 (2002), 877–887.

[95] Mukhopadhyay, S. Thermoelastic interactions without energy dissipation in an unbounded body with a spherical cavity subjected to harmonically varying temperature. *Mech. Res. Comn. 31* (2004), 81.

[96] Mukhopadhyay, S. A problem on thermoelastic interactions without energy dissipation in an unbounded body with a spherical cavity subjected to harmonically varying stresses. *Bull. Cal. Math. Soc. 99*, 3 (2007), 261–270.

[97] Muller, I. The coldness, a universal function in thermoelastic bodies. *Arch. Rat. Mech. Anal. 41* (1971), 319–332.

[98] Muratikov, K. L., and Glazov, A. L. Theoretical and experimental investigation of the photoacoustic effect in solids with residual stresses. *Central European Journal of Physics 1*, 3 (2003), 485–515.

[99] Narasimha Murthy, H. *Studies in generalized thermoelasticity.* PhD thesis, Bangalore University, Bangalore, 1993.

[100] Navier, C. Me'moires de l'acade'mie des sciences, paris, vol. 7. see also Bulletin de la socie'te philomathique, Paris (1823), pp. 127.

[101] Nettleton, R. Relaxation theory of thermal conduction in liquids. *Physics of fluids 3* (1960), 216–225.

[102] Neumann, F. Vorlesungen, uben die theorie der elasticitat der festen korper and des lichta'thers. *Breslam* (1885).

[103] Nowacki, W. *Thermoelasticity.* Addison-Wesley, London, 1962.

[104] Nowacki, W. *Dynamic problems of thermoelasticity.* Noordhoff Int. Pub., Leyden, Netherlands, 1975.

[105] Othman, M., Atwa, S., Eraki, E., and Ismail, M. The initial stress effect on a thermoelastic micro-elongated solid under the dual-phase-lag model. *Applied Physics A 127* (2021).

[106] Othman, M., Atwa, S., Eraki, E., and Ismail, M. A thermoelastic micro-elongated layer under the effect of gravity in the context of the dual-phase lag model. *ZAMM Journal of Applied Mathematics and Mechanics: Zeitschrift für angewandte Mathematik und Mechanik 101* (2021).

[107] Othman, M., and Ismail, M. The gravitational field effect on a micro-elongated thermoelastic layer under a fluid load with two theories. *Multidiscipline Modeling in Materials and Structures 18* (2022).

[108] Othman, M., and Song, Y. Effect of rotation on the reflection of magneto-thermoelastic waves under thermoelasticity without energy dissipation. *Acta Mech 184* (2006), 189–204.

[109] Othman, M. I. A., and Abbas, I. A. Eigenvalue approach for generalized thermoelastic porous medium under the effect of thermal loading due to a laser pulse in dpl model. *Indian Journal of Physics 93* (2019), 1567–1578.

[110] Othman, M. I. A., and Atwa, S. Y. Response of micropolar thermoelastic solid with voids due to various sources under green naghdi theory. *Acta Mechanica Solida Sinica 25* (2012), 197–209.

[111] Othman, M. I. A., and Lotfy, K. The effect of a magnetic field and rotation of the 2-d problem of a fiber-reinforced thermoelastic under three theories with the influence of gravity. *Mechanics of Material 60* (2013), 129–143.

[112] Othman, M. I. A., Tantawi, R. S., and Eraki, E. Propagation of the photothermal waves in a semiconducting medium under l-s theory. *Journal of Thermal Stresses 39*, 11 (2016), 1419–1427.

[113] Othman, M. I. A., Tantawi, R. S., and Eraki, E. Effect of rotation on a semiconducting medium with two-temperatures under l-s theory. *Archives of Thermodynamics 38*, 2 (2017), 101–122.

[114] Othman, M. I. A., Tantawi, R. S., and Eraki, E. E. M. Effect of initial stress on a semiconductor material with temperature dependent properties under dpl model. *Microsystem Technologies 23* (2017), 5587–5598.

[115] Pal, P., and Kanoria, M. Thermoelastic wave propagation in a transversely isotropic thick plate under green-naghdi theory due to gravitational field. *J. Therm. Stresses 40*, 4 (2017), 470–485.

[116] Paria, G. Magnetoelasticity and magnetothemoelasticity. *Advances in Applied Mechanics 10* (1967), 73.

[117] Parkus, H. *MagnetoThermoelasticity.* Springer-Verlag, Vienna, 1971.

[118] Peng, W., Ma, Y., Li, C., and He, T. Dynamic analysis of the fractional order thermoelastic diffusion problem of an infinite body with a spherical cavity and variable material properties. *Journal of Thermal Stresses 43* (2020), 38–54.

[119] Poisson, S. Mémoire sur l'équilibre de le movement des corps élastiques. *Mém. acad. 8* (1829).

[120] Povstenko, Y. Fractional radial heat conduction in an infinite medium with a cylindrical cavity and associated thermal stresses. *Mech. Res. Commun. 37* (2010), 436–440.

[121] Povstenko, Y. Z. Fractional heat conduction equation and associated thermal stress. *Journal of Thermal Stresses 28*, 1 (2004), 83–102.

[122] Quintanilla, R. Exponential stability in the dual-phase-lag heat conduction theory. *Journal of Non-Equilibrium Thermodynamics 27* (2002), 217–227.

[123] Quintanilla, R., and Racke, R. A note on stability in three-phase-lag heat conduction. *International Journal of Heat and Mass Transfer 51*, 1-2 (2008), 24–29.

[124] Rice, R. G., and Duong, D. D. *Applied Mathematics and Modeling for Chemical Engineers.* John Wiley and Sons, Inc., New York, 1995.

[125] Riemann, B. Uber die anzahl der primzahlen unter eine gegebenen grösse. *Gesammelte Math. Werke 144* (1876), 136.

[126] Roy, S., and Lahiri, A. A study on fractional order thermoelastic half space. *International Journal of Applied Mechanics and Engineering 25* (2020), 191–202.

[127] Roy, S., and Lahiri, A. Fractional order thermoelastic model with voids in three-phase-lag thermoelasticity. *Comput. Sci. Math. Forum 7* (2023), 57.

[128] Roy Choudhuri, S. On a thermoelastic three-phase-lag model. *Journal of Thermal Stresses 30*, 3 (2007), 231–238.

[129] Roy Choudhuri, S., and Dutta, P. Thermoelastic interaction without energy dissipation in an infinite solid with distributed periodically varying heat sources. *International Journal of Solid and Structures 42* (2005), 4192–4203.

[130] Sardar, S. S., Ghosh, D., Das, B., and Lahiri, A. On a multi-phase lag model of three-dimensional coupled thermoelasticity in an anisotropic half-space. *Waves in Random and Complex Media* (2022).

[131] Sarkar, N., and Lahiri, A. The effect of gravity field on the plane waves in a fiber-reinforced two temperature magneto-thermoelastic medium under lord-shulman theory. *Journal of Thermal Stresses 36* (2013), 895–914.

[132] Sherief, H., and Abd El-Latief, A. Application of fractional order theory of thermoelasticity to a 1d problem for a half-space. *ZAMM - Journal of Applied Mathematics and Mechanics / Zeitschrift für Angewandte Mathematik und Mechanik 94*, 6 (2014), 509–515.

[133] Sherief, H., and Anwar, M. Problem in generalized thermoelasticity. *Journal of Thermal Stress 9*, 2 (1986), 165–181.

[134] Sherief, H., and Anwar, M. Problems in generalized thermoelasticity. *Journal of Thermal Stresses 9* (1986), 165–181.

[135] Sherief, H., El-Sayed, A., and El-Latief, A. Fractional order theory of thermoelasticity. *International Journal of Solids and Structures 47* (2010), 269–275.

[136] Sneddon, I. *Linear theory of thermoelasticity.* Springer–Verlag, Wien, 1974.

[137] Sokolnikoff, I. S. *Mathematical theory of elasticity*, 2nd ed. McGraw-Hill Book Co., New York, 1956.

[138] Song, Y., Bai, J., and Ren, Z. Study on the reflection of photothermal waves in a semiconducting medium under generalized thermoelastic theory. *Acta Mechanica 223* (2012), 1545–1557.

[139] Song, Y., Todorovic, D., Cretin, B., and Vairac, P. Study on the generalized thermoelastic vibration of the optically excited semiconducting microcantilevers. *International Journal of Solids and Structures 47*, 14-15 (2010), 1871–1875.

[140] Song, Y., Todorovic, D. M., Cretin, B., et al. Study of photothermal vibrations of semiconductor cantilevers near the resonant frequency. *J Phys D: Appl Phys 41*, 15 (2008), 155106.

[141] Suhubi, E. *Thermoelastic solids in Continuum physics*, vol. 2. Academic Press, New York, 1975.

[142] Todorovic, D. Photothermal and electronic elastic effects in microelectromechanical structures. *Review of Scientific Instruments 74*, 1 (2003), 578–581.

[143] Todorovic, D. Plasma, thermal, and elastic waves in semiconductors. *Rev Sci Instrum 74*, 1 (2003), 582–585.

[144] Todorovic, D., Nikolic, P., and Bojicic, A. Photoacoustic frequency transmission technique: electronic deformation mechanism in semiconductors. *Journal of Applied Physics 85* (1999), 7716–7726.

[145] Tzou, D. Experimental support for the lagging behavior in heat propagation. *Journal of Thermophysics and Heat Transfer 9*, 4 (1995), 686–693.

[146] Tzou, D. A unified field approach for heat conduction from macro- to microscales. *Journal of Heat Transfer 117*, 1 (1995), 8–16.

[147] Tzou, D. Unified field approach for heat conduction from micro- to macroscales. *ASME Journal of Heat Transfer 117* (1995), 8–16.

[148] Tzou, D. *Macro- to Microscale Heat Transfer: The Lagging Behavior*. Taylor and Francis, Washington, DC, 1997.

[149] Tzou, D. Y., and Guo, Z.-Y. Nonlocal behavior in thermal lagging. *International Journal of Thermal Sciences 49*, 7 (2010), 1133–1137.

[150] Vernotte, M. Les paradoxes de la theorie continue de l'equation de la chaleur. *Comptes Rendus de l'Academie des Sciences Paris 246* (1958), 3154–3155.

[151] Youssef, H. Theory of two-temperature-generalized thermoelasticity. *IMA Journal of Applied Mathematics 71* (2006), 383–390.

[152] Youssef, H. M. State-space approach to fractional order two-temperature generalized thermoelastic medium subjected to moving heat source. *Mechanics of Advanced Materials and Structures 20*, 1 (2013), 47–60.

[153] Youssef, H. M., and Al-Lehaibi, E. A. Fractional order generalized thermoelastic infinite medium with cylindrical cavity subjected to harmonically varying heat. *Scientific Research 3* (2010), 32–37.

[154] Zakaria, M. Effects of hall current and rotation on magneto micropolar generalized thermoelasticity due to ramp-type heating. *International Journal of Electrical Applications 2* (2012), 24–32.

[155] Zakian, V. Numerical inversion of laplace transform. *Electronics Letters 5*, 6 (1969), 120–121.

[156] Zenkour, A. M. Refined microtemperatures multi-phase-lags theory for plane wave propagation in thermoelastic medium. *Results in Physics 11* (2018), 929–937.

[157] Zenkour, A. M. Refined multi-phase-lags theory for photothermal waves of a gravitated semiconducting half-space. *Composite Structures 212* (2019), 346–364.

[158] Zenkour, A. M. Exact coupled solution for photothermal semiconducting beams using a refined multi-phase-lag theory. *Optics and Laser Technology 128* (2020), 106233.

[159] Zenkour, A. M. Magneto-thermal shock for a fiber-reinforced anisotropic half space studied with a refined multi-dual-phase-lag model. *Journal of Physics and Chemistry of Solids 137* (2020), 109213.

[160] Zenkour, A. M. On generalized three-phase-lag models in photothermoelasticity. *International Journal of Applied Mechanics 14*, 02 (2022), 2250005.

[161] Zenkour, A. M., and El-Mekawy, H. F. On a multi-phase-lag model of coupled thermoelasticity. *International Communications in Heat and Mass Transfer 116* (2020), 104722.